STATEMENT OF AWARD FOR DEGREE
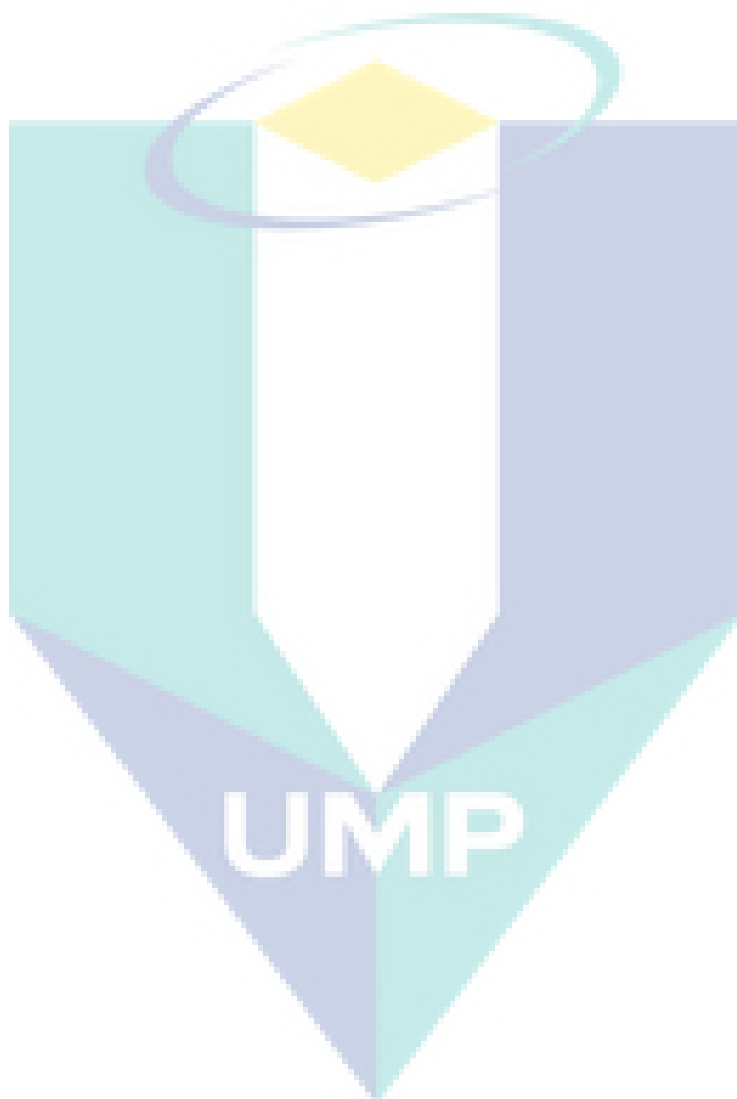
Master of Engineering (by Research)

Thesis submitted in fulfilment of the requirements for the award of the degree of Master of Engineering in Chemical
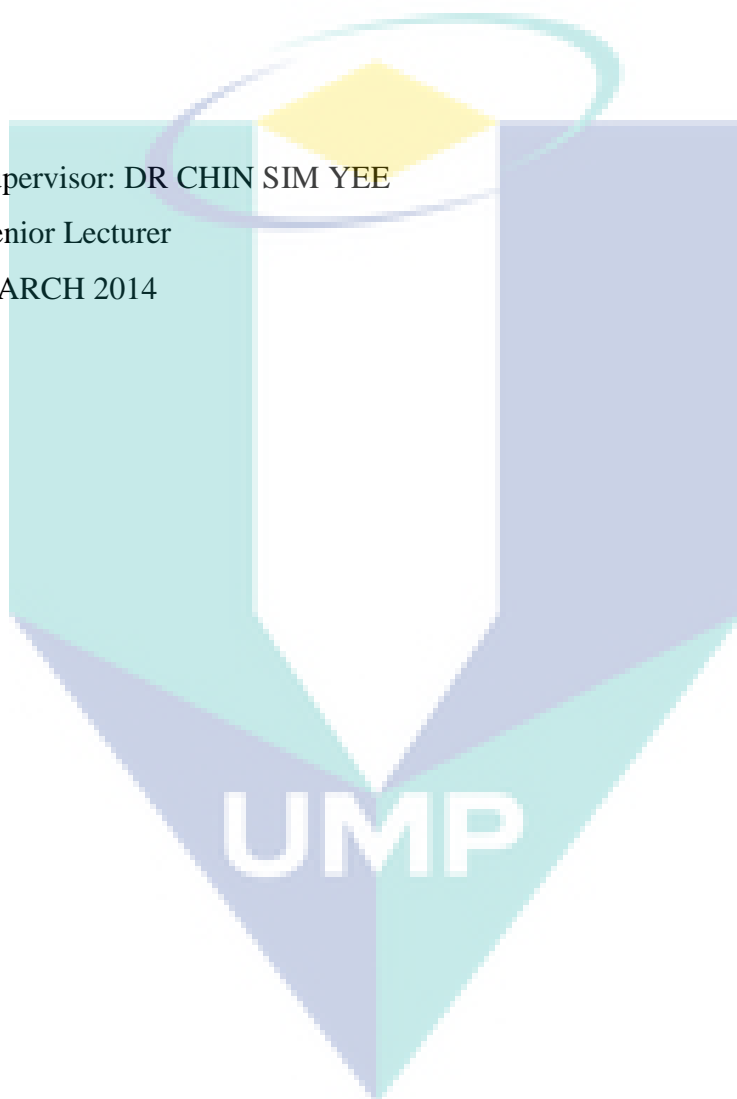
SUPERVISOR'S DECLARATION

I hereby declare that I have checked this thesis and in my opinion, this thesis is adequate in terms of scope and quality for the award of the degree of Master of Engineering in Chemical

Signature
Name of Supervisor: DR CHIN SIM YEE
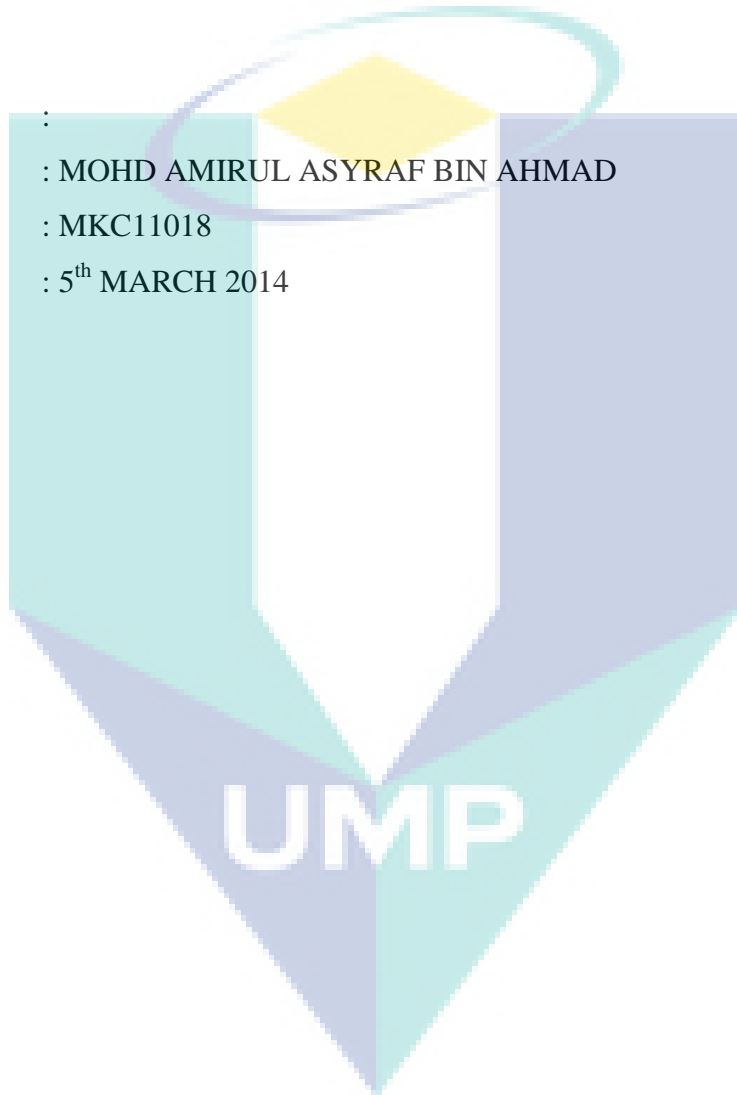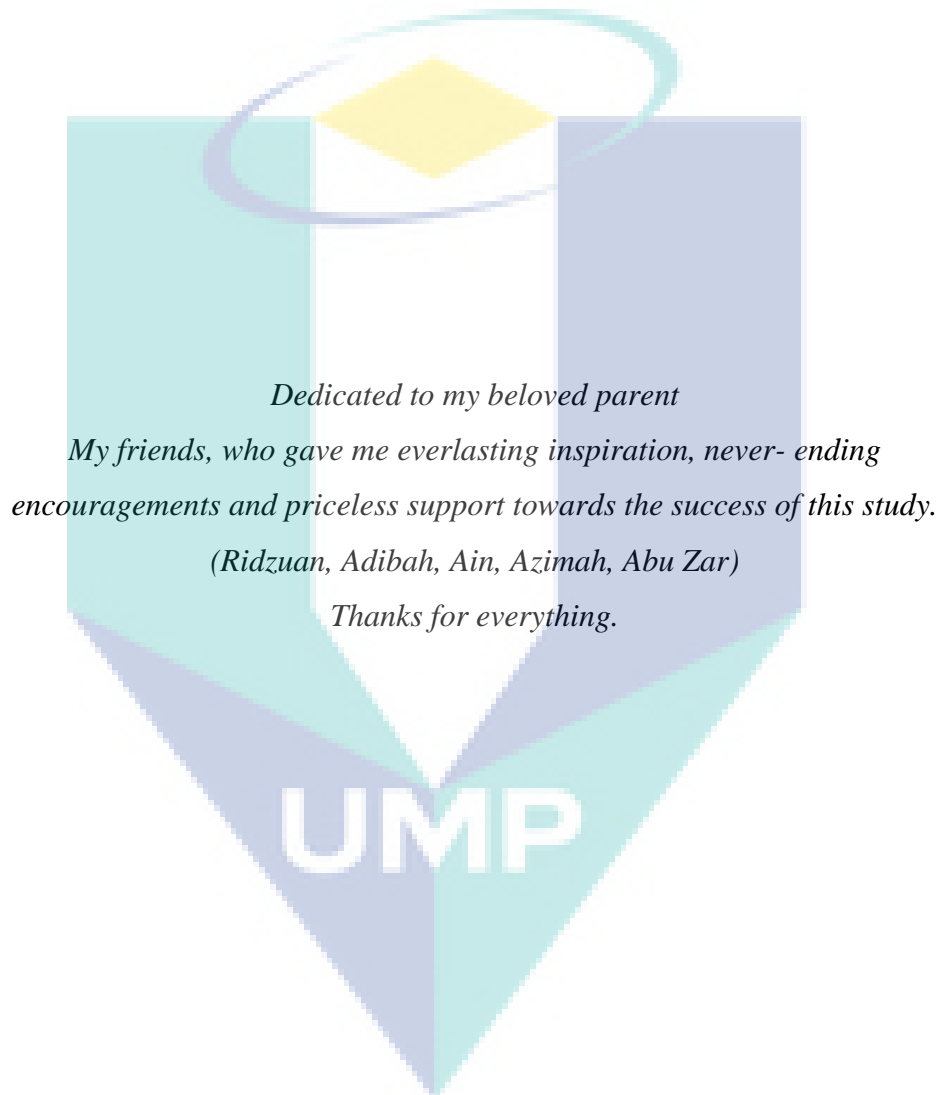Position: Senior Lecturer
Date: 5th MARCH 2014

STUDENT'S DECLARATION

I hereby declare that the work in this thesis is my own expect for quotations and summaries which have been duly acknowledged. The thesis has not been accepted for any degree and is not concurrently submitted for the award of other degree.

Signature   :

Name   : MOHD AMIRUL ASYRAF BIN AHMAD

ID Number   : MKC11018

Date   : 5th MARCH 2014

DEDICATION

Dedicated to my beloved parent
My friends, who gave me everlasting inspiration, never- ending
encouragements and priceless support towards the success of this study.
(Ridzuan, Adibah, Ain, Azimah, Abu Zar)
Thanks for everything.

ACKNOWLEDGEMENTS

ABSTRACT

In a typical acrylic manufacturing unit, waste water contains acrylic acid (AA) in a range of 4–15 wt% contributes to the high value of chemical oxygen demand. Due to the toxicity of AA to the aquatic organism, this wastewater should be treated before it is discharged. Recovery of AA from the waste water via esterification reaction in a reactive distillation column (RDC) could be a promising method to treat this waste water. Activity and kinetic studies using a batch system are important to examine the practicability of this method. In the present work, the activity and kinetic studies of the esterification of AA and 2-ethyl hexanol (2EH) were carried out in a batch system. Ion exchange resin, Amberlyst 15 was employed as a catalyst. The effect of various variables that affecting conversion and yield such as agitation speed, catalyst particle size, temperature, catalyst loading and initial reactant molar ratio were studied. The effect of the initial water content was studied using both the batch systems with total reflux (TR) and dean stark for continuously water removal (CWR). The increase of equilibrium conversion with the temperature indicated the endothermicity of the reaction. Temperature was the most significant variable that affected the conversion and yield. The highest conversion and yield were obtained at the temperature of 388 K, initial reactant molar ratio of AA to 2EH of 1:3 and catalyst loading of 10 wt%. The yield for the reactions of the AA solutions with different AA concentrations except the AA concentrations of 10-20 wt%, was enhanced significantly when the reactions were carried out using the CWR setup. Catalyst poisoning occurred during the reactions of the very dilute AA solutions (10-20%) due to the water inhibition and poly-acrylic acid deposition on the catalyst surface as validated by the catalyst characterisation studies. The pseudo-homogeneous (PH), Eley-Rideal (ER) and Langmuir-Hinshelwood-Hougen-Watson (LHHW) kinetic models were used to interpret the kinetic data. The best fit kinetic model for the main esterification reaction was shown by the non-ideal ER model while the side reaction, AA polymerisation was best interpreted by PH model. The kinetic data for the esterification of dilute AA was well described by the inclusion of the correction factor to the kinetic model of the esterification.

ABSTRAK

Kebiasaannya, unit penghasilan asid akrilik menghasilkan air sisa yang mengandungi asid akrilik (AA) dalam komposisi 4-15% nisbah berat. Air sisa ini menyumbang kepada nilai permintaan oksigen kimia (COD) yang tinggi Air sisa ini perlu dirawat sebelum dilepaskan disebabkan oleh sifat toksiknya kepada organisma akuatik. Perawatan air sisa menggunakan kaedah pengesteran dalam turus penyulingan reaktif (RDC) menunjukkan potensi yang tinggi. Kajian tentang aktiviti dan kinetik menggunakan sistem reaktor berkelompok penting untuk mengkaji kesesuaian kaedah ini. Dalam kajian ini, kajian aktiviti dan kinetik pengesteran AA dan alkohol 2-ethylhexyl (2EH) telah dijalankan dalam sistem reaktor berkelompok. Ion bertukar resin komersial, 'Amberlyst 15' telah dipilih sebagai bahan pemangkin. Kesan pelbagai pemboleh ubah yang mempengaruhi kadar tindak balas kimia seperti kelajuan adukan reaktor, saiz zarah pemangkin, suhu tindak balas, kadar muatan pemangkin dan nisbah awal mol bahan tindak balas telah dikaji. Kesan kandungan awal air diuji menggunakan kedua-dua sistem reaktor berkelompok pada keadaan refluks keseluruhan (TR) dan penyingkiran air berterusan (CWR). Peningkatan penukaran pada keseimbangan dengan peningkatan suhu membuktikan sifat endotermik tindak balas ini. Suhu ialah pemboleh ubah yang paling memberi kesan kepada penukaran dan hasil tindak balas. Penukaran dan hasil tindak balas tertinggi diperoleh pada suhu 388 K , nisbah molar awal bahan tindak balas, AA kepada 2EH pada 1:3 dan kuantiti bahan pemangkin 10% nisbah berat. Hasil bagi tindak balas AA dengan kepekatan berbeza (melainkan kepekatan AA 10-20% berat), telah dipertingkatkan dengan ketara apabila tindak balas dijalankan dengan menggunakan set radas CWR. Keracunan pada pemangkin dilihat berlaku semasa tindak balas pada kepekatan AA yang sangat rendah (10-20 %) disebabkan oleh perencatan oleh air dan pemendapan polimer akrilik pada permukaan mangkin sepertimana yang disahkan oleh kajian pencirian pemangkin. Model kinetik Pseudo-homogen (PH), Eley-Rideal (ER) dan Langmuir-Hinshelwood-Hougen-Watson (LHHW) telah diguna pakai untuk mentafsir data kinetik. Model kinetik terbaik bagi aktiviti tindak balas pengesteran utama ialah model ER tidak ideal manakala bagi tindak balas sampingan, pempolimeran AA, ditafsirkan dengan baik oleh model PH. Data kinetik untuk pengesteran cairan AA boleh ditafsirkan dengan pertambahan faktor pembetulan kepada model kinetik pengesteran.

TABLE OF CONTENTS

CHAPTER 1   INTRODUCTION

CHAPTER 2   LITERATURE REVIEW

LIST OF TABLES

LIST OF FIGURES

LIST OF SYMBOLS

%	Percent
C_M	Mears parameter
$r_{A,obs}$	observed reaction rate
R_C	catalyst particle radius
ρ_b	bulk density of catalyst
C_{Ab}	bulk concentration
k_C	mass transfer coefficient
D_{AB}	diffusivity of the solute A in solution
d_p	diameter of the catalyst particle
μ_C	viscosity of the solution
g	gravitational acceleration
ρ_l	density of the solution
C_{WP}	Weisz–Prater parameter
D_{eff}	effective diffusivity
ΔG^0	Gibbs energy
ΔH_r^{0}	standard enthalpy of reaction
ΔH_{rxn}	Heat of reaction
Å	Armstrong
A_{cs}	adsorbate cross sectional area
a_i	Activity coefficient of component i
b_i	ith adjustable variable
C_{BET}	BET constant
C_i	Concentration of component

d_p	Particle diameter
E_f	Activity energy of reaction
K_a	Thermodynamic equilibrium constant
K_{eq}	Equilibrium constant
k_f	Rate constant
k_{f0}	Pre-exponential factor
K_i	Adsorption equilibrium constant for species i
K_x	Apparent equilibrium constant
M	number of adjusted variables
M	Molecular weight of adsorbate
N	number of experimental points
N_{Av}	Avogadro's number
$P/P°$	Relative pressure
R	Gas constant
R^2	Coefficient of determination
r_i	Rate of reaction of component
T	Reaction temperature
T	Reaction time
W	Weight of gas adsorbed
W	Catalyst weight
W_m	Weight of adsorbate
X_e	Degree of equilibrium conversion
x_i	Mole fraction of component I
γ_i	Gamma of component I
σ	standard deviations

LIST OF ABBREVIATIONS

2EH	2 ethyl hexanol
2EHA	2 ethyl hexyl acrylate
AA	Acrylic acid
BET	Brunauer, Emmett and Teller
BJH	Barrett-joyner-halenda
COD	Chemical oxygen demand
CWR	Continuous water removal
DBSA	Dodecyl benzene sulfonic acid
EQA	Environment quality act
ER	Eley Rideal
FID	Gas chromatography flame ionization detector
FTIR	Fourier transform infrared
GC	Gas chromatography
IUPAC	International Union of Pure and Applied Chemistry
LHHW	Langmuir Hinshelwood Hougen Watson
PH	Pseudo Homogeneous
PVC	Polyvinyl chloride
RDC	Reactive distillation column
SEM	Scanning electron microscope
SMBR	Simulated-moving-bed reactor
TOC	Total organic content
TR	Total reflux
UNIFAC	Universal functional activity coefficient

W   Water

XRF   X-ray flourencence

CHAPTER 1

INTRODUCTION

1.0   INTRODUCTION

Acrylic acid (AA) has served for more than 30 years as an essential component in the production of acrylate polymers from acrylate ester such as methyl acrylate, butyl acrylate, ethyl acrylate and 2-ethyl hexyl acrylate, which are applied in the industry of paints, coatings, textiles, adhesives, and plastics (Xu *et al*., 2006).

Wastewater containing 4-10 wt% AA could be generated after the extraction and distillation process in the AA manufacturing plant. AA is categorized as hazardous chemical compound. Release of AA to the effluent can cause serious damage to the environment due to the high toxicity to the aquatic organism. The prolonged exposure may cause destructive to the mucous membranes and upper respiratory tract, even cause fatal as a result of spasm, inflammation and edema of the larynx and bronchi, chemical pneumonitis and pulmonary edema (Sigma-Aldrich, 2013).

High value of total organic content (TOC) and chemical oxygen demand (COD) of the wastewater from a typical acrylic manufacturing unit were attributed to the high concentration of AA (Li *et al.*, 2008). Wastewater containing AA has been treated with various methods in order to fulfil the standard limit set by the local environmental authority. Most of the AA manufacturers have burned this type of wastewater using incinerator (Alison *et al.*, 2011). However, this method is neither environmental friendly nor economical feasible. High content of COD also has restricted to the application of biological treatment and adsorption to this type of wastewater (Scholz, 2003).

1.1   PROBLEM STATEMENT

In view of the shortcomings of the existing treatment method, esterification of AA with alcohol could be a promising method to recover the AA from the wastewater stream. AA could be recovered as a useful polyester compound while the wastewater is purified

2-ethyl hexyl acrylate is widely known for the use in the polymer industries for the production of different copolymers, such as those with AA and it's salts, amides, methacrylates, acrylonitriles, styrene vinyls and butadiene (Klien *et al.*, 2012; Peykova *et al.*, 2012). It is normally produced by the esterification of prop-2-enoic acid or commonly known as AA with 2-ethyl hexanol (2EH). It is a classical reaction system where the conversion achieved is limited by equilibrium. Unfortunately, this method alone show low performance in diluted compound and has difficulty in product separation.

Reactive distillation column (RDC) is an intensified process in which reaction and separation occur simultaneously in a column. It is used to enhance particularly the reversible reaction by removing product from the system continuously. RDC was used to overcome the equilibrium limitation of the esterification reaction. A typical commercialised example is esterification of methanol with acetic acid and esterification of fatty acid with isopropyl alcohol. Numerous researches were carried out for the esterification of different type of pure/diluted carboxylic acids with alcohols. These acids include formic acid, phthalic acid, succinic acid and lactic acid (Saha and Sharma, 1996; Bock *et al.,*1997; Choi and Hong, 1999; Sanz *et al.,* 2002). Esterification in a RDC is one of the promising methods to recover AA from wastewater (Saha *et al.,* 2000; Bianchi *et al.,* 2003; Calvar *et al.,* 2007).

Catalyst is used in the esterification process to accelerate the chemical reaction process by lower the activation energy required for the reaction. Homogeneous acid catalyst such as sulphuric acid, hydrofluoric acid, para-toluenesulfonic acid and heteropolyacid are often used in industrial processes for this purpose (Lilja *et al*., 2002 Jaques and Leisten, 1964; Sejidova *et al.*, 1990; Gonçalves *et al.*, 2012; Santia *et al.*,

2012; Pappu *et al.*, 2013). Nevertheless, these corrosive homogeneous catalysts are difficult to be removed from the reaction medium (Farnetti *et al.,* 2004). Meanwhile, esterification reaction catalysed by biocatalyst/enzymatic catalyst suffers with poor thermal stability (about 323-328 K) and longer reaction time despite the low energy consumption and operating cost (Gómez-Castro *et al.,* 2012; Demirbas, 2008; Gerpen, 2005). Heterogeneous catalysts are claimed to be more relevant and appropriate as it is easy and cheap for recovery purpose, good in thermal stability, besides having better conversion and selectivity (Kiss, 2011). The usage of heterogeneous catalyst in esterification reaction could produce clean reaction product solution and reduce waste water (Sejidov *et al.,* 2005; Cordeiro *et al.,* 2008).

The suitability of commercially available solid acid catalyst such as macroporous sulfonic acid resin (Indion 130 and Amberlyst 15), gelular or microreticular cation-exchange resin (amberlite IR 120), acid-treated montmorillonite clay (Engelhard F 24), Zeolite (ZSM-5 and MCM-41) sulfated zirconia, and heteropolyacids (12-tungstophosphoric acid) were assessed for the esterification of carboxylic acid/ waste water containing carboxylic acid with alcohol (Bianchi *et al.,* 2003; Peters *et al.,* 2006; Fernandes *et al.,* 2012). The organic resin is preferable compared to solid oxides due to higher conversion (Chen *et al.,* 1999; Komoń *et al.,* 2013).

To the best of our knowledge, the study about esterification of AA with 2EH catalysed by Amberlyst 15 Dry (an acidic cation-exchange resin) is yet to be reported in the literature. In the present study, which is a part of a wider project with the aim of designing RDC for the AA recovery from the wastewater stream, diluted AA with different concentration (model wastewater) was reacted with 2EH in a stirred batch reactor. Amberlyst 15 Dry was used as catalyst. Information required for RDC design such as the important operating variables and kinetic model were identified. The practicability of carrying out this reaction in RDC was examined.

1.2   OBJECTIVES

The objectives of the study of esterification of AA with 2EH catalysed by Amberlyst 15 Dry are:

- To study the effect of important operating variables to the reaction kinetics.
- To develop the kinetic model of the reaction.
- To determine the effect of water inhibition toward the reaction.

1.3   SCOPES OF STUDY

The scopes of study include:

- The study on the effect of external and the internal diffusion on the reaction.
- The study on the effect of the operating variables such as initial concentration of AA, reaction time, catalyst loading, temperature and ratio of reactants.
- The equilibrium study.
- The kinetic data correlation with pseudo-homogeneous (PH), Eley Rideal (ER), and Langmuir Hinshelwood Hougen Watson (LHHW) models.

1.4   SIGNIFICANCE OF STUDY

The outcome of the present research serves as a basis for the analysis of the prospect and feasibility of the AA recovery from the waste water stream using RDC. The range of the important operating variables and the kinetic model identified in the present study can be adopted in the modelling and simulation of the RDC for AA recovery. The feasibility can be examined based on the results obtained from the simulation study. The success of the present work would lead to a breakthrough of new treatment method for wastewater containing acrylic acid from the petrochemical industries. Hence, the environmental impact of the wastewater generated by petrochemical industries could be reduced. More revenue would also be generated from the ester produced from the wastewater stream.

1.5   ORGANISATION OF THIS THESIS

This thesis is divided into five chapters. Chapter 1 (Introduction) presents the application of AA and the impact of the wastewater containing AA in brief. The motivation and problem statement of the present study are initiated by the shortcomings of the existing methods used to treat the wastewater containing AA. The objectives, scopes and significance of study are then elucidated accordingly. The organization of the thesis is given in the last section.

Chapter 2 (Literature review) compares the existing treatment methods for wastewater containing carboxylic acid. Esterification via reactive distillation column is identified as one of the promising methods to recovery AA from the wastewater stream. The operating conditions and catalysts used in the esterification reactions carried out in RDC are reviewed. The relevant kinetic models are assessed.

The materials, apparatus and equipment used in the present study are listed with their function in Chapter 3 (Methodology). Schematic diagrams of the experimental setup are drawn. The experimental procedures for the catalyst characterisation, esterification reaction studies and sample analysis are illustrated in detail.

Chapter 4 (Result and discussion) is divided into 6 main sections: In section 1, catalyst characterisation for fresh catalysts were performed and compared with the technical data existing. The equilibrium studies were reported based on thermodynamicity in section 2. In order to develop an accurate kinetic model, the mass transfer effect was studies in the next section. The effects of different operating variables and water to the reactions are analysed and discussed in sections 4 and 5 respectively. In the last section, the experimental kinetic data generated from the experimental studies are then used to discriminate the models proposed for the reaction kinetics.

In chapter 5, the conclusion and recommendations based on the current studies are given. The conclusions are drawn based on each individual study covered in the present research, while the recommendations are given based on the conclusions

obtained by considering their significance and importance to the future research in the related field.
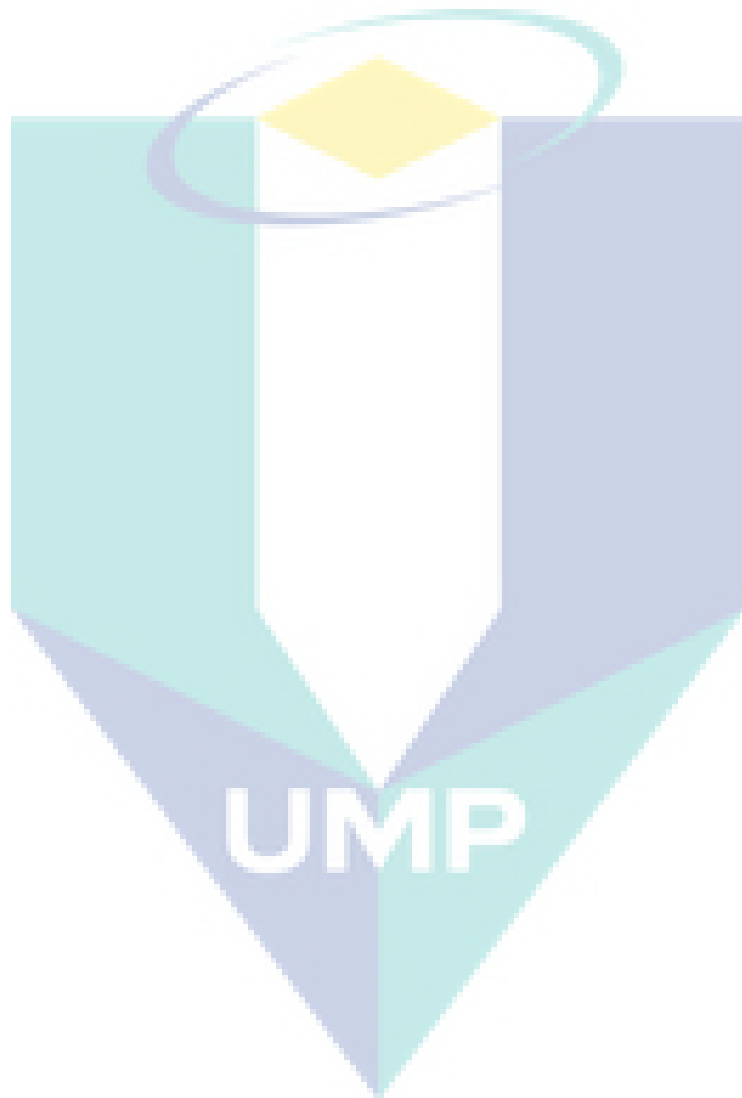
CHAPTER 2

LITERATURE REVIEW

2.0   INTRODUCTION

The present chapter reviews the methods used to treat waste water containing carboxylic acid. The method of carboxylic acid recovery via esterification was focused and the potential of treating the dilute acrylic acid aqueous solution is particularly reviewed. Comprehensive elaboration is given on the type of catalyst used and their performance under certain operating conditions. The review on the relevant kinetic models was also included.

2.1   WASTEWATER CONTAINING ACRYLIC ACID

Acrylic acid (AA), or in IUPAC name is 2-pronenoic acid, under normal conditions is a clear, colourless liquid with a pungent smell. Table 2.1 summarizes the physic chemical properties of AA.

This substance has been classified as flammable. It is harmful by inhalation (in contact with skin and if swallowed), corrosive (can causes severe burns) and dangerous for the environment, which is very toxic to aquatic organisms.

AA has been in production over 30 years for commercial purposes mainly from petrochemical industry by two-step gas-phase oxidation of propylene (Falbe *et al.*, 1995). In addition, AA can be prepared by hydrolysis of acrylonitrile (ECETOC, 1995). It is also produced naturally by several different types of algae. AA is an important intermediate for polymer industry. It has the major markets in the production of surface

coatings, textiles, adhesives, paper treatment, and plastics beside polishes, leather, fibers, detergents, and super-absorbent material (Xu *et al.*, 2006).

Table 2.1: Physico-chemical properties of AA

Properties	Value	Reference
Physical state	liquid at 20°C	
Melting point	14°C	Merck Index (1996)
Boiling point	141°C at 1 bar	Merck Index (1996)
Density	1.0621 g/cm^3 at 20°C	Merck Index (1996)
Vapour pressure	3.8 hPa at 20°C – (dynamic method)	BASF AG (1994)
Surface tension	59.6 mN/m c= 1 g/L – (ring method)	Hüls AG (1995)
Water solubility	miscible in all ratios	Merck Index (1996)
Dissociation constant	pK_a = 4.25	Weast (1989)
Partition coefficient	log P_{ow} 0.46 at 25°C – (shake flask method)	BASF AG (1988)
Flash point	48 – 55°C	CHEMSAFE
Auto flammability	395°C – DIN 51794	CHEMSAFE
Flammability	Flammable	Rohm and Haas (2006)
Explosive properties	not explosive	Rohm and Haas (2006)
Oxidizing properties	no oxidizing properties	Rohm and Haas (2006)

Fox *et al.* (1990) estimated the Western European production of AA in 1987 at about 342,000 tonnes. In 1995, the worldwide productivity of AA was more than 3 million tons annually and it was expected to grow 4 - 5% per year (Falbe *et al.*, 1995; Rohe, 1995). The world demand for crude AA and glacial AA were forecasted to grow at 3.7% per year and 4% per year respectively from year 2006 to 2011 (ICB Chemical Profile, 2008).

With the massive production and usage, substantial amount of wastewater containing AA has been generated. The wastewater containing AA is normally within the range of 3,000 – 85,000 mg/L of chemical oxygen demand (COD) (Bhattacharyya *et al.* 2013). This wastewater has drawn the attention of the local authorities due to the toxicity which harms the aquatic organisms if it is released untreated. Malaysian department of environment has set the rules and regulation to prevent the environmental pollution through the Environment Quality Act (EQA). This act prescribes ambient water quality standards and discharge standards, and specifying the maximum permissible loads that may be discharged by any source into inland waters, with reference either generally or specifically to the body of waters concerned. Due to the shortcomings of the existing treatment methods, the more effective methods, either recovery or removal of AA from the waste water stream should be further explored.

2.2 TREATMENT METHODS FOR WASTEWATER CONTAINING CARBOXYLIC ACID

Currently, most of the AA manufacturers are using the incineration approach to treat the wastewater containing AA. This method is neither economical nor environmental friendly. Some of producers integrate the distillation or evaporation with incineration to lower the energy consumption. However, this distillation and evaporation methods still require substantial amount of energy to vaporize the water (Kuila and Ray, 2011). Several patents and researches have reported on the recovery and removal techniques of carboxylic acid group such as biodegradation, catalytic degradation, adsorption, extraction, membrane separation and several hybrid processes include reactive distillation and extractive distillation.

Biodegradation is used to mineralize the chemical compound to the less hazardous or intoxicated compound by the activity of bacteria (Kimura and Ito, 2001). However, the time required for the degradation is impractical if this method is used to treat the large amount of waste water that continuously flow out or wastewater containing substantial amount of AA (4-10 wt%). Several chemical species was additionally found to resist the biological degradation (Scholz, 2003).

Catalytic degradation mineralizes the chemical compound via catalytic reaction such as ozonation, photocatalytic reaction, and wet oxidation. In recent years, a new set of oxidation process for the treatment of pollutants in waste water has become the focus of several researchers. A more efficient and low cost process in removing the unwanted compound from waste water stream was developed (Shafaei *et al.*, 2010). Despite the high efficiency of catalytic degradation, the operating cost is relatively high when comparing with the other methods.

Adsorption is another popular physical treatment. There are many established and commercial adsorbents available in the market. These include activated carbon, alumina, silica, bentonite, piet, chitosan, and ion-exchange resins (Allen, 2005). Adsorption has been proven as an effective method to remove the carboxylic acid from the waste water stream. Nevertheless, this is only valid for a very much diluted aqueous solution in which the concentration of adsorbate is in ppm level (Ayranci and Duman, 2006; Kumar *et al.*, 2008). This method is not appropriate for the waste water that contains high AA concentration as it requires bulk usage of absorbent (Kumar *et al.*, 2008).

Yu *et al.* (2003) treated the wastewater containing acetic acid through electrodialysis using membrane. Although it is effective, the wastewater requires necessary pre-treatments such as active carbon filtration and flocculation to enhance the separation. This increases capital investment. On top of this, this method also was reported to have high energy consumption resulting from the weak dissociated ability of the weak organic acid at the electrode (Xu and Yang, 2002; Wang *et al.*,2006; Zhang *et al.*,2011; Yu *et al.*, 2003). Another treatment method that uses membrane is pervaporation. Most of researchers modified the existing membrane to treat the waste water containing unsaturated monocarboxylic acid. They used several mix and match techniques such as grafting (Chiang and Huang, 1993; Shantora and Huang, 1981; Chiang and Hu, 1991; Hsiue and Yang, 1987), crosslinking, blending (Ping *et al.,* 1994; Wu *et al.*, 1994; Yuzhang *et al.*, 1993), annealing (Yuzhang *et al.*, 1993; Kojima *et al.*, 1985), composite (Wesslein *et al.*, 1990; Will and Lichtenthaler, 1992; Takegami *et al.*, 1992; Ohya *et al.*, 1992; Hayashi *et al.*, 1983), heat treatment (Katz and Wydeven, 1982; David *et al*., 1992), and solution casting (Gref *et al.*, 1993). The efficiency of this

treatment method has shown improvement from time to time. The great challenge of this method is to identify the optimal product flux and also selectivity. One needs to compromise the product flux due to the selectivity. On top of this, it is economic feasibility is still questionable.

Extraction shows an impressive efficiency in the treatment process of the waste water containing monocarboxylic acid such as acetic acid, fumaric acid, picolonic acid and propionic acid. Table 2.2 shows the concentration of the carboxylic acid in the waste water stream during the recovery studies using extraction. Most of the researches reported the efficiency of more than 90% efficiency of recovery (Chang *et al.*,2009; Tuyun *et al.*,2011; Li *et al.*,2008; Rahmanian *et al.*, 2008). Extraction alone is not effective as it needs to be integrated with other appropriate methods such as distillation column to separate the product from the extractant. This has initiated the idea of integrating the extraction process with the distillation process in a single process called hybrid extractive distillation process (Lei *et al.*, 2004; Berg, 1992). Other promising hybrid techniques to recover monocarboxylic acid are reactive distillation and pervaporation distillation. All these techniques result in saving the operating cost by reducing the energy consumption (Saha *et al.*, 2000; Kiss, 2011).

Among these hybrid methods, heterogeneously catalysed reactive distillation (catalytic distillation) is more preferable because it could ease or minimize the downstream separation processes. Reactive distillation has yielded promising result in the recovery of organic compound such as acetic acid with the range of 30 – 50% from waste water (Saha *et al.*, 2000; Singh *et al*., 2006; Saha *et al.*, 2000), as the reaction itself saves the energy consumption and prevents water inhibition toward the reaction (Saha *et al.*, 2000; Lam *et al*, 2010; Vicente *et al*., 2004). Prior to reactive distillation process, a preliminary study should be conducted to evaluate the effectiveness of esterification reaction in a batch system in order to identify the best operating condition and to obtain the kinetic data.

Table 2.2 : List of literature studies using extraction as the method of recovery

Carboxylic acid	Acid concentration in waste water (g/L)	References
Fumaric acid	6.47	Li *et al.* (2007)
Picolinic acid	28.3–141.3	Tuyun *et al.* (2011)
Propionic acid	3.7–29.6	Keshav *et al.* (2009)
Acetic acid	2	Ingale and Mahajani (1996)
Maleic and phthalic acid	0.1–5.0	Rahmanian *et al.*, 2008
Acetic acid	260 – 290	Chang *et al.*,2009

2.3   REACTIVE DISTILLATION COLUMN (RDC)

Reactive distillation column (RDC) is a unit operation in which chemical reaction and distillative separation are carried out simultaneously within a fractional distillation apparatus. Despite the difficulties in identifying a common operating window between the reaction and separation that provides acceptable and controllable reaction rates and appropriate volatilities in the reactive zone, RDC offers the following advantages (Sundmacher and Kienle, 2003; Taylor and Krishna, 2000; Gorak *et al.*, 2007):

- Improved conversion for a reversible reaction by removing products from the reactive zone.
- Circumventing/overcoming of azeotropes by reacting away the contributing components.
- Reduced side-product formation by removing products from the liquid reaction phase.
- Direct heat integration and avoidance of hot-spots for the exothermic reactions.
- Capital savings with the simplified downstream processing of reactants and products.
- Reduced the quantity of catalyst used for a comparable conversion of the reactants.

RDC has been explored as a potentially important process for several other chemicals and reactions. Along with esterifications and etherification, other reactions like hydrogenation, hydrodesulphurisation, isomerisation, and oligomerisation are some of the unconventional examples to which RDC has been successfully applied on a commercial scale. Moreover, hydrolysis, alkylation, acetilazation, hydration, and transesterification have also been identified as potential candidates for RDC. Another important area of application is the removal of small amounts of impurities for high quality product such as phenol. RDC also can be used for the recovery of valuable products like acetic acid, glycols, and lactic acid from waste stream (Saha *et al.*, 2000; Singh *et al*., 2006)

2.3.1   Esterification in Reactive Distillation Column (RDC)

Esterification is one of the equilibrium limited reactions. RDC was adopted to simplify the traditional process. The most remarkable example of the benefits of RDC is in the production of methyl acetate. The homogeneously acid catalysed conventional processes used multiple reactors with a large excess of one of the reactants to achieve high conversion. The formation of methyl acetate-methanol and methyl acetate-water azeotropes has upset the product purification. The atmospheric and vacuum distillation columns or extractive distillation were used to dissociate these azeotropes. A typical process as shown in Figure 2.1(b) is complex and yet capital intensive. It contains two reactors and eight distillation columns. The traditional process is compared with the RDC process in Figure 2.1. Nearly 100% conversion of the reactant is achieved with only one column required in the RDC process (refer Figure 2.1(a)). The capital and operationg costs are significantly reduced (Siirola, 1995).

(a) Reactive distillation process

(b) Traditional process
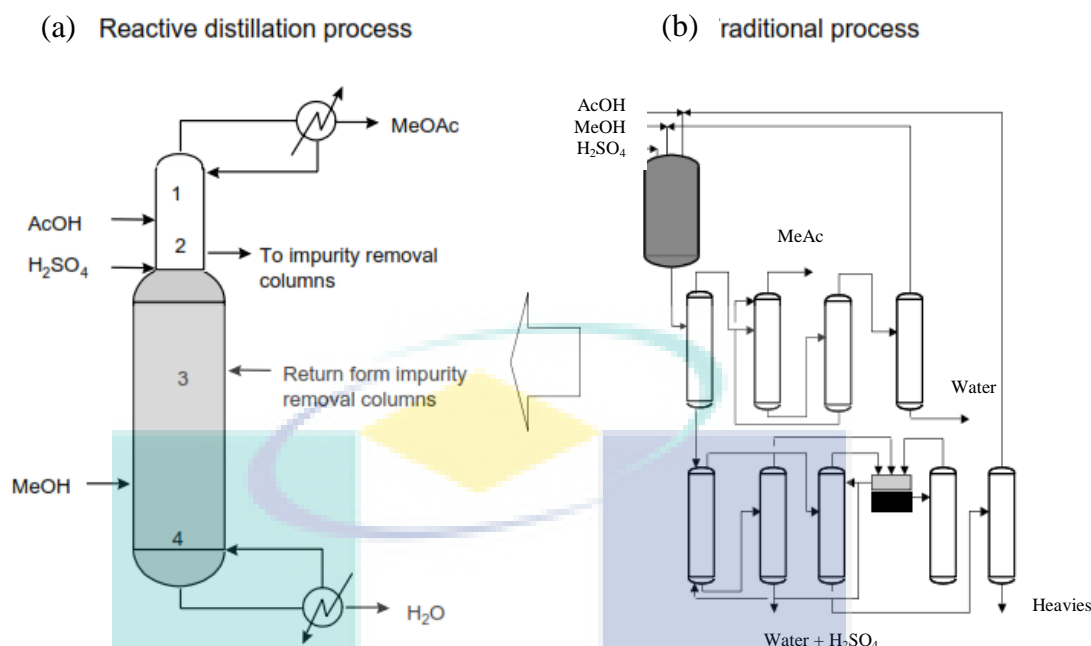
Figure 2.1: (a) RDC and (b) traditional process for methyl acetate

Source: Agreda *et al.,* 1990

Heterogeneously catalysed methyl acetate production by ion exchange resins and other solid acidic catalysts were investigated extensively (Agreda *et al.*, 1990; Dirk-Faitakis *et al.*, 2009; Kumar and Kaistha, 2009). These include the rigorous analysis of the reacting system in the RDC with the aid of experiments and modelling. For all practical purposes, chemical and phase equilibria can be assumed to explain the experimental findings. The system may deviate slightly from this assumption at high reflux ratios. The role of reflux ratio is crucial to dictate the capital cost and the energy requirements. An optimum reflux ratio is required to maintain the good separation and extent of reaction.

Esterification of pure carboxylic acids in RDC

Numerous research works were carried out to study the esterification of pure carboxylic acid with alcohol in the RDC. Most of the studies of RD analyse one-main-

product-one-reaction systems using highly pure reactants (Kumar and Kaistha, 2009; Lutze *et al.,* 2010; Hanika *et al.*, 2001; Zhicai *et al.*, 1998; Calvar *et al.,* 2007).

Apart from methyl acetate, RDC was used for the production of other esters such as ethyl acetate, isopropyl acetate, and butyl acetate (Calvar *et al.*, 2007; Zhicai *et al.*, 1998). The conversion achieved was in the range of 50 – 55%. The applications of RDC for the esterification of pure carboxylic acid are given in Table 2.3.

Table 2.3 : Applications of RDC for the esterification of pure carboxylic acid.

Reaction	Catalyst	Reference
Production of methyl acetate from acetic acid and methanol	Sulphuric acid	Agreda *et al.* (1990)
Production of ethyl acetate from ethanol and acetic acid	Amberlyst 15	Calvar *et al.* (2007)
Production of butyl acetate from butanol and acetic acid	Sulphuric acid	Zhicai *et al.* (1998)
Production of 2-methyl propyl acetate from 2-methyl propanol and acetic acid	acidic ion exchange resin	Hanika *et al.* (2001)
Production of isopropyl acetate from isopropanol and acetic acid	para-toluenesulfonic acid	Lee and Kuo (1996)

Esterification of diluted carboxylic acid in RDC

RDC has been used to recover of carboxylic acid such as acetic acid, lactic acid and mysristic acid from the waste stream (Saha *et al.*, 2000; Scates *et al.,* 1997; Choi and Hong, 1999; Bock *et al.,* 1997). Theoretically, esterification alone with the presence of large amount of water at the beginning of the reaction may shift the reaction equilibrium towards the reagent (thermodynamically favourite) rather than towards the ester (product).

Diluted acetic acid was produced in large quantities in the manufacturing processes of cellulose esters, terephthalic acid, and dimethyl terephthalate. The conventional methods of recovery are azeotropic distillation, simple distillation and

liquid-liquid extraction. Esterification of diluted acetic acid with methanol in a RDC seems to be an attractive alternative. Neumann and Sasson (1984) carried out laboratory experiments to recover acetic acid in an RDC through esterification with methanol. Commercially available ion exchange resin particles were used along with Raschig ring in the column. The use of a solid acid catalyst offered non-corrosive conditions and hence a less expensive material of construction can be used. Up to 84% of acetic acid was recovered as methyl acetate. Xu *et al.* (1999) have performed detailed experimental and simulation work on recovery of acetic acid from about 10% (w/w) aqueous solutions using the same reaction with Amberlyst 15 in the the catalyst baskets. More than 50% recovery was obtained. Hoechst Celanese Corporation (1992) has reported a work on RDC for the recovery of acetic acid from aqueous solutions as methyl acetate. Acidic ion exchange resin was used as catalyst and more than 90% recovery from 5-30% aqueous acetic acid was achieved. The use of Koch Engineering's Katamax packing was suggested to accommodate the catalyst (Scates *et al.,* 1997).

Apart from the esterification with methanol, esterification of dilute acetic acid with other alcohols was studied. Saha *et al.* (2000) have explored the possibility of esterifying acetic acid from aqueous solution with n-butanol in RDC. In this case, one can get an overhead product of composition close to the ternary heterogeneous azeotrope of butanol, butyl acetate and water. Acetic acid was recovered as the bottom product with approximately 58% conversion. The high-molecular weight acids such as lactic acid and myristic acid have been successfully recovered through esterification with methanol and isopropanol respectively at about 99% conversion (Choi and Hong, 1999; Bock *et al.,* 2000). The same approach was used to recover the succinic acid and trifluoroacetic acid from the waste water stream (Orjuela *et al.*, 2012; Mahajan *et al.*, 2008). Table 2.4 summarizes the studies about the recovery of diluted carboxylic acid using RDC.

To the best of our knowledge, the recovery of acrylic acid from the diluted aqueous solution through esterification has not been reported in the open literature.

Table 2.4 : The recovery of diluted carboxylic acid via esterification in RDC.

Process	Catalyst	Alcohol	Reference
Recovery of acetic acid from diluted streams (30 – 60% w/w)	Dowex 50 W X-8	Methanol	Neumann and Sasson (1984)
Recovery of diluted acetic acid from diluted streams (30% w/w)	Indion 130	n-butanol	Saha *et al.* (2000)
Recovery of diluted acetic acid in carbonylation process	Sulphuric acid	Methanol	Scates *et al.* (1997)
Recovery of lactic acid from fermentation broth	Dowex 50-W	Methanol	Choi and Hong (1999)
Recovery of succinic acid/acetic acid	Amberlyst 70	Ethanol	Orjuela *et al.* (2012)
Recovery of tricholoacetic acid	T-63 (cation-exchange resin)	2-propanol	Mahajan *et al.* (2008)
Recovery of myristic acid	Not available (NA)	Isopropanol	Bock *et al.* (1997)

2.4   CATALYST FOR THE ESTERIFICATION

Catalyst is used in the esterification process to enhance or accelerate chemical reaction process by lower the activation energy required for reaction. Catalysts can be divided into 3 types; there are homogenous catalysts (Sert, 2013; Malshe and Chandalia, 1977; Chubarov *et al.*, 1984), heterogeneous catalyst (Chen *et al.*, 1999), and biocatalyst (Tsukamoto and Franco, 2004).

2.4.1 Homogeneous Catalyst

Carboxylic esters such as methyl carboxylate, ethyl carboxylate, and butyl carboxylate are generally manufactured by esterifying the corresponding carboxylic acid with the corresponding alcohol. Homogenous acid catalysts are often used in these processes. It can be classified into Brønsed acid catalysts and Lewis acid catalysts.

Homogeneous catalysts for the esterification of other carboxylic acids

Simple Brønsted acid catalysts are the most frequently used catalyst especially when the esterification is generally slower due to more sterically hindered alcohol or acid, as in the case of long-chain fatty alcohols, or of the tertiary acid abietic acid (Hui, 1996). These catalysts include sulphuric acid, hydrochloric acid, hydrofluoric acid, dissolved arylsulfonic acids, para-toluenesulfonic acid, heteropolyacid, polyphosphoric acid and the mixtures of these catalysts (Khurana *et al.*,1990; Schwegler *et al*., 1991; Paumard, 1990).

Diphenylammonium triflate is an effective Brønsted acid catalyst for esterification of an equimolar acid : alcohol mixtures at 110 °C, without a need for specific dehydrating agents or removal of water by azeotropic distillation (Wakasugi *et al.*, 2000).

Sulfonic acid detergent such as dodecylbenzenesulfonic acid (DBSA) was used to catalyse the esterification of lauric acid with 3-phenyl-1-propanol. The equilibrium conversion of 84% was reached within 2 h using 10 mol% of DBSA at 40 °C. Tensioactive and acid properties of this catalyst can be combined. This detergent formed micelles in the aqueous solution, and the interior of these micelles was sufficiently apolar to drive the reaction of two hydrophobic reactants to the right (Manabe *et al.,* 2002).

Lewis acids may be preferred over Brønsted acids in order to avoid alcohol dehydration or racemization or, in order to create conditions that are compatible with acid labile groups. However, the distinction between Lewis and Brønsted acids is often

unsharp in a reaction producing water such as the direct esterification. For instance, Lewis acid compounds such as boron trifluoride form protonic acids in contact with water or an alcohol (Kadaba, 1974).

Several groups of Lewis acids, containing titanium, tin, hafnium or zirconium were applied with clear advantages over protonic acids. Titanium compounds include $TiCl_4$, $TiCl_2(ClO_4)_2$ and $TiCl(OTf)_3$, titanium alkoxides, and even peroxy titanium complexes have acceptable activity, but their selectivity for the esterification of primary versus secondary alcohols is poor, since they also have pronounced transesterification activity (Thil *et al.,* 2000; Disteldorf *et al*., 2002). In the group of tin catalysts, Me_2SnCl_2, Ph_2SnCl_2, n-BuSnO, and especially 1,3disubstituted tetraorganodistannoxanes have received attention (Otera *et al.,* 1991).

Distannoxanes were applied as catalysts in the esterification, albeit at high tin concentration at 80 °C. The reactions were susceptible to steric bulk, especially for the acid. Since the distannoxane core was surrounded by hydrophobic groups, water can hardly access the active sites, and this seems to impede the reverse hydrolytic reaction. Consequently, reactions can be driven almost to completion with just heating, without specific water removal (Otera *et al.*, 1991). In a further evolution, the distannoxane was modified with fluoroalkyl tails, resulting in $[\{Cl(C_6F_{13}C_2H_4)_2SnOSn(C_2H_4C_6F_{13})_2Cl\}_2]$. Esterification with this catalyst was performed at 150°C in a fluorocarbon solvent, resulting in rapid elimination of produced water. Often, yields are beyond 99%, but not with sterically hindered alcohols like borneol or menthol, or with benzoic and cinnamic acid (Xiang *et al.,* 2002).

High ester yields have also been obtained with hafnium (IV) chloride tetrahydrofuran complex (HfCl$_4$.2THF), zirconium(IV) chloride tetrahydrofuran complex (ZrCl$_4$.2THF), cyclopentadienyl hafnium (IV) dichloride (Cp$_2$HfCl$_2$) and with the alkoxides of zirconium and hafnium (Ishihara *et al*., 2000; Ishihara *et al*., 2001; Ishihara *et al*., 2002). Particularly, HfCl$_4$.2THF was effective for the alcohol : acid mixtures (molar ratio 1:1) at concentrations between 0.2 and 1 mol%. These compounds were rather moisture stable. Strong preference for esterification of primary versus secondary or aromatic alcohols was observed. Secondary alcohols like menthol, or

aromatic acids like benzoic acid were converted for over 95%. It was assumed that hafnium or zirconium carboxylates are the actual active catalysts.

Similar with the tris(methoxyphenyl)bismuthanes (Ogawa *et al.*, 1994), high concentrations of hydrated NiCl can be used to obtain moderate ester yields (Ram and Charles, 1997). Scandium (III) triflate (Sc(OTf)$_2$) is well known as a water-tolerant Lewis acid, and hence it was successfully used for the esterification of polyethylene glycols with aromatic carboxylic acids in Dean–Stark conditions (Chandrasekhar *et al.*, 2002). Cerium (IV) triflate (Ce(OTf)$_4$) has been used for menthol esterification, with retention of the configuration at the secondary alcohol group (Iranpoor and Shekarriz, 1999).

Homogeneous catalysts for the esterification of AA

Saha and Sharma (1996) reported that the acrylate esters could be produced through the reaction of acrylic acid with an excess of cyclohexene, 1-hexene, 1-octene, 1-decene, 1-dodecene, 2-octene at 333-383 K using 95% H$_2$SO$_4$ as catalyst. H$_2$SO$_4$ was employed as a catalyst by Fomin *et al.* (1991) and Sert (2013) for the esterification of acrylic acid and 2-ethylhexanol and hexanol respectively in the isothermal semi-batch reactor. Reaction conversion of more than 95% was observed. H$_2$SO$_4$ with different concentrations was also adopted as the catalyst for the esterification of acrylic acid with n-octanol and 2-ethyl hexanol (Nowak, 1999) in an isothermal semibatch reactor. Hydroquinone (0.2 wt%) was used as an effective polymerization inhibitor. The initial molar ratios of acrylic acid : n-octanol (or 2-ethyl hexanol) 1:2 – 1:10 were used while the temperatures were varied between 333-403 K. A 95% conversion was obtained at the temperature of 403 K, initial molar ratio of acid: alcohol of 1:5 of and 0.1%wt catalyst

Saha and Sharma (1996) stated in their paper that cyclohexyl acrylate could be prepared with good yield in a short time by reacting acrylic acid with cyclohexene in the presence of heteropoly acids supported on molybdenum oxides and tungsten oxides with conversion of 95% with 99% selectivity.

Even though homogeneous has shown the higher activity in the esterification reaction, it is found to be toxic and corrosive and hence increasing the maintenance cost. In addition, homogeneous catalyst was also difficult to be recovered from the process (Farnetti *et al*., 2004; Essayem *et al,* 2007). Heterogeneous acidic catalyst such as zeolite, alumina or resin could be the alternative to substitute the homogenous catalysts in order to overcome the drawbacks of homogeneous catalyst (Chen *et al.*, 1999; Saha and Sharma, 1996; Komon *et al.*, 2013).

2.4.2 Heterogeneous Catalyst

The use of heterogeneous catalyst could promote the advantages of reducing equipment corrosion and ease of product separation. The most attractive part is most of this solid catalyst are more facile regeneration of used catalyst (Essayem *et al,* 2007; Paul and Samuel, 1995).

Heterogeneous catalysts for the esterification of other carboxylic acid

The suitability of commercially available solid acid catalysts such as macroporous sulphonic acid resin (Indion 130 and Amberlyst 15), gelular or microreticular cation-exchange resin (Amberlite IR 120) and acid-treated montmorillonite clay (Engelhard F 24) was commonly studied (Qu *et al.,* 2009; JagadeeshBabu *et al.,* 2011; Gangadwala *et al.*, 2003; Yadav *et al.,* 2003; Osorio-Viana *et al.,* 2013; Merchant *et al.*, 2013; Saha and Streat, 1999).

Pappu *et al.* (2013) has studied the esterification of butyric acid with various types of alcohol with different length of carbon chain (methanol, ethanol, 1-propanol, 2-propanol, 2-butanol, 3-butanol, iso-butanol and 2-ethylhexanol). The reactions were catalysed by the commercial ion exchange resin catalysts (Amberlyst 15, Amberlyst 36, Amberlyst BD 20, and Amberlyst 70). It was found that the rate of reaction decreased with the increase of the length of alcohol carbon chain. Amberlyst 70 showed the best performance for the reaction of butyric acid with 2-ethylhexanol attributing to the higher activity per active site (H$^+$) and higher thermal stability. Teo and Saha (2004), Izci & Bodur (2007) and Akbay and Altiokka (2011) has studied the esterification of

acetic acid with isoamyl alcohol, isobutanol and n-amyl alcohol catalysed by ion exchange resin. Amberlyst 70 has given the maximum conversion in the range of 85 – 93% within 5 hours. The operating condition for the heterogeneously catalysed esterification reaction of carboxylic acid other than AA is included in Table 2.5.
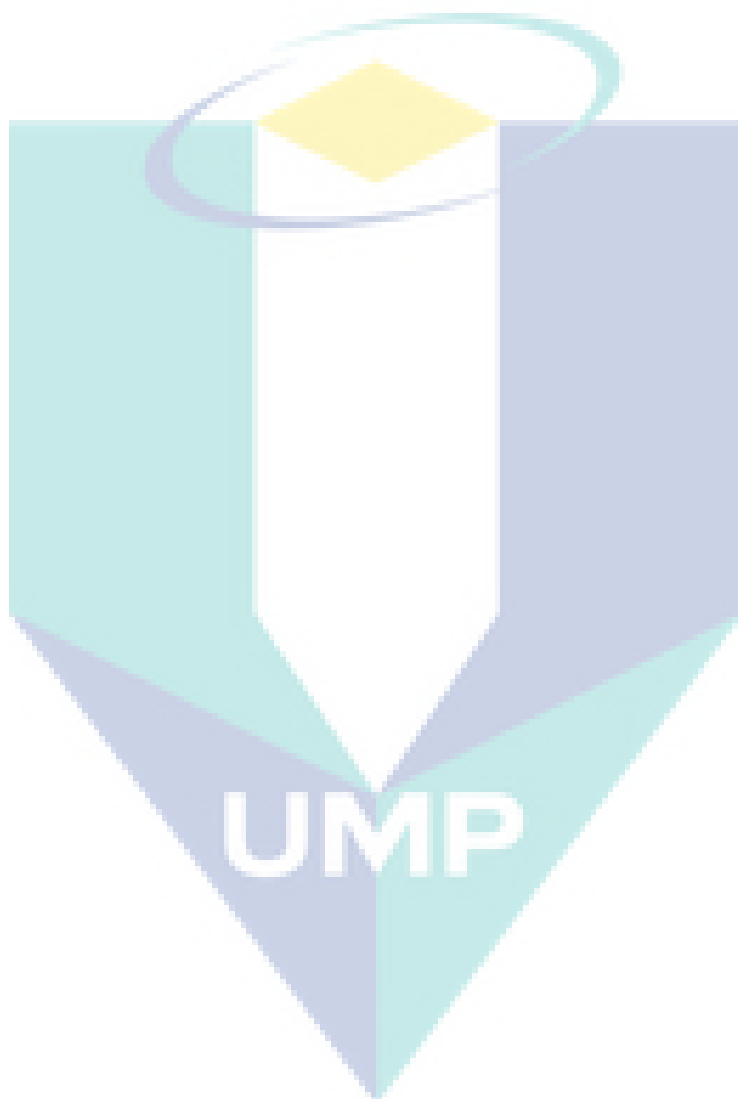
Table 2.5 : Operating condition of the heterogeneously catalysed esterification of carboxylic acids other than AA

References	Reaction time (h)	Temperature (K)	Molar Ratio (Acid to alcohol)	Catalyst loading	Remarks
Qu *et al.* (2009)	20-50	333-363	1:1-1:4	1.5-6 % w/v	• Reactant: Lactic acid and butanol • Catalyst: Weblyst D009
JagadeeshBabu *et al.* (2011)	3	333-353	1:1-1:4	0.01-0.05 g/cm^3	• Reactant: Acetic acid and methanol • Catalyst: Indion 130
Gangadwala *et al.* (2003)	5	373-393	1:12-1:100	0.01-0.04 g/cm^3	• Reactant: Phthalic anhydride and methanol • Catalyst: Amberlyst 36
Yadav and Rahuman (2003)	5	373-393	1:12-1:100	0.008-0.05 g/cm^3	• Reactant: Anthranilic acid and methanol • Catalyst: Amberlyst 36
Osorio-Viana *et al.* (2013)	8	322–362	3:1-1:3	20-60 g/L	• Reactant: Acetic acid with isoamyl alcohol • Catalyst: Amberlite IR 120
Merchant *et al.* (2013)	5	298-328	3:1-1:3	5% w/w	• Reactant: acetic, propanoic and pentanoic acids and ethanol • Catalyst: Amberlite IR 120

Table 2.5 : Continued

References	Reaction time (h)	Temperature (K)	Molar Ratio (Acid to alcohol)	Catalyst loading	Remarks
Saha and Streat (1999)	5	393-433	1:2-1:4	5-10% w/w	• Reactant: cyclohexyl acrylate n-butanol • Catalyst: Engelhard F-24
Teo & Saha (2004)	4-6	333-358	1:2-1:10	2.5-10% w/w	• Reactant : Acetic acid and isomyl alcohol • Catalyst : Purolite CT-175
Akbay & Altiokka (2011)	8	333-358	N/A	0.12-0.65 mol H^+/L	• Reactant: Acetic acid and n-amyl alcohol • Catalyst: Amberlyst-36
Izci & Bodur (2007)	12	318-348	0.5-1.5 G	N/A	• Reactant: Acetic acid and isobutanol • Catalyst: Dowex 50 Wx2 and Amberlite IR-120
Pappu et al. (2013)	3	373 – 423	1:4 – 1:6	0.01 kg cat/ kg soln	• Reactant: Butyric acid and 2-ethylhexanol • Catalyst: Amberlyst 70

Heterogeneous catalysts for the esterification of AA

The heteropoly compound $Cs_{2:5}H_{0:5}PW_{12}O(Cs_{2.5})$ is a strong acid heterogeneous catalyst, which is stable in water (Okuhara 2002). In the liquid-phase esterification of acrylic acid with 1-butanol, the following activity order was found (Hino and Arata, 1981):

$$Nb_2O_5 < J\text{-}ZSM\text{-}5 < Amberlyst\ 15 < Cs_{2.5}$$
$$\sim SO_4^{2-}/ZrO_2 \ll H\text{-}Nafion$$
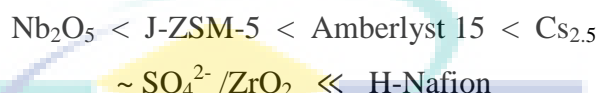
Chen *et al.* (1999) has compared the performance of $Cs_{2.5}H_{0.5}PW_{12}O_{40}$ with $H_3PW_{12}O_{40}$ solid oxides and organic resins for the reaction of acrylic acid with 1-butanol. Organic acid ($Cs_{2.5}H_{0.5}PW_{12}O_{40}$) was more preferable compared to solid oxides as the conversion was higher and Amberlyst 15 showed the second highest conversion after Nafion-H. The activity of $Cs_{2.5}H_{0.5}PW_{12}O_{40}$ was found to be retained after the addition of water, while the activities of the organic resins were greatly decreased. Thus, $Cs_{2.5}H_{0.5}PW_{12}O_{40}$ was claimed to be water-tolerable due to the hydrophobic nature of the surface.

The esterification of acrylic acid with butanol catalysed by heteropolyacids ($H_3P_{12}W_{40}$) supported on activated carbon under batch and flow conditions were studied by Dupont *et al.* (1995). The supported heteropoly acids displayed a better activity per proton than the conventional catalysts such as sulfuric acid or resins like Amberlyst 15. The deactivation of the catalyst in flow system was found to be low due to the dissolution of the supported heteropoly acids in the reaction medium. In contrast, under batch conditions both polyanion dissolution and deposition of polymeric species resulted in deactivation of the catalyst (even in the presence of a polymerization inhibitor).

The heteropoly acids, phosphorous tungstic acid showed higher activities than the conventional acids in the esterification of methacrylic acid with tripropylene glycol (Shanmugam *et al.,* 2004). The mangan and ferum promoted sulfated zirconia was used to catalyse the reaction of acrylic acid esterification by 1-butene to sec-butyl acrylate at

343 K. It was found that Mn and Fe did not improve the catalytic activity and selectivity to sec-butyl acrylate compared with Amberlite resins or sulfuric acid. Nevertheless, the promoted sulphated zirconia strongly resisted deactivation (Essayem *et al.,* 2007).

Amberlyst 15 was used by Altıokka and Odes (2009) in their study of the esterification of acrylic acid with propylene glycol in a batch reactor at different temperature and initial reactant molar ratios. It was found that the selectivity of hydroxypropyl acrylate was significantly low at high AA conversion. Therefore, this process was recommended to operate at low conversion with a proper recycle of unreacted stream for industrial usage.

Amberlyst 15 also was used by Ströhlein *et al.* (2006) for the esterification of acrylic acid with methanol as a stationary phase in a chromatographic reactor. This process can be regarded as a possible competition for current technologies due to the low-operating temperature. Simulated-moving-bed reactor (SMBR) was claimed as a viable option to overcome the drawbacks of the conventional processes for the production of methyl acrylate. 12 moles of methanol per mole of methyl acrylate were required in order to obtain 98% conversion of acrylic acid. The separation of the reaction products could be completed at a relatively low operating temperature of 333 K.

Komon *et al.* (2013) found that Amberlyst 70 was the best among the other resin catalyst like Amberlyst 39, Amberlyst 46, and Amberlyst 131 in the esterification of acrylic acid with 2-ethylhexanol. The maximum conversion was approximately 80%.

Sert *et al.* (2013) has compared three different ion exchange resins, Amberlyst 15, Amberlyst 131 and Dowex 50Wx-400 for the esterification of acrylic acid and n-butanol. Amberlyst 131 was found to be more efficient catalyst giving the maximum conversion of acrylic acid with the conversion of 89%. The catalyst performances follow the sequence of Amberlyst 15<Dowex 50Wx-400<Amberlyst 131. The effects of temperature (338, 348 and 358 K), catalyst loading (10, 15 and 20 g/L), molar ratio of alcohol to acid (1:1, 2:1 and 3:1), and stirrer speed (600, 800, 1000 and 1200rpm) on the reaction rate were investigated. Absence of internal and external diffusion resistances

was proven experimentally and theoretically by using Mears and Weisz Prater parameters.

Table 2.6 summarises the operating conditions of the heterogeneously catalysed esterification of AA with different alcohol.

Table 2.6 : Operating conditions of the heterogeneously catalysed esterification of AA with different alcohol.

Alcohol used	Reaction time (h)	Temperature (K)	Molar Ratio (Acid to alcohol)	Catalyst and the loading	References
Propylene glycol	8.33	333-358	1:1-4:1 1:1-1:3	Amberlyst-15; 3.11-8.46 wt%	Altiokka & Odes (2009)
2-ethyl hexanol	4	353-403	1:2-1:10	Sulphuric acid; 0.1-1.0 % wt	Nowak (1999)
n-octanol	5	333-403	1:2-1:10	Sulphuric acid; 0.1-1.5 % wt	Nowak (1999)
1-butanol	5	N/A	N/A	Various catalyst (Amberlyst, Nafion, $Cs_{2.5}H_{0.5}PW_{12}O_{40}$);0-2 g	Chen et al. (1999)
2-ethyl hexanol	6	333-373	7:1-1:7	Amberlyst 70; 5% wt	Komon et al. (2013)
Methanol	1	333	1:1	Amberlyst 15;	Ströhlein et al. (2006)
1-butanol	N/A	N/A	N/A	$Cs_{2.5}H_{0.5}PW_{12}O(Cs_{2.5})$	Okuhara (2002)
Butanol	4.5	353	1:1.35-1:3	$H_3P_{12}W_{40}$	Dupont et al. (1995)
Tripropylene glycol	N/A	N/A	N/A	phosphorous tungstic acid	Shanmugam et al. (2004)
1-butene	-	473	-	Amberlite resin	Essayem et al., 2007

2.4.3 Biocatalyst

Similar to other catalysts, biocatalysts increase the speed in which a reaction takes place but do not affect the thermodynamics of the reaction. However, it offers some unique characteristics over conventional catalysts as mentioned in Table 2.7. The most interesting part is the high selectivity. This is very important in chemical process synthesis as it may minimise the side reactions for easier separation.

Table 2.7: Advantages and disadvantages of biocatalyst in comparison with chemical catalyst

Advantages	Disadvantages
Generally more efficient (lower concentration of enzyme needed)	Susceptible to substrate or product inhibition
Can be modified to increase selectivity, stability, and activity	Solvent usually water (high boiling point and heat of vaporisation)
More selectivity	Enzymes fount in nature in only one enantiomeric form
Milder reaction condition (typically in a pH range of 5 – 8 and temperature range of 20 - 40°C)	Limiting operating region (enzymes typically denatured at high temperature and pH)
Environmental friendly (completely degrade in the environment)	Enzymes can cause allergic reactions

Source : Faber, 1997

Bio catalysts for the esterification of other carboxylic acids

Among all types of biocatalyst, lipase catalysts are the most common biocatalyst for esterification process. Enzyme-catalysed esterification has acquired increasing attention in many applications, due to the significance of the derived products. The enzymatic esterification is widely used in biofuel production.

As shown in Table 2.8, most of the studies focus on the esterification of fatty acids. Garcia *et al. (*2000), Kraai *et al.* (2008), Abdul Rahman *et al* (2012) and Yin *et*

al. (2013) studied the esterification of the fatty acid with cetyl alcohol, oleyl alcohol and 1-butanol catalysed by different types of lipase obtained from different sources of microbe. Garcia *et al* (2000) and Yin *et al* (2013) were using immobilized and silica supported lipase which attracted most research attention because of the ease of catalyst separation from the reaction mixture. Kraai *et al.* (2008) employed the homogeneous lipase. The conversion and selectivity were increased with the reduction in the energy requirement of the system. Abdul Rahman *et al.* (2012) have coated the lipase with ionic liquid in order to improve the lipase activity, selectivity and stability comparing to the uncoated lipase.
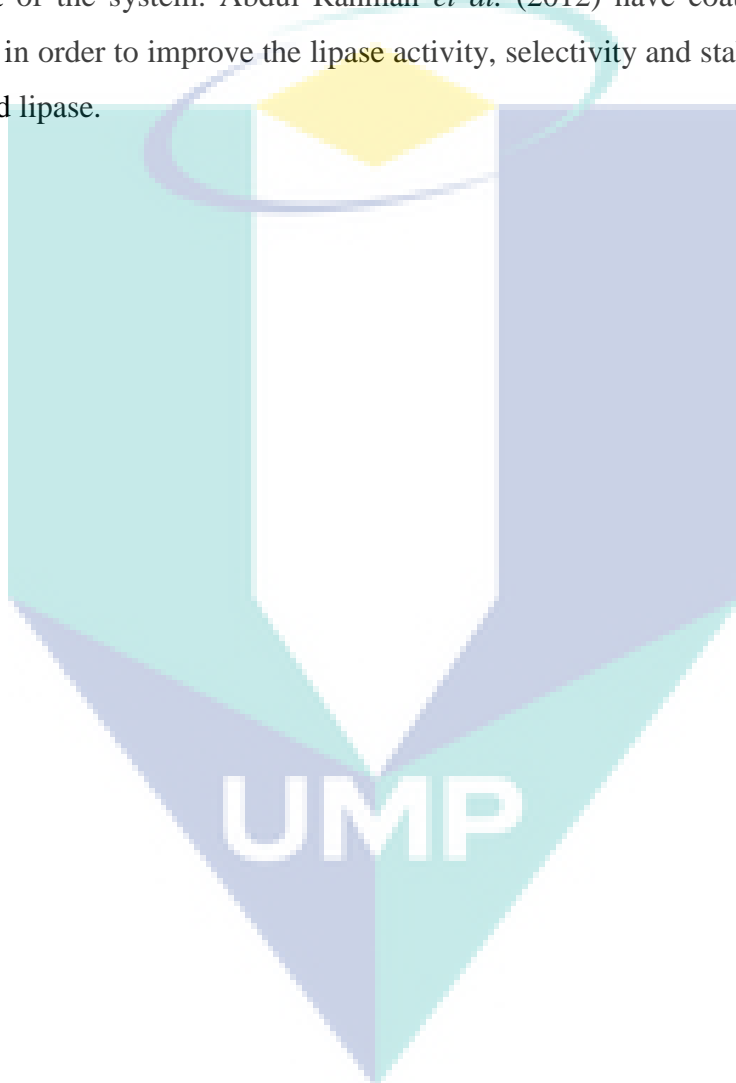
Table 2.8 : Operating condition of the biocatalyst catalysed esterification of carboxylic acids other than AA with alcohol.

Reactant	Reaction time (h)	Temperature (K)	Molar Ratio (Acid to alcohol)	Catalyst and the loading	References
cetyl alcohol with oleic acid	2	343-353	1:1-1:10	Novozym 435 (Candida Antarctica immobilized lipase); 3-7 % wt	Garcia *et al.* (2000)
Various fatty acid with oleyl alcohol	1	323	1:1	Tetraethylammonium amino acid ionic liquids-coated Candida rugosa lipase	Abdul Rahman *et al.* (2012)
oleic acid with 1-butanol	1	304	10:1-1:10	Rhizomucor miehei lipase; 0.01–0.2g/L	Kraai *et al.* (2008)
oleic acid with ethanol	N/A	293-303	1:1.1-1:1.3	lipase/organophosphonic acid-functionalized silica; 11-15%	Yin *et al.* (2013)

Biocatalysts for the esterification of AA

Biocatalyst/enzymatic catalyst consumed low energy and hence requiring low operating cost. However, the process required longer reaction time because of the poor thermal stability (about 323-328 K) of enzyme (Demirbas, 2008; Gerpen, 2005). Park *et al.* (2003) has performed the enzymatic esterification of β-methylglucoside with acrylic acid/methacrylic acid using Novozym 435 (lipase from *Candida antarctica*). The temperature was varied from 318-333K while the molar ratio was varied from 1:3-1:15. The maximum conversion achieved was 59.3% after 12 h.

Tsukamoto and Franco (2009) has esterified the AA with D-fructose using 0.7-2.1g of *Candida antarctica* lipase as catalyst. The reactions were carried out in the temperature ranged from 318-338 and molar ratio (acid to alcohol) ranged from 1:1-5:1.

2.5 REACTION KINETICS FOR THE HETEROGENEOUSLY CATALYSED ESTERIFICATION REACTION

The reaction kinetics is important for reactor design. Kinetics is required in analysing the reactive process and controlling the reaction variables. It is used to simulate the process and predict the industrial potential of the catalyst (Johannessen *et al.*, 2000; Sayyed *et al.*, 2009; Shi *et al.*, 2011; Tsai *et al.*, 2011). The reaction mechanism can be elucidated using different type of kinetic model. The model must be fitted with the experimental data which gives positive activation energy (Teo and Saha, 2004).

The pseudohomogeneous (PH) model is widely used in esterification systems (Komon *et al.*, 2013; Pappu *et al.*, 2013; Yu *et al.*, 2004). In the PH model, adsorption and desorption of all components are negligible. The PH model assumes complete swelling of the polymeric catalyst in contact with polar solvents, leading to an easy access of the reactants to the active sites. Eq. 2.1 shows the PH model.

$$-r_A = k_f \left(c_A c_{AL} - \frac{1}{K_{eq}} c_{ES} c_W \right)$$

(2.1)

Where r_A, k_f, K_{eq}, denote for reaction rate of acid, forward reaction constant, and equilibrium constant respectively and c_A, c_{AL}, c_{ES}, and c_w denote for concentration of acid, alcohol, ester and water respectively.

On the other hand, the Eley−Rideal (ER) model can be applied when reaction between one adsorbed reactant and one non-adsorbed reactant from the bulk liquid phase is assumed to occur. Depending on which of the two reactants is adsorbed, for a single site surface reaction rate-controlling step, the reaction between an adsorbed and a non-adsorbed reactant molecule on the catalyst surface can be represented by the ER model as shown in Eq. 2.2 and Eq. 2.3.

$$-r_A = \frac{k_f \left(c_A c_{AL} - \frac{1}{K_{eq}} c_{ES} c_W \right)}{(1 + K_A c_A + K_W c_W)} \tag{2.2}$$

$$-r_A = \frac{k_f \left(c_A c_{AL} - \frac{1}{K_{eq}} c_{ES} c_W \right)}{(1 + K_{ES} c_{ES} + K_{AL} c_{AL})} \tag{2.3}$$

Where K_A, K_{AL}, K_{ES}, and K_w represent adsorption constant for acid, alcohol, ester and water respectively.

The Langmuir−Hinshelwood−Hougen−Watson (LHHW) model takes into account the adsorption of all components. Assuming that the process is controlled by the reaction on the catalyst surface, the LHHW model assumes that the reaction takes place between two adsorbed molecules (Sert and Atalay,2012). Eq. 2.4 depicts the LHHW model.

$$-r_A = \frac{k_f \left(c_A c_{AL} - \frac{1}{K_{eq}} c_{ES} c_W \right)}{(1 + K_A c_A + K_{AL} c_{AL} + K_{ES} c_{ES} + K_W c_W)^2} \tag{2.4}$$

2.5.1   Reaction kinetics for the esterification of other carboxylic acids

Pseudo-homogeneous model was claimed to be well fitted with the kinetic experimental data of the esterification reaction catalysed by ion exchange resins. This conclusion was drawn by Yu *et al.* (2004) for the esterification of acetic acid with methanol catalysed by Amberlyst 15 and Pappu *et al.* (2013) for the esterification of butyric acid and hexanol catalysed by Amberlyst 70. Instead of using the concentration based PH model, Pappu *et al.*, (2013) has taken into account the non-ideality of the liquid phase by using the activity of the components. The activity coefficients were predicted using the UNIFAC group contribution method.

Kinetic studies for the esterification of lactic acid and acetic acid with methanol in batch reactor were carried out by Sanz *et al.* (2002) and Sert and Atalay (2012) respectively. The corresponding catalysts for these reactions were Amberlyst 15 and Amberlyst 131. Three kinetic models were compared and it was concluded that activity based LHHW model was well agreed with the experimental kinetic data.

Sert and Atalay (2012) and Yu *et al.* (2004) studied the kinetic of esterification of acetic acid with methanol and both employed ion exchange resin as their catalyst but using the different kinetic model that is LHHW activity based and PH concentration based. An identical activation energy was found. Adam *et al.* (2012) reacted acetic acid with ethanol and resulted a higher activation energy which employed the PH ideal kinetic modelling. This is in line with the study of Pappu *et al.* (2013).

The esterification of oleic acid with methanol and ethanol has been studied by Song *et al.* (2009) and Sarkar *et al.* (2010) respectively in a batch reactor system. Activation energy of approximately 40 kJ/mol was determined based on the pseudo homogeneous concentration base kinetic model. The other carboxylic acids such as myristic acid, lactic acid, and naphthenic acid which were studied by Rattanaphra *et al.* (2011), Sanz *et al.* (2002), and Wang *et al.* (2008) in the batch reactor exhibit the similar thermodynamic trend of exothermic also determined using pseudo homogeneous kinetic model.

2.5.2   Reaction Kinetics for The Esterification of AA

The kinetic modelling studies of the esterification of waste water containing acrylic acid with alcohol are scarce. To date, most of the kinetic studies for the esterification of AA with alcohol were using concentrated or pure acrylic acid.

Komon *et al.* (2013) has carried out the kinetic study for the esterification of AA with 2EHA. Activity based PH model was claimed to well describe the reaction. The non-ideality of the liquid phase was considered by the activity of the components where the activity coefficients were estimated using the UNIFAC method. The activation energy obtained was 50.1 kJ/mol.

Kinetic behaviour of the esterification of acrylic acid and n-butanol, leading to n-butyl acrylate and water catalysed by Amberlyst 131 was studied by Sert *et al.* (2013). The experiments were carried out in a batch reactor. The acrylic acid conversion increased with an increase in temperature, which confirmed that the reaction is intrinsically kinetically controlled. The experimental data were correlated by the LHHW model and the activation energy was found to be 57.4 kJ/mol.

LHHW model was also well fitted with the experimental reaction rate generated by Altıokka and Ödeş (2009) for the kinetic study of the esterification of acrylic acid with propylene glycol. The reaction catalysed by Amberlyst 15 was conducted in a batch reactor. The simultaneous dimerization/polymerization of acrylic acid and products, in addition to the reversible esterification reaction, was proposed as the reaction mechanism. Phenothiazine (0.3 wt%) was also used as an inhibitor to reduce the polymerization of acrylic acid and product. The activation energy was 80.37 kJ/mol. The kinetic studies reported in the preceding section were summarised in Table 2.9.

Table 2.9 : Kinetic studies for the esterification reaction of acrylic acid and other carboxylic acids with different type of alcohols.

Esterification	Thermodynamic type	Catalyst	Activation Energy	Reference
Lactic acid + methanol	Endothermic	Amberlyst 15	48.67 kJ/mol (PH activity base)	Sanz et al. (2002)
Acetic acid + methanol	Exothermic	Amberlyst 15	44.2 kJ/mol (PH concentration base)	Yu et al. (2004)
Naphthenic acid (diluted) + methanol	N/A	Tin oxide	104.2 kJ/mol (PH concentration base)	Wang et al. (2008)
Oleic acid + methanol	Endothermic	Zinc acetate	32.46 kJ/mol (PH concentration base)	Song et al. (2010)
4-methoxyphenyl acetic acid + dimethyl carbonate	N/A	mesoporous sulfated zirconia (MSZ)	75.3 kJ/mol (PH concentration base)	Devulapelli and Weng, (2009)
Oleic acid + ethanol	Endothermic	SnO_2/WO_3	39.5 kJ/mol (PH concentration base)	Sarkar et al. (2010)
Myristic acid + methanol	N/A	sulfated zirconia	22.51 kJ/mol (PH concentration base)	Rattanaphra et al. (2011)

Table 2.9 : Continued.

Esterification	Thermodynamic type	Catalyst	Activation Energy	Reference
Acetic acid + methanol	Endothermic	Amberlyst 131	37.8 kJ/mol (LHHW activity base)	Sert & Atalay (2012)
Butyric acid + hexanol	Exothermic	Amberlyst 70	41.7±2.3 kJ/mol (PH activity base)	Pappu *et al.* (2013)
Acrylic acid + n-butanol	Exothermic	Amberlyst 131	57.4 kJ/mol (LHHW activity base)	Sert *et al.* (2013)
Acetic acid + ethanol	N/A	L-(N-α-acetylphenylalanine)-ruthenium (III) complex (RHAPhe-Ru) immobilized on silica	343.92 kJ/mol (PH concentration base)	Adam *et al.* (2012)
Acrylic acid + 2-ethylhexanol	Endothermic	Amberlyst 70	(PH conc. based) 50.1±3.1kJ/mol (PH	Komon *et al.* (2013)

CHAPTER 3

RESEARCH METHODOLOGY

3.1   MATERIALS

The chemicals used in the experimental studies are listed in Table 3.1 with the purity, brand and function. All these chemicals were used without further purification.

Table 3.1: List of chemicals

Chemical/Reagent	Assay	Brand	Function
2-ethyl hexanol (2EH)	99.99%	Fluka	Reactant
Acrylic acid (AA)	99.9%	Sigma Aldrich	Reactant
n-Hexane	99.99%	Sigma Aldrich	Solvent for GC-FID analysis
2-ethyl hexyl acrylate (2EHA)	99.99%	Sigma Aldrich	Standard for GC-FID analysis
Nitrogen	99.99%	Air Product	Makeup gas for GC-FID analysis
Compressed air	99.99%	Air Product	To initiate flame in FID
Hydrogen	99.99%	Air Product	Innert gas for GC-FID analysis
Helium	99.99%	Air Product	Mobile phase and carrier for GC-FID analysis

The strong acidic ion-exchange resin, Amberlyst 15, was used as catalyst without further purification. The properties of Amberlyst 15 are shown in Table 3.2.

Table 3.2: Properties of Amberlyst 15

Characteristic	Form/Value
Physical form	Opaque beads
Concentration of acid sites	≥ 4.75 mequiv H^+/g
Surface area	53 m^2/g
Maximum operating temperature	120 °C
Macro porosity	35%
Polymer density	1410 kg/m^3
Bulk density	600 kg/m^3

Source : Rohm and Haas, 2006

3.2 APPARATUS AND EQUIPMENT

3.2.1 Catalyst Characterization

The morphology and structure of Amberlyst 15 before and after water tolerance experimental studies were identified using nitrogen physisorption measurement, Fourier Transform Infrared spectroscopy (FTIR), X-Ray Fluorescence (XRF), and Scanning Electron Microscope (SEM). The size distribution of Amberlyst 15 was analysed using particle size analyser.

3.2.2 Esterification Reaction Studies

The experiment was carried out in a stirred batch reactor. The setup comprised of 500ml three necked round bottom flask attached with rotamantle, condenser, magnetic stirrer, temperature probe and temperature controller. Figure 3.1 and Table 3.3 show the experimental set up and the function of each part in the set up.
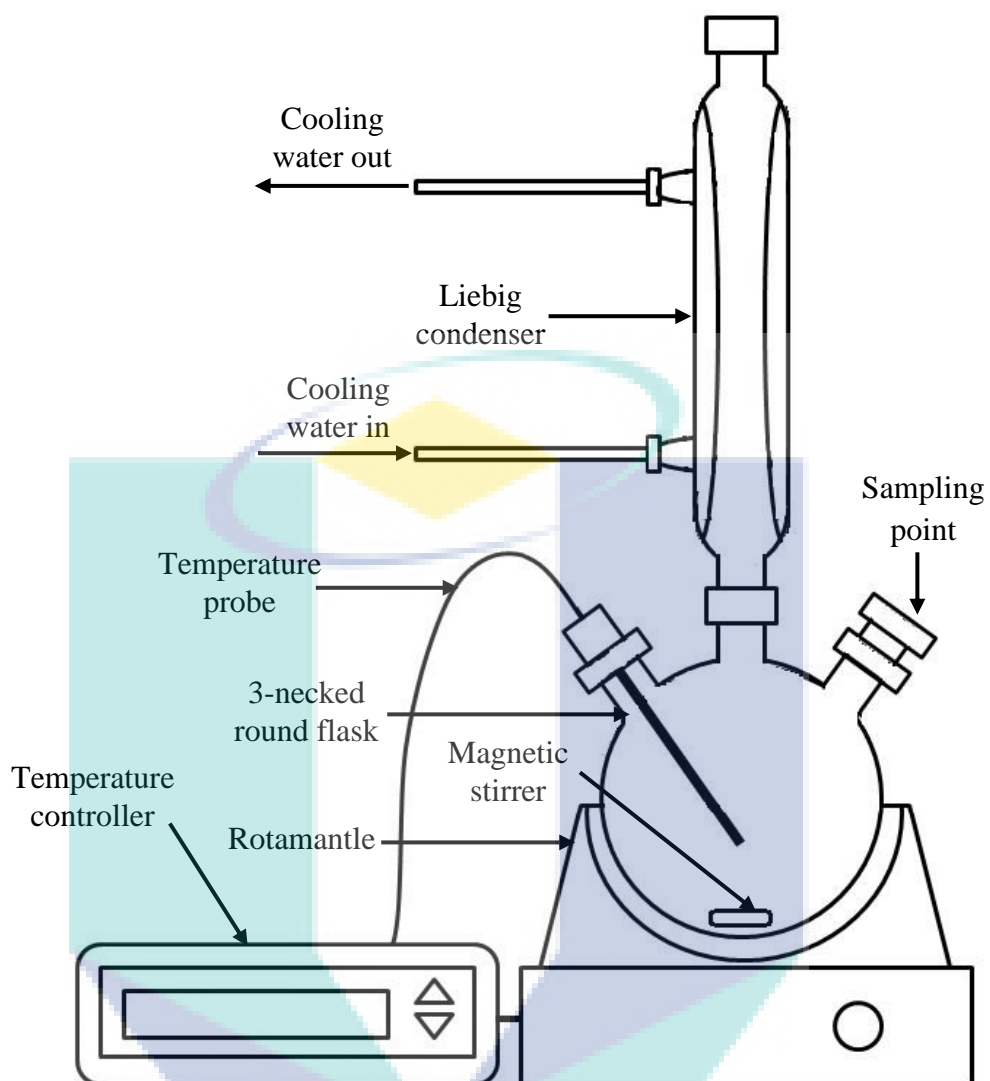
Figure 3.1: The experimental setup for the esterification reaction studies

Table 3.3 : List of main components in the experimental setup for the esterification reaction studies

Component	Description	Function
Rotamantle	Equipment which holds the 3-necked round flask. Equipped with heating and magnetic stirring system. The heating system was modified and connected to the temperature controller	To supply heat required during the esterification reaction and to provide the magnetic field to stir the reaction mixture.
3-necked round flask	A round bottom flask with capacity of 500 ml. There are three openings on the flask. The condenser was connected to the middle opening. The thermocouple was connected to the first opening. The third opening was used for charging the reactants and catalyst and sampling purposes. The reactor was equipped with digital temperature indicating controller (Cole Parmer).	As the batch reactor.
Liebeg Condenser	Glass condenser with the length of 50 cm (Fluka)	To condense the reaction mixture vapours during the esterification reaction.
Temperature probe	J-type thermocouple with the length of 10 cm.	To manipulate the process temperature during the reaction.
Temperature controller	The heat controller with function of proportional-integral-derivative controller (PID) and on/off system. Compatible with K-type, J-type, I-type, and type of thermocouple.	To control the process temperature during the reaction.
Magnetic stirrer	3 cm magnetic bar	To stir the reaction mixture continuously and thoroughly.

3.2.3   Sample Analysis

Agilent HP 1200 gas chromatography (GC) equipped with flame ionization detector (FID) was used to analyse the chemical compounds involve in the esterification reaction of 2EH and AA catalysed by Amberlyst 15. By using DB-200 column (Agilent) with diameter of 30 m, diameter of 0.32 mm and inner diameter of 0.25µm, the analysis was performed with n-Hexane as the solvent and helium gas as the carrier gas throughout the GCFID analysis.

3.3   EXPERIMENTAL PROCEDURES

3.3.1   Catalyst Characterisation

The fresh and the used catalyst was characterised using particle size analyser, physisorption analyser, scanning electron microscope, X-Ray Flourencence (XRF) and Fourier Transform Infrared Spectroscopy (FTIR) to check the possibility of catalyst poisoning. The used catalyst was retrieved from the reaction media by filtering using the filter paper and dried in oven at 373 K.

Particle Size Analyzer

Malvern Mastersizer 2000 particle size analyser was used to determine the size distribution of Amberlyst 15. The sample of Amberlyst 15 was dispersed though the measurement area of the optical bench where the system of analyser accurately measured the scattered size range of particles. The Mastersizer 2000 software was used to process and analyses the scattering data to calculate a particle size distribution.

Nitrogen Physisorption Measurement

Bruneauer-Emmet-Teller (BET) surface areas, pore volumes and pore size distribution of catalysts were quantified from the nitrogen adsorption isotherms measured using Thermo Surfer equipment at 77 K. The samples were degassed in a vacuum at 373 K for 12 h prior to the adsorption experiments. Adsorption isotherms

were generated by dosing nitrogen (>99.99% purity) onto the catalyst contained in a sample tube dipped in a bath of liquid nitrogen. The surface area was calculated using the BET method (Micropore version 2.46). The pore volume and pore size distribution was calculated using Barrett-Joyner-Halenda (BJH) method.

Scanning Electron Microscope (SEM)

The morphology of the catalysts was determined by scanning electron microscope (Model Leo Supra 50VP equipped with an Oxford INCA 400 Energy Dispersive X-ray Microanalysis (EDS) system). Prior to SEM measurements, the samples were mounted on a gold platform using polyvinyl chloride (PVC) glue and were coated with a layer of gold. The plate containing sample was placed in the electron microscope for the analysis with magnifications of 15x, 500x, 2000x, and 8000x.

X-Ray Fluorescence (XRF)

XRF analysis was used to determine the elemental composition (mainly oxide group) of the Amberlyst 15. About 10 g of dried Amberlyst 15 was used for the XRF analysis. XRF measurements were made directly on resin beads with Spectro X-lab 2000.

Fourier Transmitter Infrared (FTIR)

FTIR spectra were recorded by Perkin Elmer Series II IR spectrometer at room temperature using potassium bromide (KBr) pellet technique. The sample was ground with the spectra grade KBr to form a pellet under hydraulic pressure. The pellet was used to record the IR spectrum in the range of 400-4000 cm^{-1} under the atmospheric conditions with a resolution of 1 cm^{-1}.

3.3.2 Esterification Reaction Studies

The batch reactor was charged with 350 ml total volume of AA and 2EH. The temperature in the reactor was maintained within ±1 K. The first sample was withdrawn once the desired temperature reached. Subsequently, the required amount of catalyst was added to the mixture through the sampling port. Then the reaction was considered start. Amberlyst 15 particles were suspended in the reaction mixture through continuous stirring. The reaction was performed under total reflux conditions. Samples with individual volume of 0.5 ml were withdrawn at regular intervals and analysed using gas chromatography for the composition of 2EHA, AA and 2EH.

3.3.3 Effect of Mass Transfer

To study the reaction kinetics without mass transfer effects, it is necessary to eliminate both external and internal diffusion limitations which were reported to cause discrepancy between the experimental behaviour and model simulation results.

Preliminary experiments were conducted by varying the stirring speed, from 0 – 600 rpm, to quantify the influence of external resistances to heat and mass transfer.

The effect of internal diffusion on the catalytic reaction was studied by carrying out the experiment using catalysts with different particle sizes. Amberlyst 15 was screened into 2 different groups with the particle sizes ranged from 0.50 to 0.65 mm and 0.65 to 0.80 mm respectively.

The preliminary reaction study was performed in the absence of the resin catalyst with the aim of evaluating the contribution of the un-catalysed reaction on the overall kinetics.

3.3.4   Effect of Important Operating Variables

The yield and conversion of reaction were measured at different operating variables. The investigated variable included the temperature, catalyst loading, and initial molar ratio of acid to alcohol as shown in Table 3.4. The range of each variable was decided based on the literature review and also the limits of condition. For examples, the amberlyst 15 will deactivated beyond 393 K, which limit the maximum range to be 388 K.

Table 3.4: Important operating variable study and the range

Variable	Range
Temperature	338 – 388 K
Catalyst loading	1 – 15 % w/w acid
Initial molar ratio (in excess AA)	1:1 – 1:7
Initial molar ratio (in excess 2EH)	1:1 – 1:7

3.3.5   Reaction Water Tolerance Study

The tolerance of reaction to the presence of substantial amount of water was investigated by varying the dilution of AA from 100% AA to 10% AA in total volume of 150 ml reactant consist of AA, 2EH, and water. Two different experimental setups were used in this study. There are total reflux setup (as shown in Figure 3.1) and dean stark setup. The conversion and yield profile were generated based on the sample analysis by GC-FID.

A setup with continuous water removal using dean stark set up as shown in Figure 3.3.
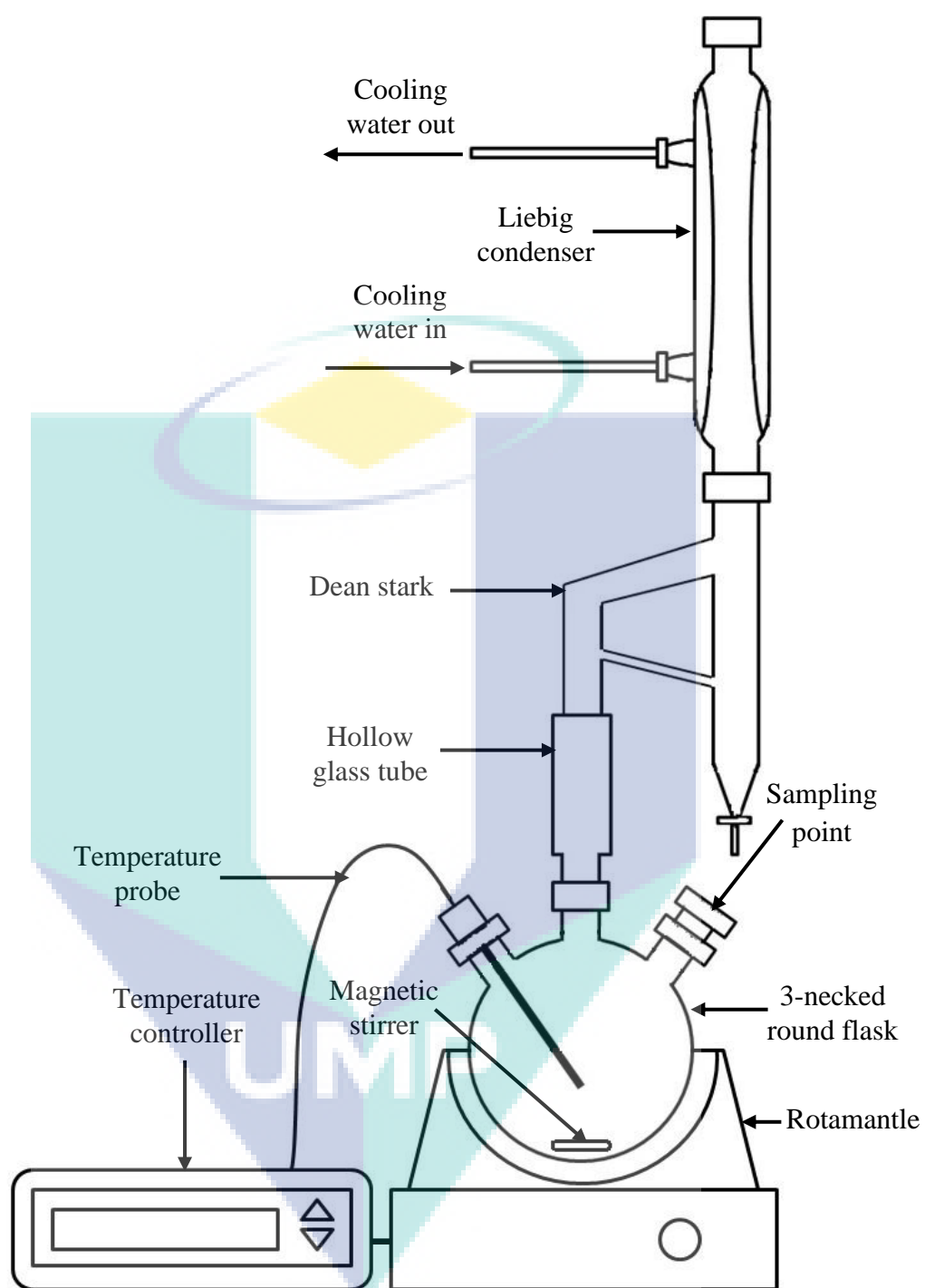
Figure 3.2 : The experimental setup with dean stark

3.4 ANALYSIS

The composition of 2EHA and AA in the collected samples were analysed using GC-FID with the injector and detector block temperatures at 503 K (with 1:10 split ratio) and 523 K respectively. The oven temperature was maintained at 308 K for 5 minutes then it was increased to 473°C at 10 K/min for 17 minutes. The carrier gas, helium flowed at a flow rate of 36.8 cm^3/s (Agilent, 2011). Figure 3.4 show one of the chromatograms for acrylates compound analysis.
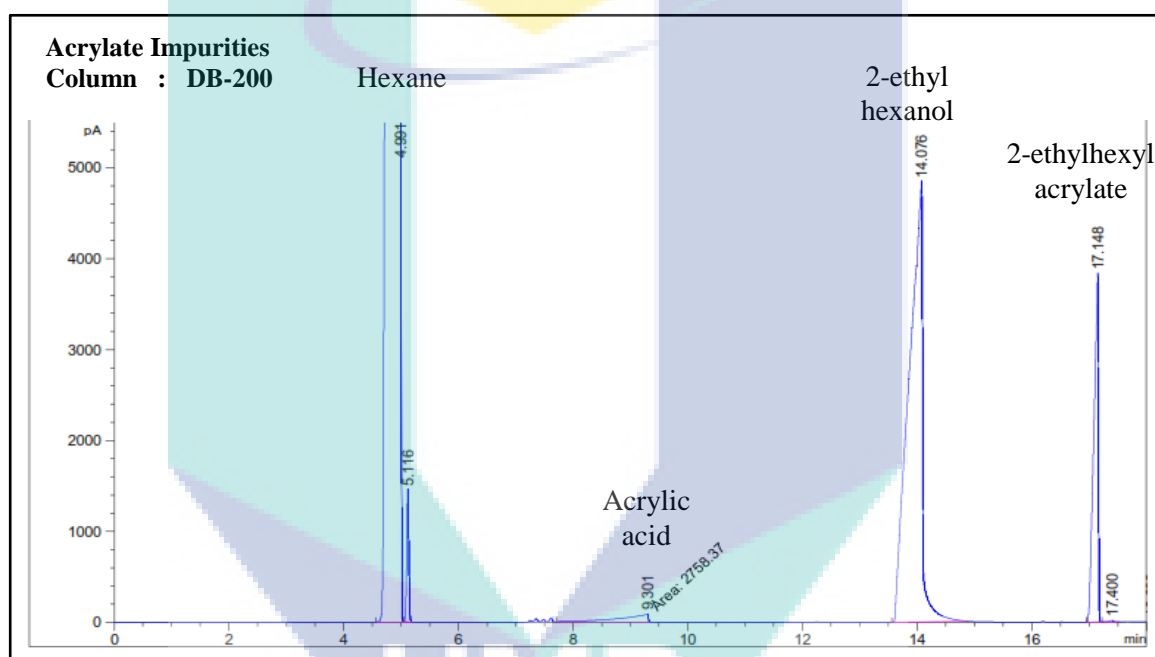
Figure 3.3 : Chromatogram obtained from the GC-FID analysis

The standard calibration curves of 2EHA, AA and 2EH from the GC-FID analysis are required to obtain the concentration of specific components in the sample. The analytical standard or HPLC standard of each component was used to generate the calibration curve.

The concentrations for the working standard samples of 2EHA were ranged from 2,000 ppm to 16,000 ppm with 2000 ppm interval for each point. While the respective concentrations for the working standard samples of AA were ranged from 6,300 ppm to 63,000 ppm with 400 ppm interval for each point. The absorbence-

concentration data for standard calibration curve for AA and 2EHA was represent respectively in Appendix A and B.

This analysis assumes that the equipment performed consistently and persistently during the experiments at any time as there is no calibration procedure during the analysis to measure the fluctuation from the equipment.

The following equation has been used to calculate yield and conversion of reaction:

$$yield\ (\%) \ = \ \frac{C_{2EHA}}{C_{AA0}} \ \times \ 100\% \tag{3.1}$$

$$conversion\ (\%) \ = \ \frac{C_{AA0} - C_{AA}}{C_{AA0}} \ \times \ 100\% \tag{3.2}$$

Where C_{2EHA} is the concentration of 2EHA produce, C_{AA} is the concentration of AA, and C_{AA0} is the initial concentration

3.5 KINETIC MODELLING

The conversion and yield profile generated from the study of the effect of temperature was used to develop the kinetic model of the esterification of AA with 2EH. The pseudo-homogeneous (PH), Eley-Rideal (ER) and Langmuir-Hinshelwood-Hougen-Watson (LHHW) kinetic models were used to fit the kinetic data. Both concentration based and activity based model are shown in Eq. 3.1 – 3.7 were used to fit the kinetic data.

Pseudo-homogeneous (PH) concentration based:

$$r_{AA} \ = \ -k_f \left(c_{AA} c_{2EH} - \frac{1}{K_{eq}} c_{2EHA} c_W \right) \tag{3.3}$$

Pseudo-homogeneous (PH) activity based:

$$\frac{r_{AA}V}{N_T} = -k_f \left(\alpha_{AA}\alpha_{2EH} - \frac{1}{K_{eq}} \alpha_{2EHA}\alpha_W \right) \tag{3.4}$$

Eley-Rideal (ER) concentration based:

$$r_{AA} = \frac{-k_f \left(c_{AA}c_{2EH} - \frac{1}{K_{eq}} c_{2EHA}c_W \right)}{(1 + K_{AA}c_{AA} + K_{2EH}c_{2EH} + K_{2EHA}c_{2EHA} + K_W c_W)} \tag{3.5}$$

Eley-Rideal (ER) activity based:

$$\frac{r_{AA}V}{N_T} = \frac{-k_1 \left(\alpha_{AA}\alpha_{2EH} - \frac{1}{K_{eq}} \alpha_{2EHA}\alpha_W \right)}{(1 + K_{AA}\alpha_{AA} + K_{2EH}\alpha_{2EH} + K_{2EHA}\alpha_{2EHA} + K_W \alpha_W)} \tag{3.6}$$

Langmuir-Hinshelwood-Hougen-Watson (LHHW) concentration based:

$$r_{AA} = \frac{-k_1 \left(c_{AA}c_{2EH} - \frac{1}{K_{eq}} c_{2EHA}c_W \right)}{(1 + K_{AA}c_{AA} + K_{2EH}c_{2EH} + K_{2EHA}c_{2EHA} + K_W c_W)^2} \tag{3.7}$$

Langmuir-Hinshelwood-Hougen-Watson (LHHW) activity based:

$$r_{AA} = \frac{-k_1 \left(\alpha_{AA}\alpha_{2EH} - \frac{1}{K_{eq}} \alpha_{2EHA}\alpha_W \right)}{(1 + K_{AA}\alpha_{AA} + K_{2EH}\alpha_{2EH} + K_{2EHA}\alpha_{2EHA} + K_W \alpha_W)^2} \tag{3.8}$$

Where K_{eq} and α_i were calculated as follow:

$$K_{eq} = \frac{k_f}{k_r} \tag{3.9}$$

The theoretical developments in the molecular thermodynamics of liquid-solution behaviour are often based on the concept of local composition, presumed to

account for the short-range order and non-random molecular orientations that result from differences in molecular size and intermolecular forces. Alternatively correlative methods, UNIFAC (UNIQUAC Functional-group Activity Coefficient) was employed to provide fitted component-specific and model variables as shown in Eq. 3.14:

$$\alpha_i = \gamma_i x_i \qquad (3.10)$$

Where γ_i is the liquid activity coefficient for component i and x_i is the concentration of each compounds. The UNIFAC model splits up the activity coefficient for each species in the system into two components; a combinatorial, γ_i^c and a residual component, γ_i^r as shown in Eq. 3.15:

$$\ln \gamma_i = \ln \gamma_i^c + \ln \gamma_i^r \qquad (3.11)$$

The UNIFAC program written in Microsoft Excel was included in Appendix C. Figure 3.6 summarises the procedures involved in the present study.
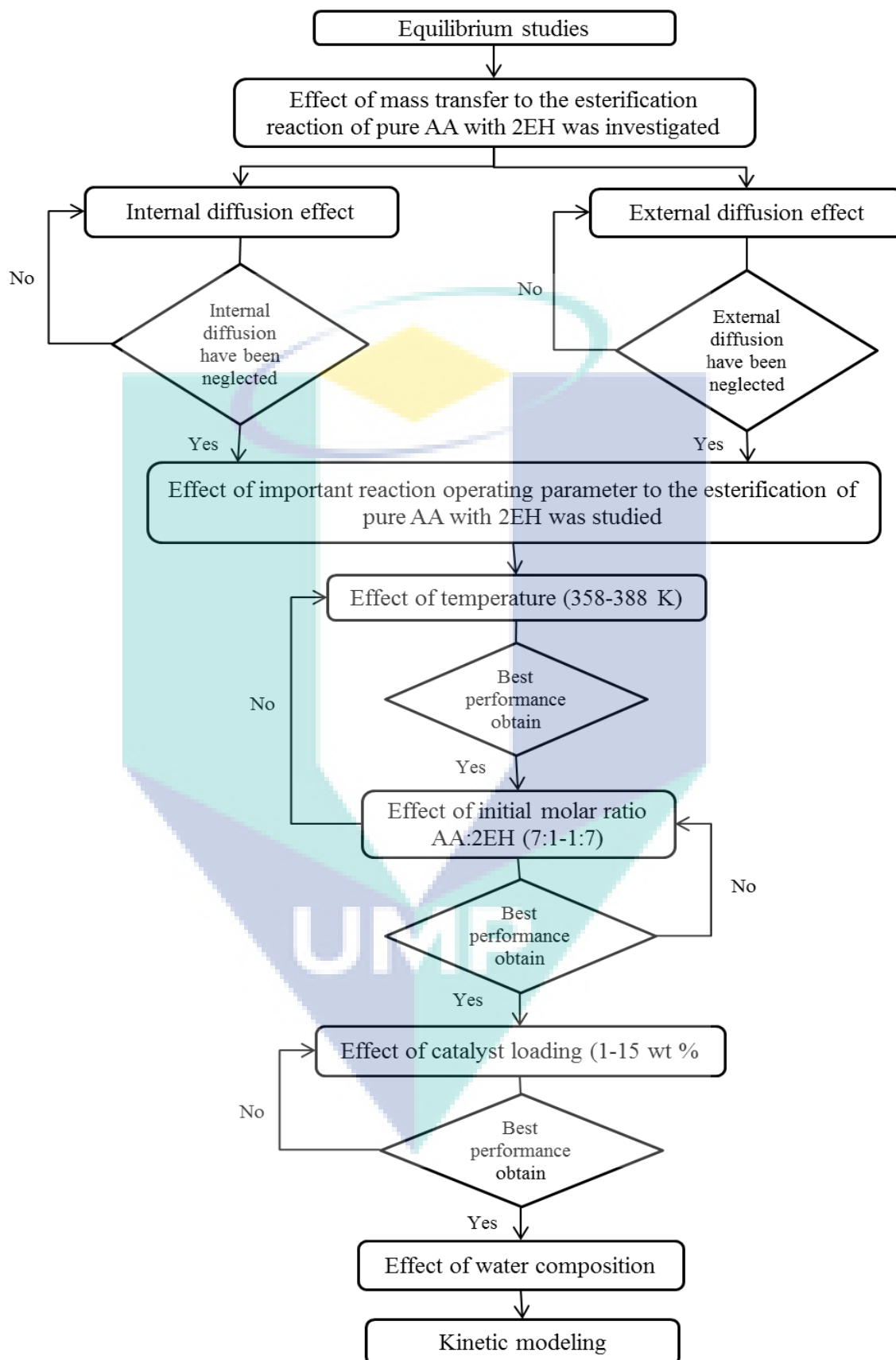
Figure 3.4 : The procedure involved throughout the research studies

CHAPTER 4

RESULTS & DISCUSSION

4.1   FRESH CATALYST CHARACTERISATION

Before the catalyst, Amberlyst 15 was used in the esterification reaction study, it was characterised using particle size analyser for the particle size distribution, physisorption analyser for the surface area and volume, scanning electron microscope of the morphology, X-Ray Flourencence (XRF) for the elemental oxide composition and Fourier transform infrared spectroscopy for the functional groups.

4.1.1   Particle Size Analyser

The particle size distribution of the fresh Amberlyst 15 was measured using Malvern Mastersizer 2000 and shown in Table 4.1. Most of the catalysts are with the particles size in between 0.42-0.72 mm and the calculated mean diameter of the resin beads was 0.65 mm. This is comparable with the results reported by Yu *et al.* (2004) and Sharma (1995). For the investigation of possible mass-transfer resistance effects, a sample of the catalyst was sieved and categorized to $d_p < 0.68$mm, 0.68mm $< d_p < 0.80$mm and $d_p > 0.80$mm.

Table 4.1 : Particle size distribution of Amberlyst 15.

Diameter (d_p) range (mm)	Mass Fraction
>1.10	0.003
0.95 - 1.10	0.027
0.83 - 0.95	0.094
0.72 - 0.83	0.167
0.63 - 0.72	0.234
0.55 - 0.63	0.223
0.42 - 0.55	0.226
<0.40	0.026

4.1.2 Nitrogen Physisorption Measurement

Nitrogen physisorption measurement was carried out to determine the surface area, pore volume, and average pore diameter of the fresh Amberlyst 15. The surface area was calculated using Brunauer, Emmett and Teller (BET) method while the pore volume and average pore diameter were quantified using Barrett-Joyner-Halenda (BJH) method.

The nitrogen adsorption-desorption isotherm in Figure 4.1 is a typical irreversible-type IV adsorption isotherm with H1 hysteresis loop as defined by IUPAC. The initial part of the Type IV isotherm is attributed to monolayer-multilayer adsorption. The hysteresis loop is a typical feature of mesoporous materials with the average pore diameter in between 20 – 500 Å. It is associated with capillary condensation taking place in mesopores, and the limiting uptake over a range of high $P/P°$. Type H1 is often associated with porous materials known to consist of agglomerates or compacts of approximately uniform spheres in a regular array, and hence to have narrow distributions of pore size (Sing, 1982). The average diameters of primary mesopores as shown in Table 4.2 were obtained from the maximum of a pore size distribution calculated using the BJH method applied to the desorption part of the isotherm. The results obtained from the nitrogen physisorption measurement are comparable with the technical data provided by Rohm and Hass (2007).
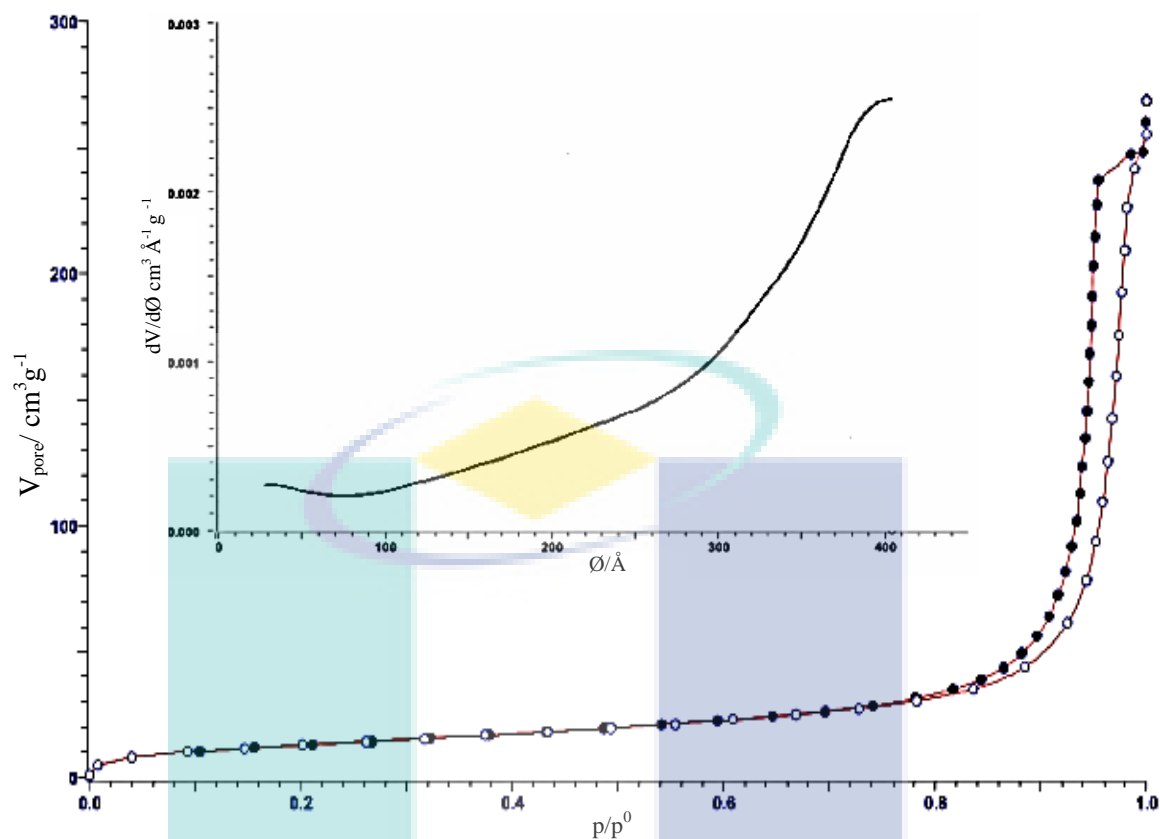
Figure 4.1: Nitrogen adsorption/desorption isotherm at -195 °C for the fresh Amberlyst
15. Inset shows the pore size distribution

Table 4.2 : Comparison of the nitrogen physisorption results of the fresh Amberlyst
with the data obtained from the Rohm & Haas technical sheet

Properties	Present study	Rohm and Hass technical sheet
BET surface area (m²/g)	56	53
Pore volume (cm³/g)	0.32	0.40
Average pore diameter (Å)	326	300

4.1.3   Scanning Electron Microscope (SEM)

The SEM micrographs of the fresh Amberlyst 15 outer surface under the magnifications of 15 and 2000 are shown in Figure 4.2 (a) and (b) while the SEM micrograph of the Amberlyst 15 inner surface under the magnification of 8000 is shown in Figure 4.2 (c). It can be clearly seen that Amberlyst 15 comprises of the sphere particles with the particle size in the range as reported in section 4.1.1. The surface of the fresh catalyst is smooth like other gel resins. Some minute pores and cracks are observed on the outer surface of the catalyst while the cabbage like porous structure is observed in the inner surface. The thin line cracks are responsible for the pore volume of the catalyst. The pores of the catalyst attribute to the increase of catalyst surface area and it allows the penetration of the reactants to ensure the chemical reaction.
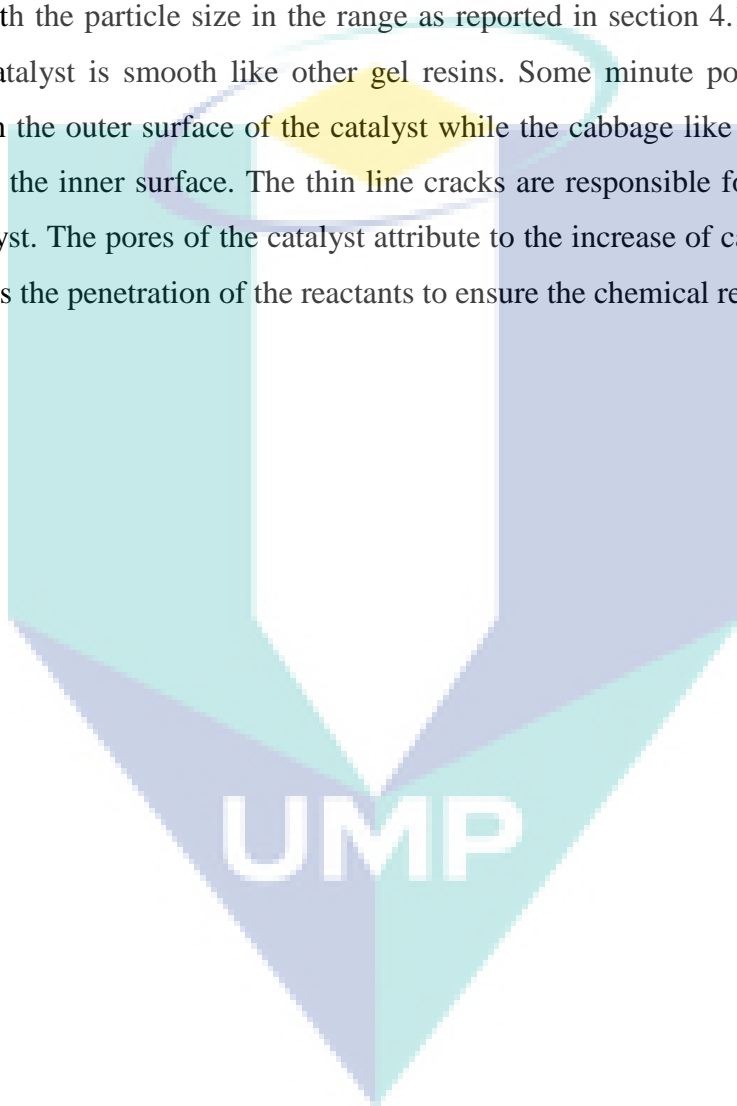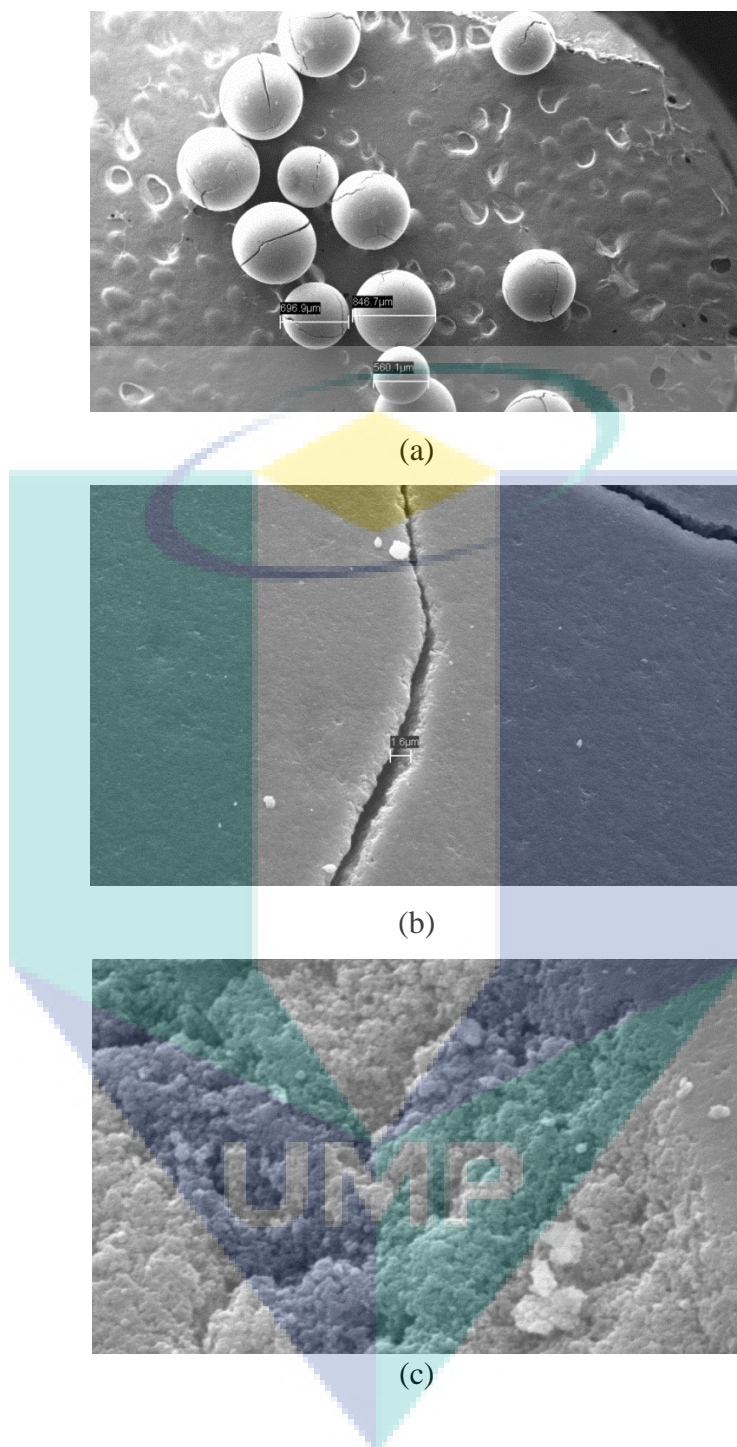
Figure 4.2 : Micrographs of fresh Amberlyst 15 outer surface under magnification , a) 15x, b) 2000x, and inner surface under magnification c) 8000x.

4.1.4   X-Ray Fluorescence (XRF) analysis

Table 4.3 shows that sulphonic group (from the analysis is sulphur trioxide) is the main oxide component of this catalyst. This sulphonic group is the active group to catalyse the esterification reaction.

Table 4.3 : Results of the elemental analysis using XRF analyser

Element	Result	Unit
Sulphur Trioxide (SO_3)	47.07	%
Phosphorus Pentoxide (P_2O_5)	0.18	%
Calcium Oxide (CaO)	0.07	%
Molybdenum Trioxide ($MoO_{3)}$)	0.03	%

4.1.5   Fourier Transform Infrared Spectroscopy (FTIR) analysis

Figure 4.3 illustrates the spectra of FTIR analysis for the fresh Amberlyst 15. The peaks observed at 580 cm^{-1}, 1600 cm^{-1}, and 2920 cm^{-1} are the aromatic ring stretching of the polystyrene supports of Amberlyst 15. The peak at wavenumber of 1030 cm^{-1} represents the sulfur-oxygen double bonds of the catalyst while peaks at wavenumbers of 1600 cm^{-1} and 1645 cm^{-1} associate with the Lewis and Bronsted acid sites respectively (Salem, 2001).
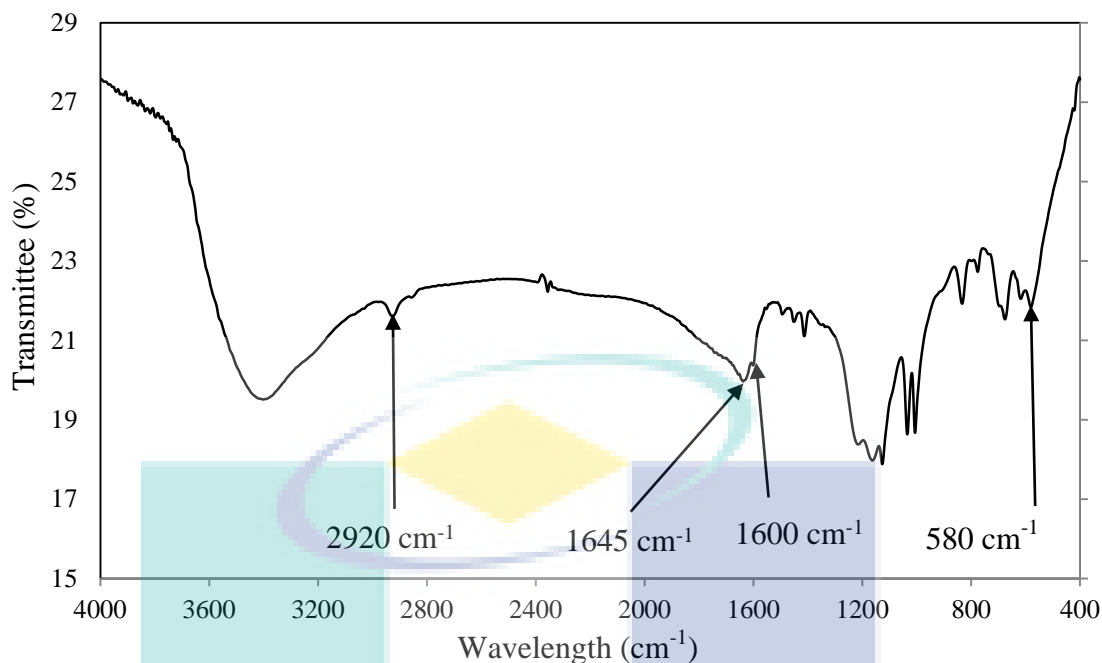
Figure 4.3 : FTIR spectra of the fresh Amberlyst 15.

4.2 CHEMICAL EQUILIBRIUM STUDY FOR THE ESTERIFICATION OF PURE AA WITH 2EH

The esterification reaction of AA with 2EH occurs based on the following chemical equation:

$$
\begin{array}{ccccccc}
CH_2CH & + & CH_3(CH_2)_3CH & \rightleftharpoons & CH_2CHCOOCH_3(CH_2)_3 & + & H_2O \\
COOH & & (C_2H_5)CH_2OH & & CH\ (C_2H_5)CH_2 & & \\
AA & & 2EH & & 2EHA & & W
\end{array}
\tag{4.1}
$$
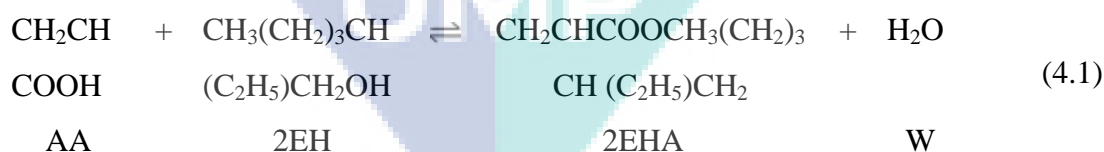
This reaction is a typical acid catalysed, equilibrium limited esterification. The thermodynamic equilibrium constant of reaction, K_a is shown in Eq. 4.2.

$$
K_a = \exp\left(-\frac{\Delta G^0}{RT}\right) = \prod a_i^{v_i} = \prod_i (x_i \gamma_i)^{v_i}
\tag{4.2}
$$

where x_i is the mole fraction of component i at equilibrium and a_i is the activity coefficient of component i calculated by the UNIFAC model.

The equilibrium constant was calculated experimentally according to the following formula:

$$K_a = \frac{x_{2EHA}x_W}{x_{AA}x_{2EH}} \frac{\gamma_{2EHA}\gamma_W}{\gamma_{AA}\gamma_{2EH}} \tag{4.3}$$

The apparent equilibrium constant of the reaction, K_x, expressed in terms of mole fractions can be written as Eq. 4.4:

$$K_x = \sum x_i^{v_i} = \frac{x_{2EHA}x_W}{x_{AA}x_{2EH}} = \frac{x_{2EHA}^2}{(x_{AA}^0 - x_{2EHA})(x_{2EH}^0 - x_{2EHA})} \tag{4.4}$$

The experimental runs were undertaken at the temperatures of 338, 368, 378 and 388 K, molar ratio of acid to alcohol of 1:1, and catalyst loading of 10 % (wt catalyst/ wt acid) to determine the equilibrium mole fractions of AA, 2EH, 2EHA and W.

The calculated activity coefficients for the corresponding experimental mole fractions of all the components at equilibrium state in the temperature range of 338–388 K are shown in Table 4.4.

Table 4.4 : Mole fractions and the evaluated activity coefficients of components at the equilibrium state of the reaction at various temperatures.

T (K)	AA		2EH		2EHA		W	
	Mole fraction	Activity coefficient	Mole fraction	Activity coefficient	Mole fraction	Activity coefficient	Mole fraction	Activity coefficient
338	0.180	0.138	0.180	0.209	0.320	0.528	0.320	1.211
368	0.127	0.094	0.127	0.152	0.373	0.597	0.373	1.454
378	0.108	0.079	0.108	0.131	0.392	0.620	0.392	1.546
388	0.102	0.073	0.102	0.123	0.398	0.628	0.398	1.578

The thermodynamic and the apparent equilibrium constants calculated based on Eq. 4.3 and 4.4 are tabulated in Table 4.5 and plotted against temperature in Figure 4.4. The variation of K_x and K_a with temperature in Figure 4.4 indicates that the latter is more sensitive to the temperature changes.

Table 4.5 : The apparent and activity based equilibrium constants (K_x and K_a respectively), the corresponding enthalpy of reaction and the equilibrium conversion of AA (X_e).

T (K)	K_x	ΔH_r^0 (kJ mol^{-1})	K_a	ΔH_r^0 (kJ mol^{-1})	X_e
338	3.185	22.699	22.187	23.874	0.641
368	8.574	33.264	60.429	33.559	0.745
378	13.091	36.986	92.693	36.970	0.783
388	15.336	40.807	108.767	40.472	0.797

The temperature dependence of the K_x and K_a can be described by Eq. 4.5:

$$K = \exp(b_1 + \frac{b_2}{T} + b_3 T) \tag{4.5}$$
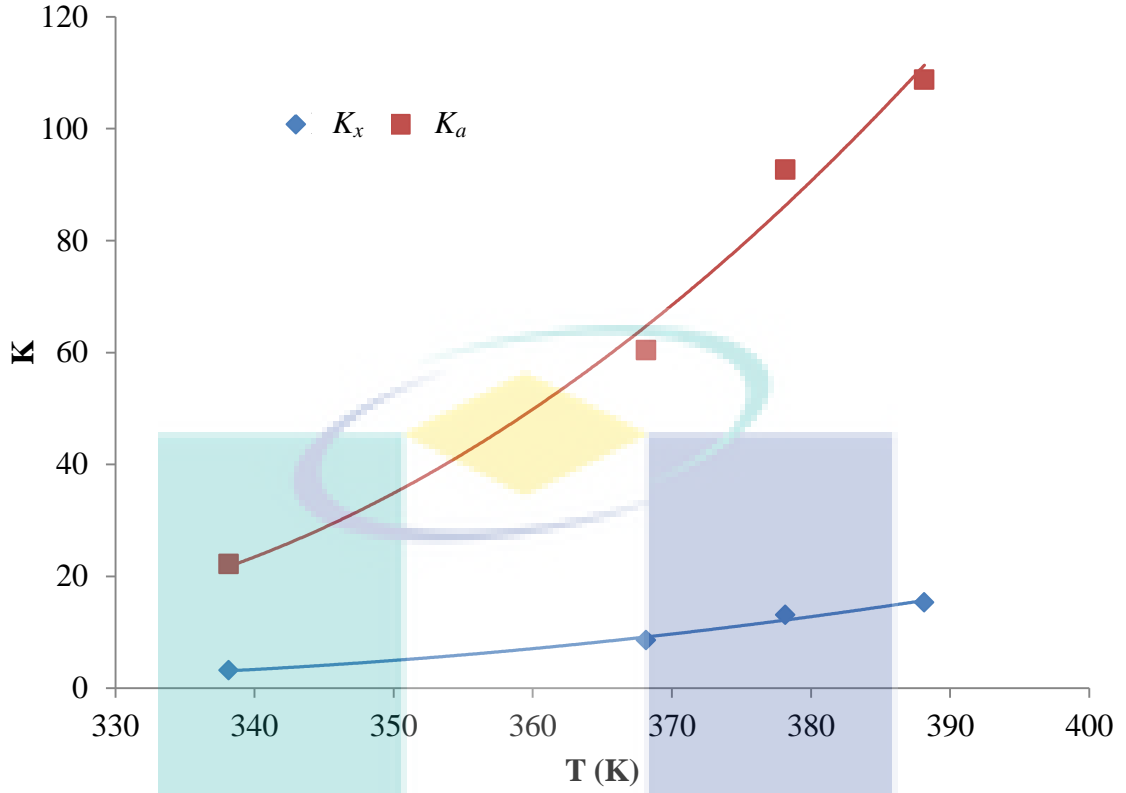
Figure 4.4 : The temperature dependence of the apparent (K_x) and thermodynamic (K_a) equilibrium constant of the esterification of AA with 2EH at 1:1 molar ratio of AA to 2EH, catalyst loading of 10 % w/w, at 400 rpm stirring speed

where b_i, the adjustable varible of ith can be fitted to the experimental data using the least squares method. The sum of squared deviations between experimental and calculated values were evaluated for all experimental points as the objective function., The standard deviation as shown in Eq. 4.6 can be used as a measure of the quality of the fit:

$$\sigma(K) = \sqrt{\sum_{i=1}^{N} \frac{\left(K_i^{\exp tl} - K_i^{calc}\right)^2}{(N-m)}} \qquad (4.6)$$

where N is the number of experimental points and m is the number of adjusted variables. The fitted variables of Eq. 4.5 and their standard errors are tabulated in Table

4.6. The corresponding standard deviations for K_x, σ_{K_x} and standard deviations for K_a, σ_{K_a} are 1.21 and 8.45 respectively.

Table 4.6 : The b_i variables and their standard errors, $\sigma(b_i)$

I	1	2	3
K_x			
b_i	-31.134	4124.454	0.060
$\sigma(b_i)$	7.883	3040.025	0.012
K_a			
b_i	-25.400	3411.866	0.055
$\sigma(b_i)$	7.867	3020.069	0.022

Based on the Van't Hoff equation as shown in Eq. 4.7, the thermodynamic equilibrium constant is related to the standard enthalpy of reaction, ΔH_r^0:

$$\left(\frac{d \ln K_a}{dT}\right) = \frac{\Delta H_r^0}{RT^2} = \frac{\Delta G^0}{RT^2} \tag{4.7}$$

ΔG^0 is equivalent to the ΔH_r^0 calculated based on the activity based equilibrium constant. The enthalpy of reaction was calculated using Eq. 4.8. This equation was yielded by combining Eqs. 4.5 and 4.7 for both K_a and K_x The values of the enthalpy of reaction calculated for discrete temperatures are given in Table 4.5.

$$\Delta H_r^0 = -R(b_2 - b_3 T^2) \tag{4.8}$$

The calculated enthalpies of the reaction for activity based and mole fraction based thermodynamic equilibrium constant at 373 K are 35.11 kJ/mol (K_a) and 35.26 kJ/mol (K_x) respectively. The results are slightly different from the study of Komoń *et al.* (2013), in which the estimated enthalpies of reaction are 43.8 kJ/mol (K_a) and 43.8

kJ/mol (K_x) respectively. The estimated enthalpy of reaction obtained by Fomin *et al.* (1991) was remained at 70.1-72.3 kJ/mol for temperature in the range of 363-383 K. Comparing Eq. 4.2 and 4.7, ΔH_r^0 in Eq 4.7 is equivalent to ΔG^0.

The enthalpy of the reaction estimated based on the appropriate combinations of standard enthalpies of formation $\Delta_f H_i^0$ as shown in Eq. 4.9 was done for the comparison purposes.

$$\Delta H_r^0 = \sum_{product} v_i \Delta_f H_i^0 - \sum_{reactant} v_i \Delta_f H_i^0 \tag{4.9}$$

The enthalpies of formation of each component in the liquid state at 298 K are given in Table 4.7. Considering that the temperature dependence of the enthalpy of reaction at 298 K, the calculated enthalpy based on Eq. 4.8 is 10.053 kJ/mol and 12.282 kJ/mol , for K_x and K_a, respectively. The enthalpy of reaction calculated by Eq 4.9 was found to be 14.8 kJ/mol at 298 K. Komon *et al.* (2013) reported that the enthalpies of reaction at 298 K were calculated 9.9 kJ/mol and 10.5 kJ/mol for K_x and K_a respectively. Comparing with the study carried out by Komon *et al.* (2013), the calculated enthalpy of the present study is relatively closer to the enthalpy calculated from the heat of reaction.

Table 4.7 : Enthalpy of formation of the selected components.

Compound	Enthalpy of formation (kJ mol^{-1})
Acrylic acid	-383.8
2 ethyl hexanol	-432.8
2 ethyl acrylate	-516.0
Water	-285.8

Source: Daubert and Danner, 1998

4.3 STUDY OF THE MASS TRANSFER EFFECT ON THE ESTERIFICATION OF PURE AA WITH 2EH

4.3.1 Effect of External Mass Transfer

In order to develop an accurate kinetic model for the reactions catalysed by heterogeneous catalysts, the external and internal mass transfer resistances should be minimised. The external mass transfer resistance was eliminated by carrying out the reaction at agitation speeds ranged from of 0 to 600 rpm. The results in Figure 4.5 show that there are no significant increments in the yield of 2EHA when the stirring rate is increased to 200 rpm above. Therefore, all the other experimental measurements were carried out at 400 rpm to ensure that there was no external mass transfer resistance. The similar finding was also obtained in other researches for the esterification reaction using various reactants catalysed by Amberlyst 15 (Ragaini *et al.*, 2006; Akbay and Altıokka, 2011; Pappu *et al.*, 2011). Ragaini *et al.* (2006) stated that 100 rpm was the best speed among the speed of 60-200 rpm for the esterification of diluted acetic acid with 2 ethyl hexanol catalysed by Amberlyst 15. Akbay and Altıokka (2011) who employed Amberlyst 36 in the batch reaction system of acetic acid with n-amyl alcohol, stated that particularly above 500 rpm, the differences effect of stirring effect can be considered to be negligible. Pappu *et al.* (2011) also in line with the other two researchers in which the stirring speeds ranging from of 100-850 rpm showed no significant effect to the reaction system of butyric acid with 2 ethyl hexanol catalysed by Amberlyst 70.
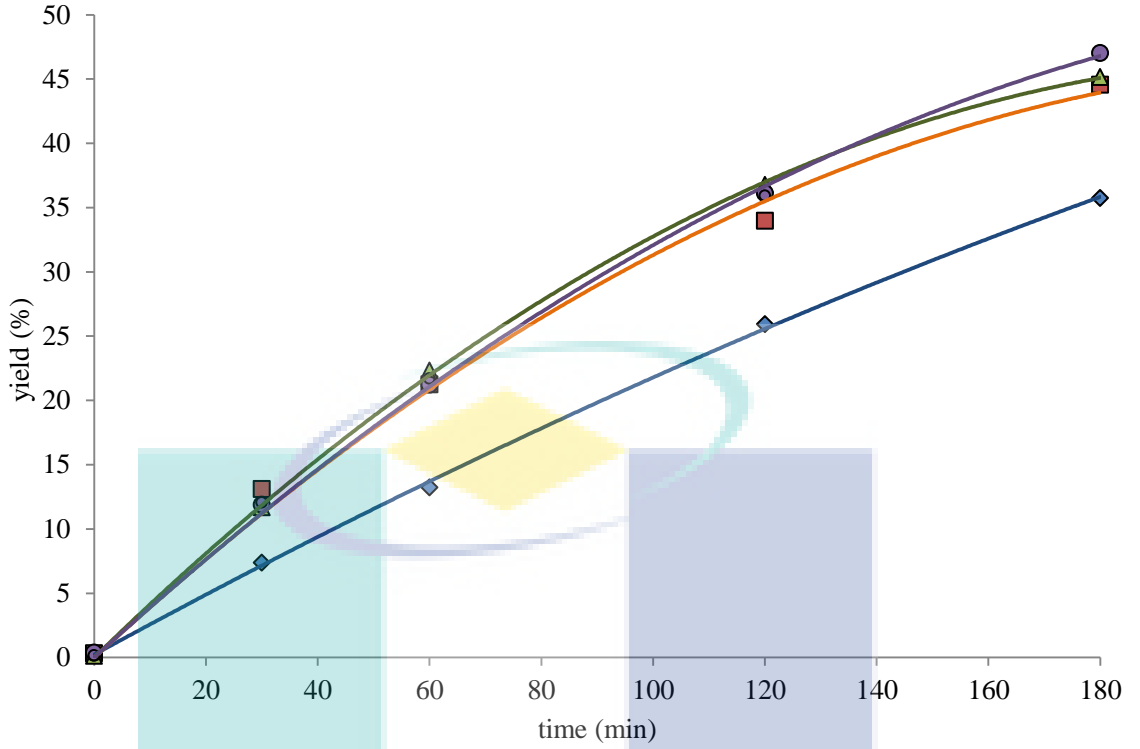
Figure 4.5 : The yield of 2-ethylhexyl acrylate at stirring effect of 0 – 600 rpm ($\Diamond$ 0 rpm $\Box$ 200 rpm Δ400 rpm $\circ$ 600 rpm) temperature of 388 K and catalyst loading of 10 wt% with the initial molar ratio acid to alcohol of 1:3.

To consider the effect of external mass transfer resistance on the rate of reaction, the Mears criterion for external diffusion was examined and the dimensionless Mears parameter (C_M) was calculated as follows:

$$C_M \;=\; \frac{r_{A,obs}\,\rho_b\,R_C\,n}{k_C C_{Ab}} \;<\; 0.15 \qquad (4.10)$$

Where n is the reaction order, R_C is the catalyst particle radius, ρ_b is the bulk density of catalyst, $r_{A,obs}$ is observed reaction rate, C_{Ab} is the bulk concentration of AA and k_C is the mass transfer coefficient. Figure 4.6 shows the observed reaction rate at 60 min at different stirring speed under identical condition of other variables. The rate of reaction is increased by approximately 30% when stirring is introduced during the reaction.
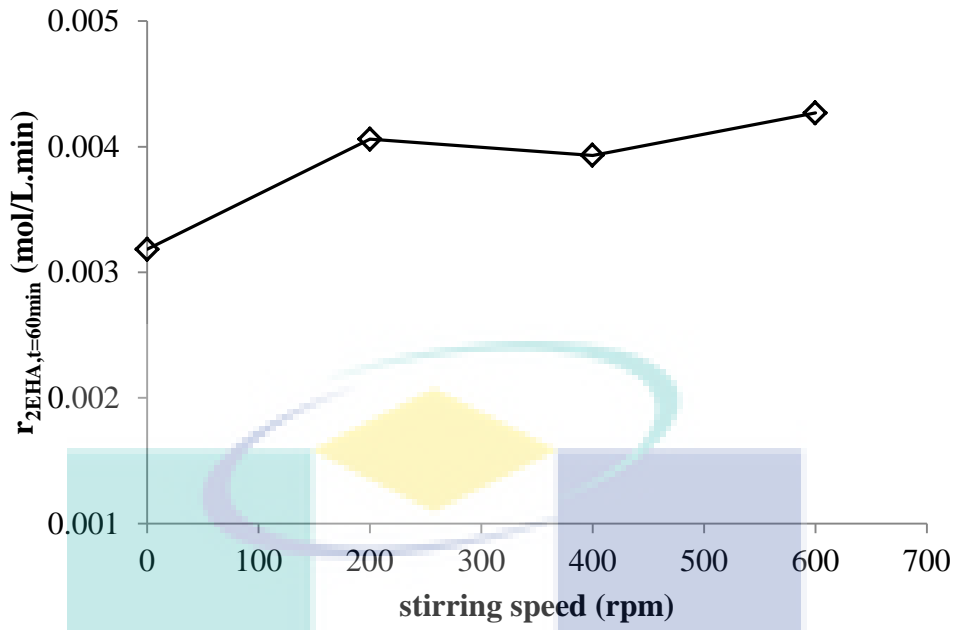
Figure 4.6 : Effect of stirring speed on the initial rate of reaction at temperature of 388 K and catalyst loading of 10 wt% with the initial molar ratio acid to alcohol of 1:3.

To estimate the mass transfer coefficient (k_C), the following equation was employed:

$$k_C \ = \ \frac{2D_{AB}}{d_p} + 0.31 \, N_{Sc}^{-2/3} \left(\frac{\Delta\rho\mu_C g}{\rho_c^2} \right)^{1/3} \tag{4.11}$$

Where D_{AB} is the diffusivity of the AA in solution, d_p is the diameter of the catalyst particle, μ_C is the viscosity of the solution, g is the gravitational acceleration, N_{Sc} is the Schmidt number (defined as $\mu_C/\rho_c D_{AB}$) and $\Delta\rho = |\rho_l - \rho_c|$| where ρ_l and ρ_c are the density of the solution and the density of the catalyst, respectively.

Table 4.8 shows that the calculated Mears parameters (C_M) are less than 0.15, indicating that the external mass diffusion can be neglected during the esterification of AA with 2EH (Fogler, 2008).

Table 4.8 : The Mears parameter for external diffusion.

Run	C_{Ab} (kmol/m^3)	$r_{A,obs}$ at 60 min (kmol/k$_{cat}$.s)	Mears parameter, C_M
0 rpm	1.604	5.858e^{-6}	0.067
200 rpm	1.455	7.270e^{-6}	0.092
400 rpm	1.435	8.029e^{-6}	0.103
600 rpm	1.455	7.843e^{-6}	0.099

4.3.2 Effect of Internal Mass Transfer

Internal mass transfer resistances were evaluated by conducting reactions at identical condition with three different categories of particle size. The experimental data in Figure 4.6 shows that there is insignificant difference in yield for the catalyst particle sizes of d_p<0.68mm 0.68mm<d_p<0.80mm and d_p>0.68mm. This validates that intraparticle diffusional resistances of the reactant in the ion-exchange resin are not important. This observation is in line with the research studies done by Yu *et al.* (2004) and Pappu *et al.* (2011), which indicating that intra-particle diffusion resistances are negligible for Amberlyst 15 catalysed esterification.
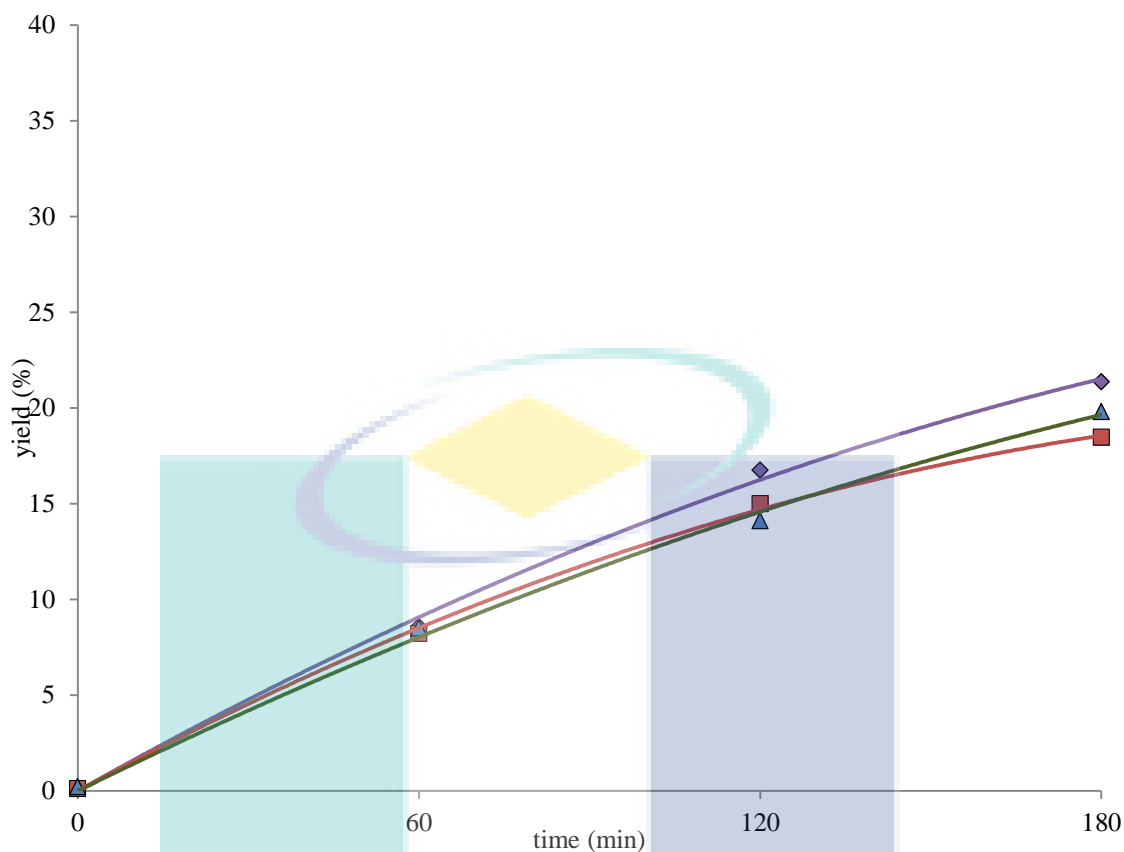
Figure 4.7 : The yield of 2-ethylhexyl acrylate at different catalyst particle sizes (◊ <0.68mm □ between 0.68mm and 0.80mm Δ >0.80mm) stirring speed of 400 rpm, temperature of 388 K and catalyst loading of 5 wt% with the initial molar ratio acid to alcohol of 1:3.

The occurrence of any internal pore diffusion limitation is determined on the basis of the Weisz–Prater criterion, where the dimensionless Weisz–Prater parameter (C_{WP}) is calculated as follows:

$$C_{WP} = \frac{-r_{A,obs}\,\rho_c\,R_c^2}{D_{eff}C_A} \tag{4.12}$$

The symbols R_c, D_{eff}, and C_A represent the effective radius of the catalyst, the effective diffusivity and the limiting reactant concentration in the mixture.

Figure 5 shows the observed reaction rate at 60 min at different particle sizes under identical condition of other variables. The corresponding Weisz–Prater parameters as listed in Table 7 are less than 1, implying that the resistance to internal pore diffusion is sufficiently small and the internal diffusion can be ignored in the present study (Fogler, 2008).
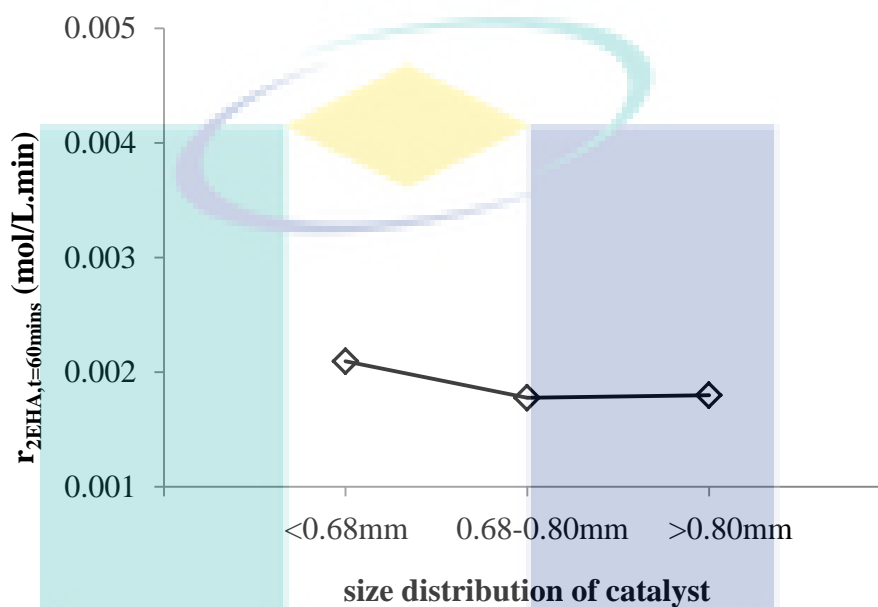
Figure 4.8 : Effect of catalyst particle size on the initial rate of reaction at temperature of 388 K and catalyst loading of 10 wt% with the initial molar ratio acid to alcohol of 1:3.

Table 4.9 : The Weisz–Prater parameter for internal diffusion.

Run	C_A (kmol/m^3)	$r_{A,obs}$ at 60 min (kmol/k$_{cat}$.s)	Weisz–Prater parameter, C_M
<0.68mm	1.690	7.205e^{-6}	0.5530
0.68-0.80mm	1.697	6.216e^{-6}	0.5995
>0.80mm	1.692	5.966e^{-6}	0.7282

4.4 STUDY OF THE EFFECT OF DIFFERENT OPERATING VARIABLES ON THE ESTERIFICATION OF PURE AA WITH 2EH

4.4.1 Effect of Temperature

For the study of the temperature effect on the esterification reaction, the molar ratio of AA to 2EH was fixed at 1:6 while the catalyst amount was fixed at 10 wt% with 400 rpm agitation speed. Figure 4.9 (a) and (b) illustrate the conversion and yield for the temperatures within the range of study. Increasing the reaction temperature would increase the kinetic energy of the reactant molecules and hence more of the reactant molecules would obtain the minimum amount of energy required to form products. Temperature of 388 K was chosen and used in the subsequent experimental studies.
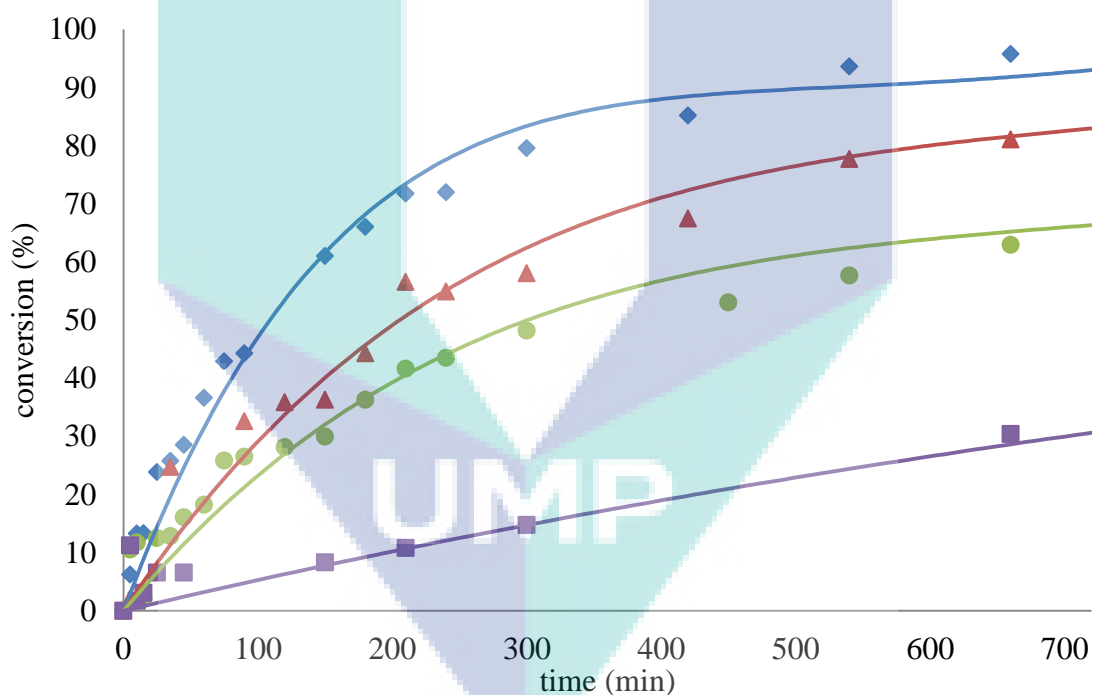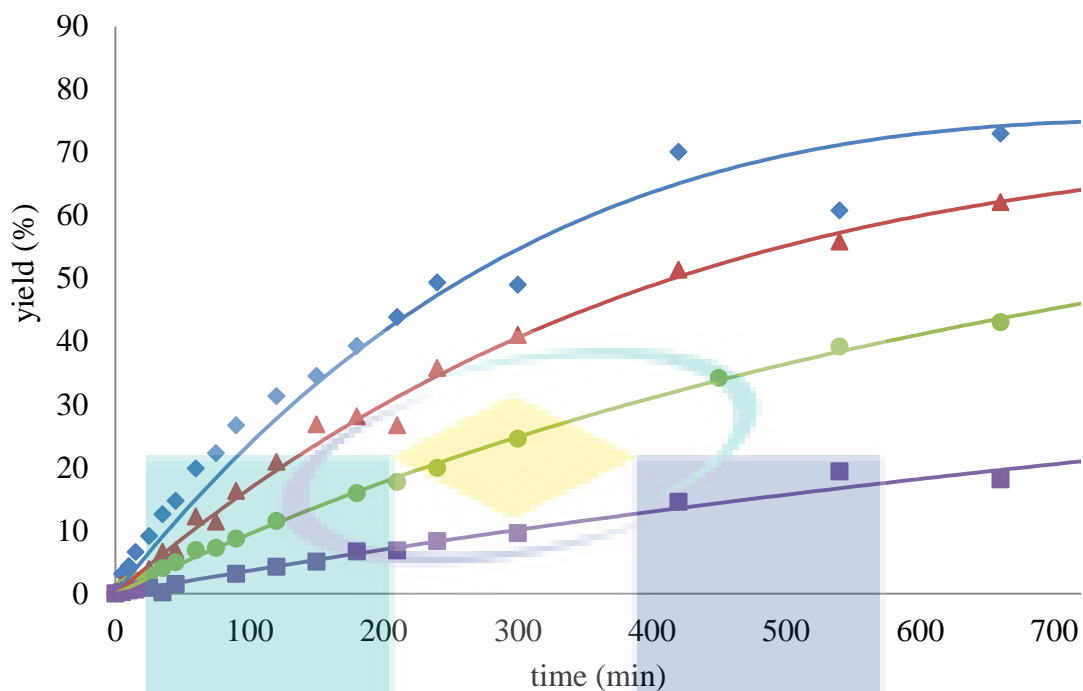
Figure 4.9: a) The AA conversion b) The yield of 2EHA at the temperatures of 358–388 K (□ 358 K ○368 K △378 K ◇ 388 K), stirring speed of 400 rpm, initial molar ratio acid to alcohol of 1:6 and catalyst loading of 10 wt%.

A plot of the reaction rate calculated using Eq. 4.13 versus temperature is given in Figure 4.10. It shows that the reaction rate increases with temperature. Every increment of temperature with 10 K doubles the initial rate of reaction. The reaction rate strongly depends on temperature hence indicating the reaction is controlled by surface reaction.

$$r_{2EHA0} = \left(\frac{dC_{2EHA}}{dt}\right)_{t=0} \tag{4.13}$$
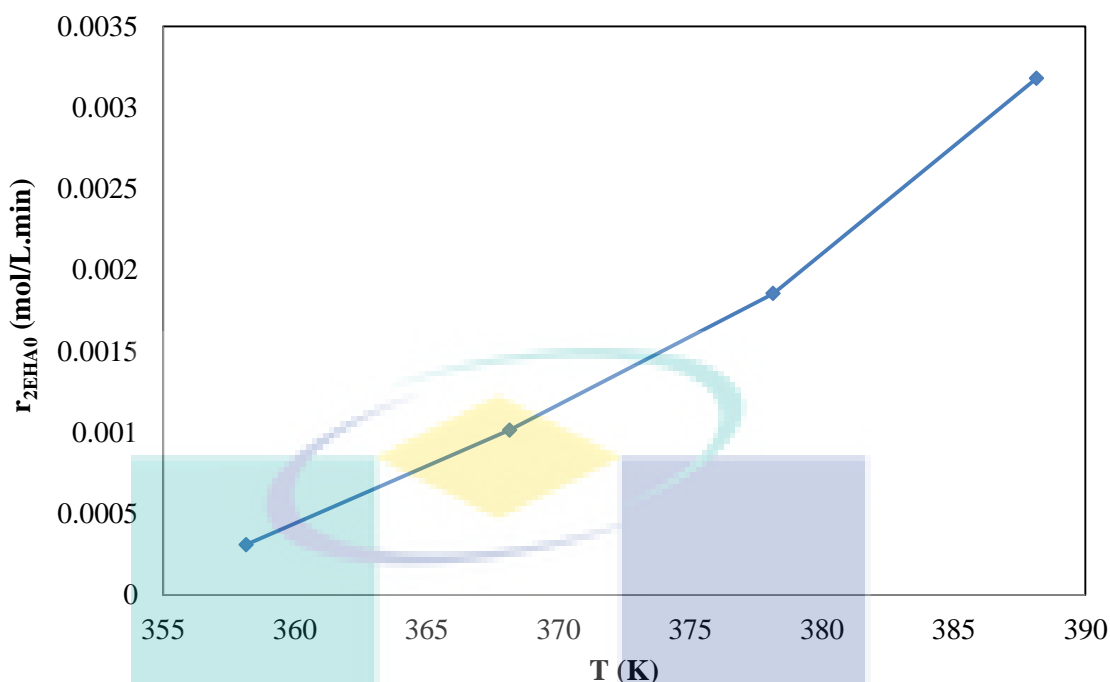
Figure 4.10: Effect of reaction temperature on the initial rate of reaction at stirring speed of 400 rpm, initial molar ratio acid to alcohol of 1:6 and catalyst loading of 10 wt%

4.4.2   Effect of Initial Reactant Molar Ratio

The effect of initial molar ratio of AA to 2EH ($M_{AA/2EH}$) was investigated by varying the molar ratio of AA to 2EH both in excess of alcohol (1:1, 1:3, 1:5, 1:7) and excess in acid (1:1, 3:1, 5:1, 7:1). Figure 4.11 shows the effect of $M_{AA/2EH}$ on the product selectivity after 6 hours with the catalyst amount of 15 wt%. The highest yield was observed at $M_{AA/2EH}$ of 1:3. The excess of 2EH could drive the reaction equilibrium to product side and hence shorten the time needed to achieve equilibrium conversion. Nevertheless, the excess of 2EH also could promote the side reactions which would lower the yield of 2EHA. For instance the excess of 2EH enhances the side reaction of polymerisation and etherification. Similarly, the excess of acid may promote the side reaction of polymerisation and hence reducing the selectivity. Therefore, the best initial molar ratio 1:3 of AA:2EH was chosen and used in the subsequent experimental studies, based on the selectivity, compromising both conversion and yield. The concentration-time data for the reaction study at different initial reactant molar ratio are shown in Appendix F. was
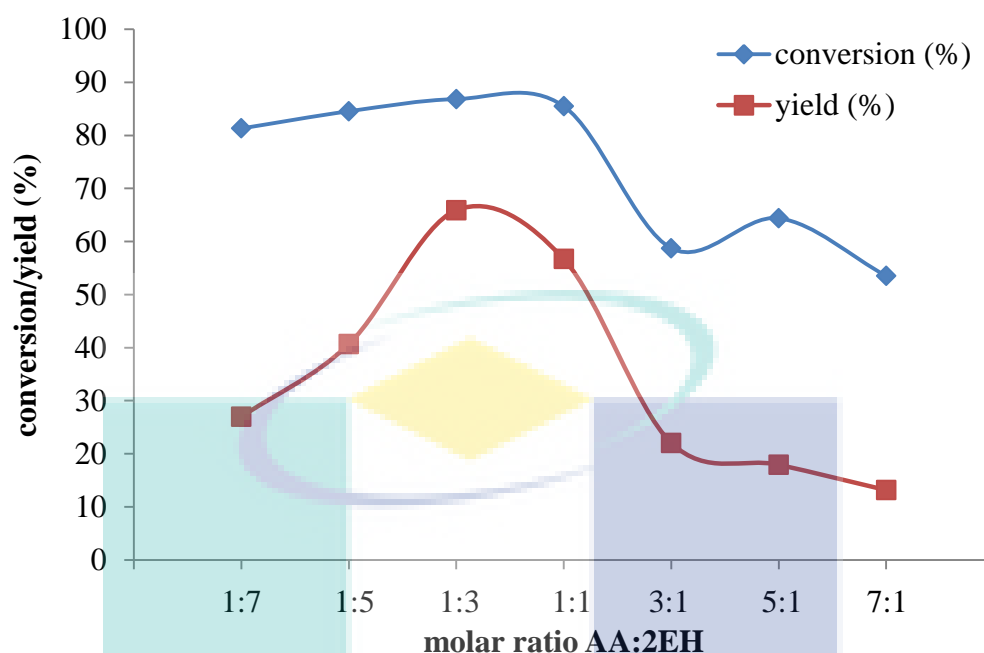
Figure 4.11: The AA conversion and yield of 2EHA for different initial molar ratio of AA to 2EH at 6 hrs. Operating condition: stirring speed of 400 rpm, temperature of 388 K and catalyst loading of 15 wt%.

4.4.3 Effect of Catalyst Loading

The effect of the amount of catalyst on the 2EHA yield was studied by varying the catalyst loading from 1-15 wt% and keeping all other reaction variables identical. Each reaction was carried out for 6 hours. Based on the results illustrated in Figure 4.12, the increase in product yield is significant when the catalyst amount is increased from 1 to 10 wt%. This is due to the increase of active site with increasing catalyst loading. There was no enhancement anymore in the rate of reaction was observed when the catalyst amount is increased later from 10 to 15 wt%. This can be attributed to the fact that beyond a certain catalyst loading, there exists an excess of catalyst sites than actually required by the reactant molecules and hence there is levelling off of the reaction rate (Fogler, 2008). In additional, this has also proven that the process is economic feasible since the amount of catalyst used is less than 10 wt% (Teo and Saha, 2004). Thus, the 10 wt% of catalyst loading was chosen as the best condition for esterification of AA with 2EHA.
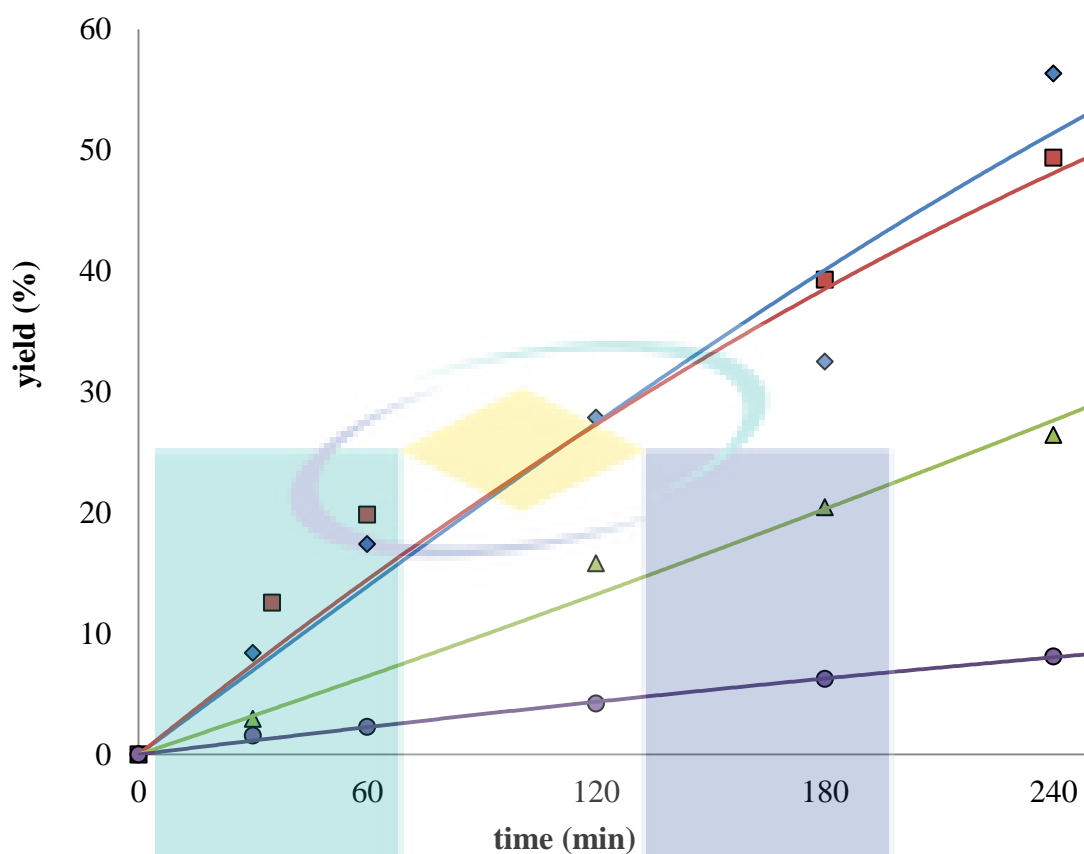
Figure 4.12 : The 2EHA yield for the catalyst loading of 1 – 15 wt% (○ 1 wt% Δ 5 wt% □ 10 wt% ◊ 15 wt%) at stirring speed of 400 rpm, temperature of 388 K and $M_{AA/2EH}$ of 1:3.

The initial rate was obtained using Eq. 4.10. A plot of the initial reaction rate versus catalyst loading is given in Figure 4.13. It shows that the initial rate for the reaction with the catalyst loading of 1-10 wt%, as expected, is increasing linearly with catalyst loading since the active surface area is proportional to the amount of catalyst. There is no increment found in the initial rate of reaction when the catalyst loading is more than 10wt%. The concentration-time data for the reaction studies using different catalyst loading is shown in Appendix E.
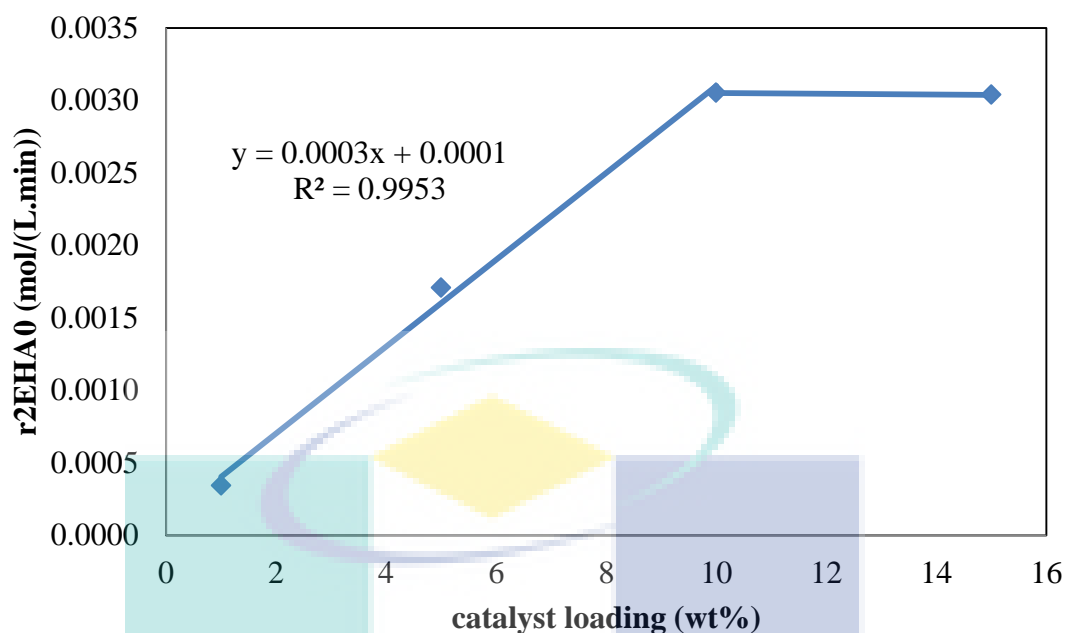
Figure 4.13 : Effect of reaction catalyst loading on the initial rate of reaction at stirring speed of 400 rpm, initial molar ratio acid to alcohol of 1:3 and temperature of 388 wt%.

The mathematical expression relating the initial reaction rate to the catalyst loading can be derived from Figure 4.14 as follows:

$$r_{2EHA0} \ (mol \ L^{-1} \ min^{-1}) \ = \ 0.0001 \ + \ 0.0003 \ C_{cat} \ (mol \ L^{-1}) \qquad (4.14)$$

Eq 4.11 is only valid at the temperature of 388 K with $M_{AA/2EH}$ of 1:3 at which the experiments were performed.

4.4.4 Recyclability Study

Ion exchange resins can be deactivated due to hydrolysis of the functional groups and/or blocking of the active sites as a result of polymerization or polycondensation products, depolymerisation, and release of oligomeric sulphonic acids because of oxygen sensitivity and desulphonation (Neier, 1991). It was reported that partial desulphonation occurred and the shrinkage of the three dimensional network

took place in Amberlyst 15 when the temperature was increased up to 413K (Teo and Saha, 2004). In the present study, Amberlyst 15 was reused up to 5 times for 6 hours at 388 K. Based on the results reported in Figure 4.14, a reduction of 20% in the yield of 2EHA is observed after the catalyst is reused for the first time while a reduction of ≤10% is observed for the subsequent reuse. The deactivation was due to the blocking of active site by the poly-acrylic acid formed through the polymerisation of AA, as validated by the catalyst characterisation results as shown in section 4.5.2.
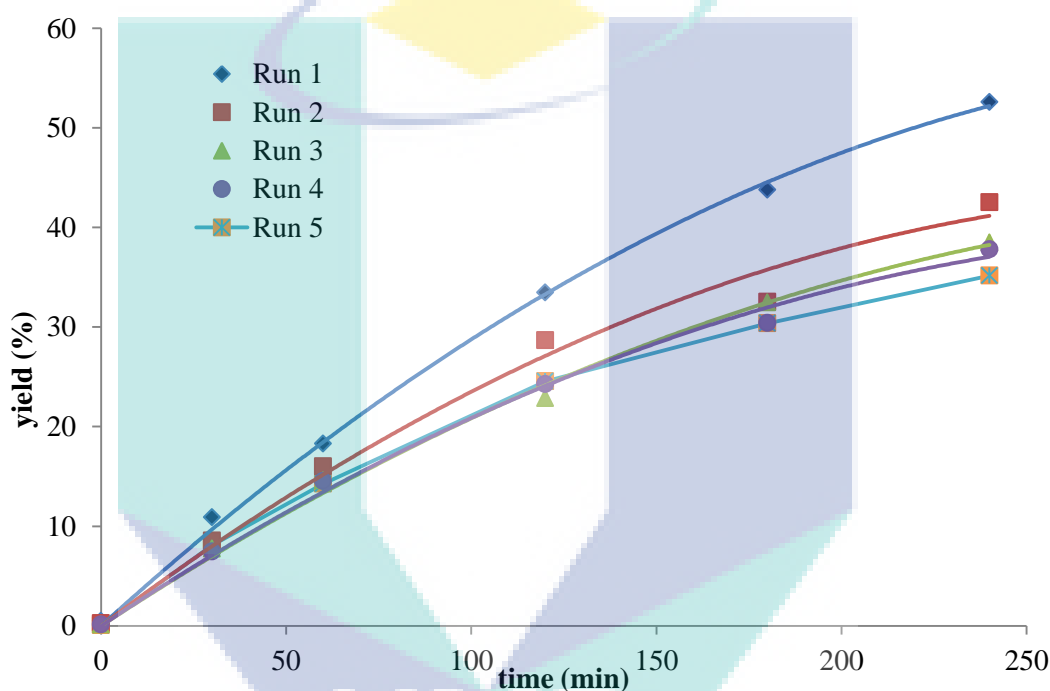
Figure 4.14: The recyclability study of Amberlyst 15 for the reaction of AA with 2EH under 388 K, molar ratio of AA:2EH, 1:3, catalyst loading of 10% w/w, with 400 rpm stirring speed.

In order to identify the deactivation mechanism, the catalyst activity was related to the reaction time as shown in Figure 4.15. Catalyst activity was calculated based on Eq. 4.15.

$$a(t) = \frac{-r'_A(t)}{-r'_A(t = 0)} \tag{4.15}$$
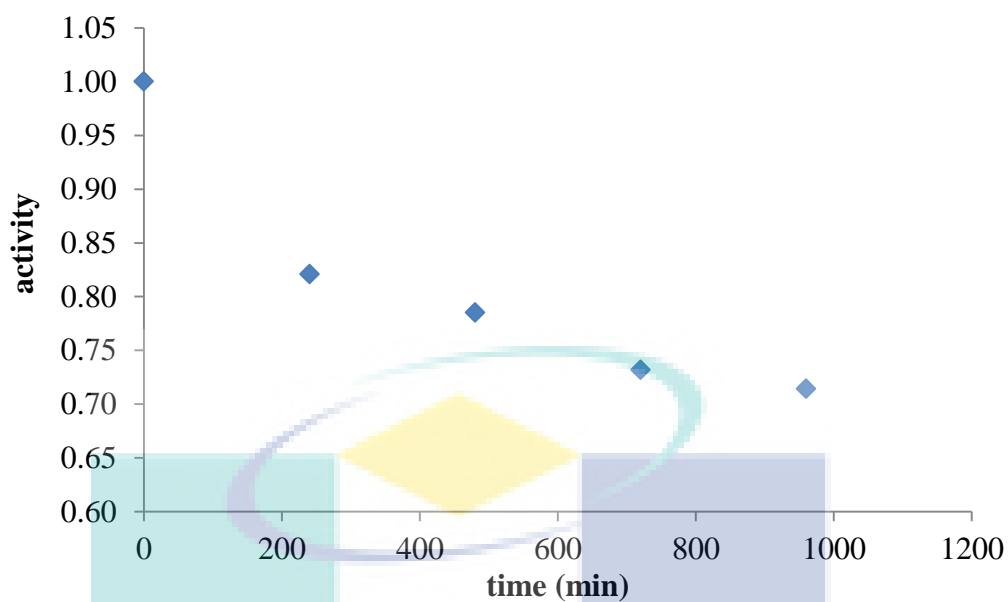
Figure 4.15: The catalyst activity for 5 cycle's usage

Where a is the catalyst activity, $-r'_A$ (t=0) is the initial rate of reaction when the catalyst was used for the 1st time and $-r'_A$ (t) is the initial rate of reaction when the catalyst was used in the subsequent experimental runs.

$1/a = 0.013t^{0.5} + 1$
$R^2 = 0.9935$
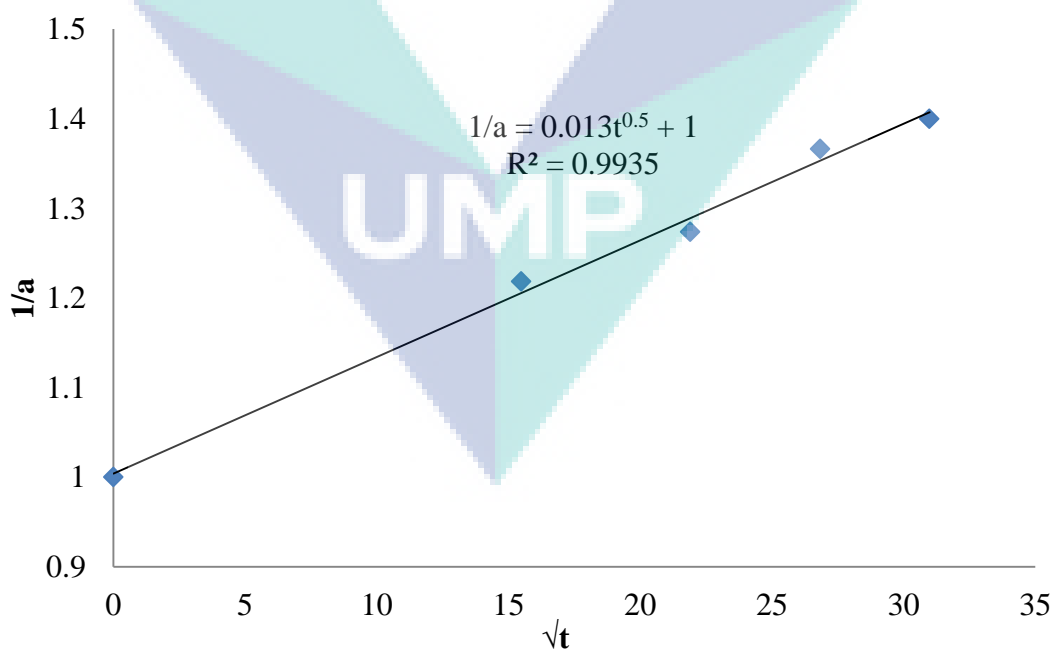
Figure 4.16: Linearized plot of the decay law

The plot of *1/a* versus $\sqrt{t}$ in Figure 4.15 shows that the best fit decay law to relate the catalyst activity and reaction time is as Eq. 4.16, implying that the deactivation is due to fouling. The catalyst active sites might be blocked by the poly-acrylic acid.

$$a(t) = \frac{1}{1 + k_D t^{0.5}} \tag{4.16}$$

Where the deactivation coefficient, k_D=0.013min$^{-0.5}$.

4.5 STUDY OF THE EFFECT OF DIFFERENT INITIAL WATER CONTENT TO THE ESTERIFICATION REACTION

The presence of water in the reactants of would affect the kinetics of the esterification reaction. The effect of the initial water content was investigated using two different experimental setups and the results are discussed in the subsequent sections.

4.5.1 Comparison Study Using Different Experimental Setup

A series of experiments were carried out with different initial amounts of water (wt% of water in AA) in order to quantify the effect of water on the kinetics of the reaction of AA with 2EH. Water and 2EH are immiscible. It was found that more than 99% of the AA remained in the organic phase. The catalyst was well dispersed in the aqueous and organic phases by mixing. Figure 4.17 shows the yield profile of the reversible reaction carried out using the total reflux (TR) setup. The reaction with 90% and 100% of AA achieves identical yield after 6 hours. A significant drop is observed when 20% of water presents in the system. A yield of less than 5% is observed when the initial water content in the reactant is more than 70%. This phenomenon may occur due to the poor accessibility of reactants to acid sites. The presence of huge amount of water (Haas, 2005; Rat *et al*., 2008) has interrupted the adsorption of the reactant to the active site of catalyst. The affinity of Amberlyst 15 with polar solvent, water, is stronger than the affinity with organic solvent, 2EH.
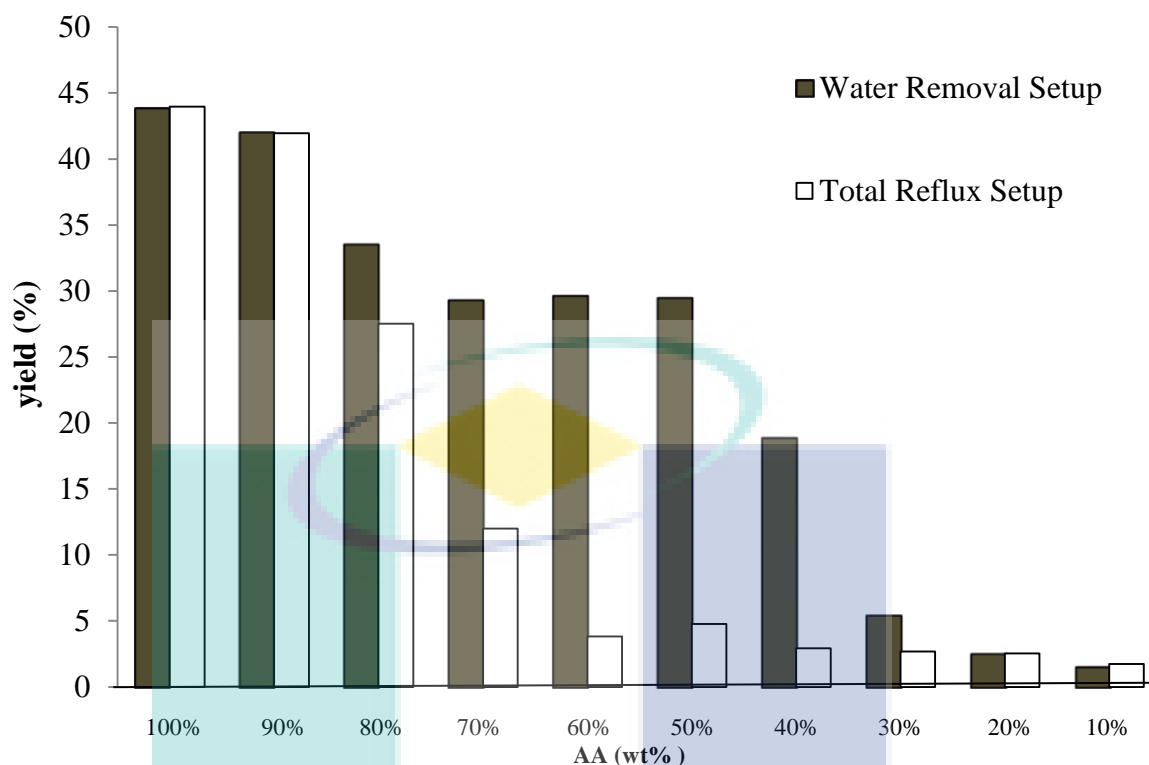
Figure 4.17 : Yield for the esterification of AA with 2EH after 6 hours reaction at catalyst loading of 10% w/w of acid; temperature of 373 K; initial molar ratio acid to alcohol of 1:3 for different concentrations of AA (10- 100% AA)

The reactions with different concentrations of diluted AA were repeated using batch reactor which was connected to a continuous water removal (CWR) system as shown in Figure 4.17, the yield for the reactions with 30-70 % of AA increases tremendously (>50% increment) by removing water from the system. The water removal efficiency for these systems is more than 95% as shown in Table 4.10. The yield for the reactions with 10% and 20% of AA in different setups does not differ much due to the catalyst poisoning by the water and poly-acrylic acid as proven by the catalyst characterisation results in sections 4.5.2 and 4.6.3. Moreover, , the efficiency of the water removal from the system reduced to 71 and 84 % for the reaction with 10 % and 20 % of AA respectively because of the insufficient surface area of the condenser. The efficiencies for the water removal for the reactions with 90 and 100% of AA are relatively low with the others due to a stronger interaction and miscibility between the acrylic acid and the minute amount of water.

Table 4.10: Percentage of water removed from the CWR system

AA concentration (%)	Initial volume			Water generated during the reaction (ml)	Total percentage water removal (%)
	AA (ml)	Water (ml)	2EH (ml)		
10	8.67	82.02	59.31	0.04	71.30
20	12.45	52.36	85.19	0.08	83.91
30	14.57	35.74	99.69	0.21	98.75
40	15.93	25.11	108.96	0.79	99.98
50	16.87	17.73	115.40	1.31	97.17
60	17.56	12.31	120.13	1.37	95.06
70	18.09	8.15	123.76	1.40	94.28
80	18.51	4.86	126.63	1.63	99.98
90	18.85	2.20	128.95	2.08	67.70
100	19.13	0.00	130.87	2.21	45.35

4.5.2   Used Catalyst Characterisation

The possibility of the catalyst poisoning was examined by characterizing the fresh and used Amberlyst 15 using SEM, physisorption analyser, FTIR and XRF. Figure 4.18 shows the SEM micrographs of Amberlyst 15 under magnification of 15x. Identical cracks of very minute size on the fresh catalyst are also observed on the used catalysts.

(a)

(b)

(c)

(d)

(e)
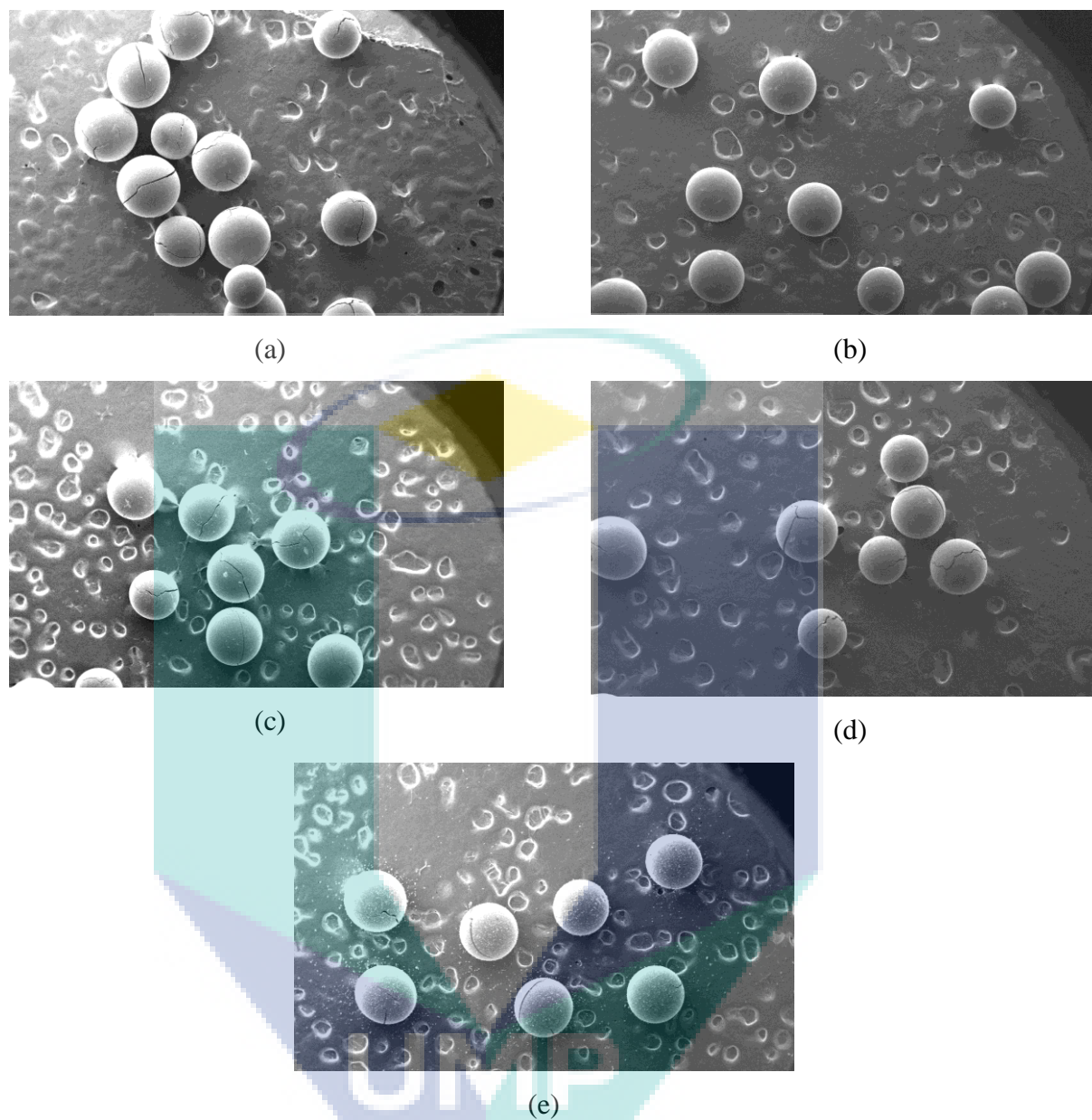
Figure 4.18: SEM micrographs (magnification: 15x) of outer surface of Amberlyst 15 under condition; a) unused catalyst, b) 50% AA in TR setup, c) 10% AA in TR setup, d) 50% AA in CWR setup, and e) 10% AA in CWR setup
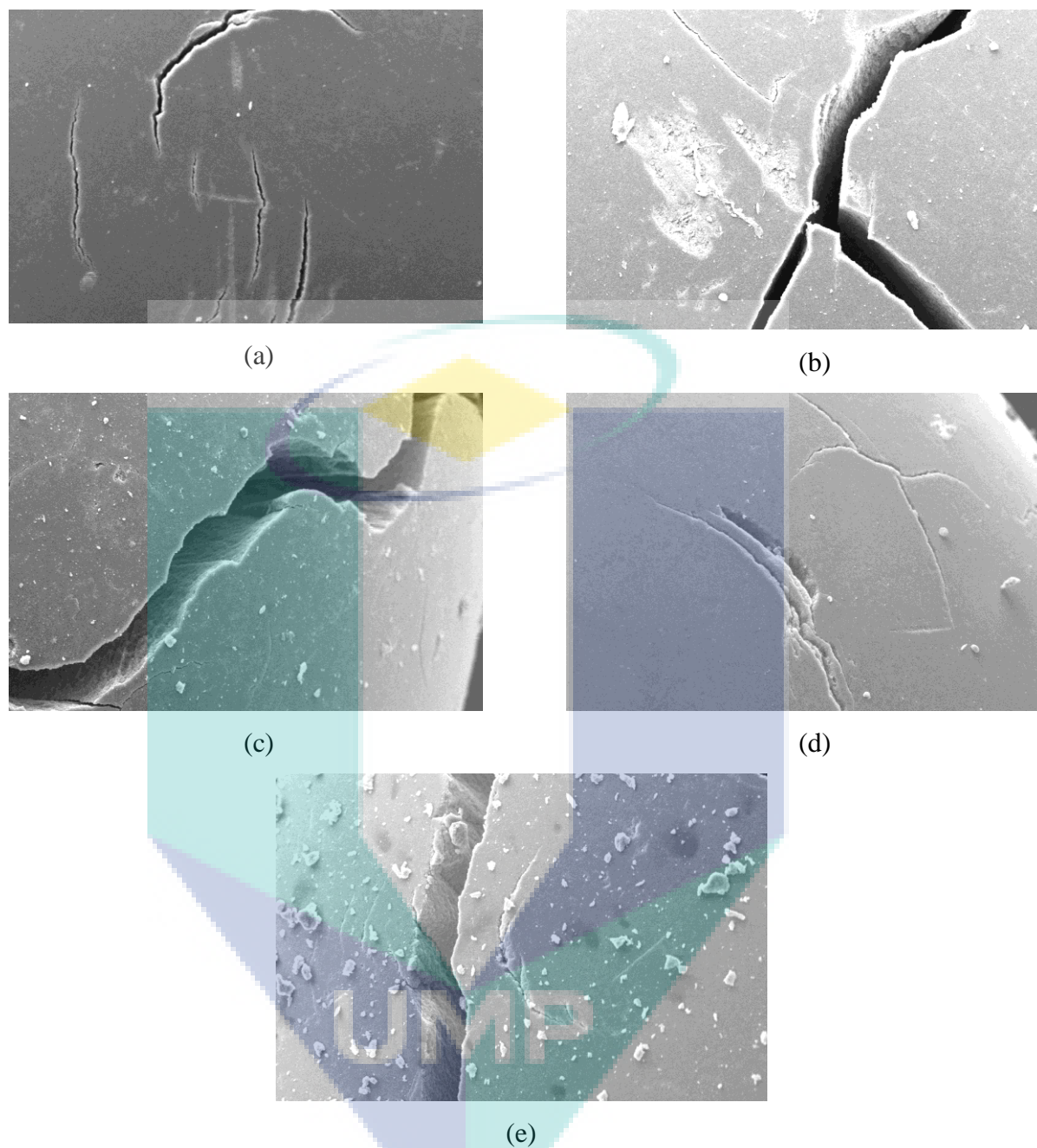
Figure 4.19 : SEM micrographs (magnification: 500x) of inner surface of Amberlyst 15
under condition; a) unused catalyst, b) 50% AA in TR setup, c) 10% AA
in TR setup, d) 50% AA in CWR setup, and e) 10% AA in CWR setup

The micrographs of Amberlyst 15 under magnification of 500x are shown in
Figure 4.19. The surface of the fresh catalyst is smooth like other gel resins. However,
some small defects are observed on the used catalyst surfaces, which are probably
caused by a small amount of poly-acrylic acid formed during the experiments. It is

observed that the used catalysts obtained from the reaction study using 10 wt% AA are deposited with more poly-acrylic acid. The polymerization was enhanced by the substantial amount of water. The AA solution was not stable and AA would be easily polymerized when the solution was heated.

Figure 4.20 shows that the formation of poly-acrylic acid has caused an increase in the conversion of AA during the reactions with 10 wt% of AA solution for both TR and CWR setups. Despite the miscibility of AA and W, more AA would be distributed in 2EH due to the mixture stability. Table 4.8 shows that the volume of 2EH in the reaction with 50 % AA solution is seven fold to the volume of water. Hence, a more stable AA and 2EH mixture was formed and AA polymerization was reduced. Less deposit was found on the catalyst surface for the reaction with 50 wt% AA solution as shown in Figure 4.19.

The results of BET surface area, pore volume and average pore diameter for the unused and used catalysts are shown in Table 4.11. The used catalysts were obtained from the reaction studies using the 10% AA solution. The properties of the unused catalyst are comparable with the specifications published by the manufacturer (Rohm and Haas, 2005). The lowest BET surface area and pore volume are acquired for the used catalyst in the CWR setup. This is in line with the findings obtained from the micrographs of SEM where this catalyst was deposited with the most poly acrylic acid. These deposits have reduced the surface area and pore volume for approximately 10 % as compared to the unused catalyst. Nevertheless, the average pore diameter does not have much change between the unused and used catalyst.
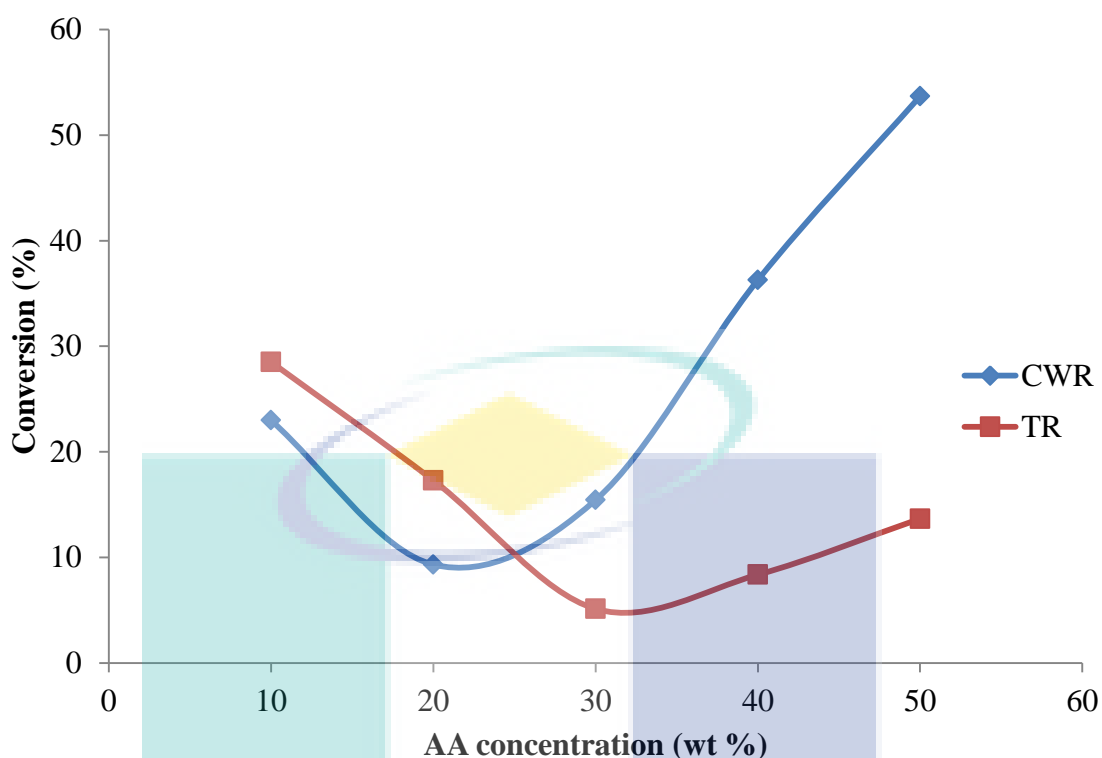
Figure 4.20: Conversion for the esterification of AA with 2EH after 6 hours reaction at catalyst loading of 15% w/w of acid; temperature of 373 K; initial molar ratio acid to alcohol of 1:3 for different concentrations of AA (10- 50% AA)

Table 4.11: The BET surface area and pore size data for used and unused catalyst

Element	Unused	Total Reflux	Continuously Water Removal
		10%AA	10%AA
BET surface area (m^2/g)	56.1	49.9	48.4
Pore volume (cm^3/g)	0.32	0.31	0.30
Average pore diameter (Å)	326.9	330.9	326.9

Figure 4.21 illustrates the spectra of FTIR analysis for unused and used Amberlyst 15. There are no obvious and significant changes of the unused and used Amberlyst 15 in terms of the pattern of the spectra. This indicates that no physical structure of catalyst was affected after the reactions with the presence of large amount

of water. Nevertheless, the peak height is reduced significantly for the used catalysts obtained from the reaction with 10% AA solution in a CWR setup. This is attributed to the deposition of the polymers on the surface of Amberlyst 15 as observed from the SEM micrograph in Figure 4.19 (e).
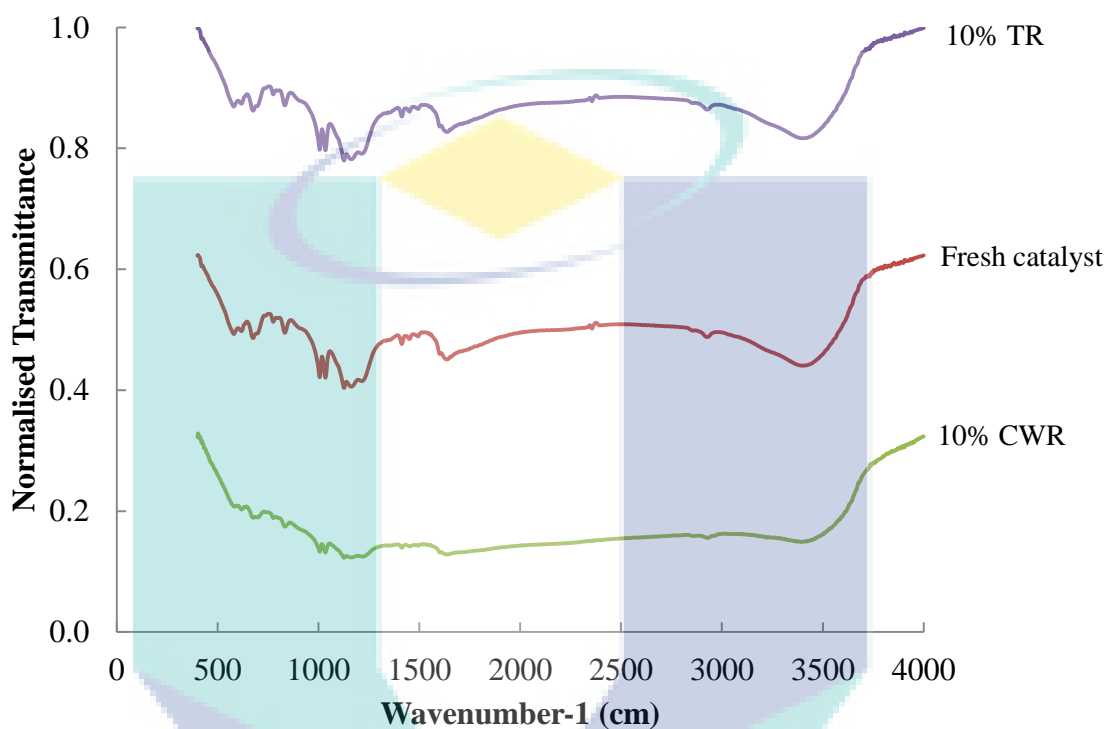
Figure 4.21: FTIR spectra of fresh and used Amberlyst 15.

This finding is also validated by the XRF results tabulated in Table 4.12 which shows that the content of sulphur trioxide has reduced more than 15% for the catalyst employed in the reaction with 10% AA solution in a CWR setup. The catalyst poisoning happened when it was significant amount of poly-acrylic acid deposited on the catalyst surface.

Table 4.12 : Results of elemental analysis using XRF analyser

Element	Unused	Total Reflux		Continuously Water Removal	Unit
		100%AA	10%AA	10%AA	
Sulphur Trioxide (SO_3)	47.07	44.60	43.28	38.76	%
Phosphorus Pentoxide (P_2O_5)	0.18	0.18	0.20	0.20	%
Calcium Oxide (CaO)	0.07	0.09	0.13	0.12	%

4.6   KINETIC STUDY

4.6.1   Main Reaction (Esterification)

The reaction rate expression of the 2EHA formation depends on the mechanism of reagent adsorption on heterogeneous catalyst. PH, ER, and LHHW model are commonly applied for correlating the kinetic data of esterification reaction.

PH model is applicable to many ion exchange resin catalysed reactions and highly polar reaction medium. The reversible PH model expression for the reaction rate is derived based on the assumption of neglecting the presence of two liquid phases. The solid phase is lumped into the single hypothetical phase.

LHHW and ER models are appropriate for heterogeneously catalysed reactions. LHHW model is applicable whenever the rate determining step is the surface reaction between adsorbed molecules. On the other hand, ER model is applicable if the rate-limiting step, surface reaction takes place between one adsorbed species and one non-adsorbed reactant from the bulk liquid phase

In the present study, activity based kinetic model was preferred due to the non-ideality of the liquids used. UNIFAC group contribution method was reported as one of

the best methods to estimate the activity coefficient for esterification mixture (Komoń *et al.*, 2013; Teo and Saha, 2004). Therefore, it was adopted to calculate the liquid activity coefficient.

In spite of the presence of inhibitor, the side reaction, AA polymerisation was alleged to occur when the reaction temperature was increased. Therefore, the rate expressions were related to the rate of reaction of 2EHA, r_{2EHA} instead of the rate of reaction of the limiting reactant AA, r_{AA}. The PH, ER and LHHW models are shown in Eq. 4.17-4.19:

$$r_{2EHA} = k_f \left(a_{AA} a_{2EH} - \frac{1}{K_a} a_{2EHA} a_W \right) \tag{4.17}$$

$$r_{2EHA} = \frac{k_f \left(a_{AA} a_{2EH} - \frac{1}{K_a} a_{2EHA} a_W \right)}{(1 + K_{AA} a_{AA} + K_W a_W)} \tag{4.18}$$

$$r_{2EHA} = \frac{k_f \left(a_{AA} a_{2EH} - \frac{1}{K_a} a_{2EHA} a_W \right)}{(1 + K_{AA} a_{AA} + K_{2EH} a_{2EH} + K_{2EHA} a_{2EHA} + K_W a_W)^2} \tag{4.19}$$

The activity based equilibrium constant, K_a was adopted from section 4.2. K_i is the adsorption equilibrium constant for species i. The rate constants, k_f can be related to the temperature with Arrhenius equations as below:

$$k_f = k_{f0} \exp\left(\frac{-E_f}{RT}\right) \tag{4.20}$$

Where k_{f0} is the pre-exponential factors for the reactions, E_f denote the activation energy of reactions, R is the gas constant and T is the temperature of the reaction.

In the case of this heterogeneously catalysed reaction, the following equation was used to determine the r_{2EHA} (Cunill *et al.*, 2000):

$$r_{2EHA} = \frac{dC_{2EHA}}{dt} \qquad (4.21)$$

Where C_{2EHA} is the concentration of 2EHA and t is the reaction time.

The kinetic variables obtained with their standard errors, σ are shown in Table 4.13. Since the residuals obtained from all the models were randomly distributed around the line of error=0 with zero mean, it is to be noted that the ER model gave the best correlation among the three models adopted because the coefficient of determination (R^2) is closest to one. The parity plot for the experimental and predicted rate of reaction is shown in Figure 4.22.
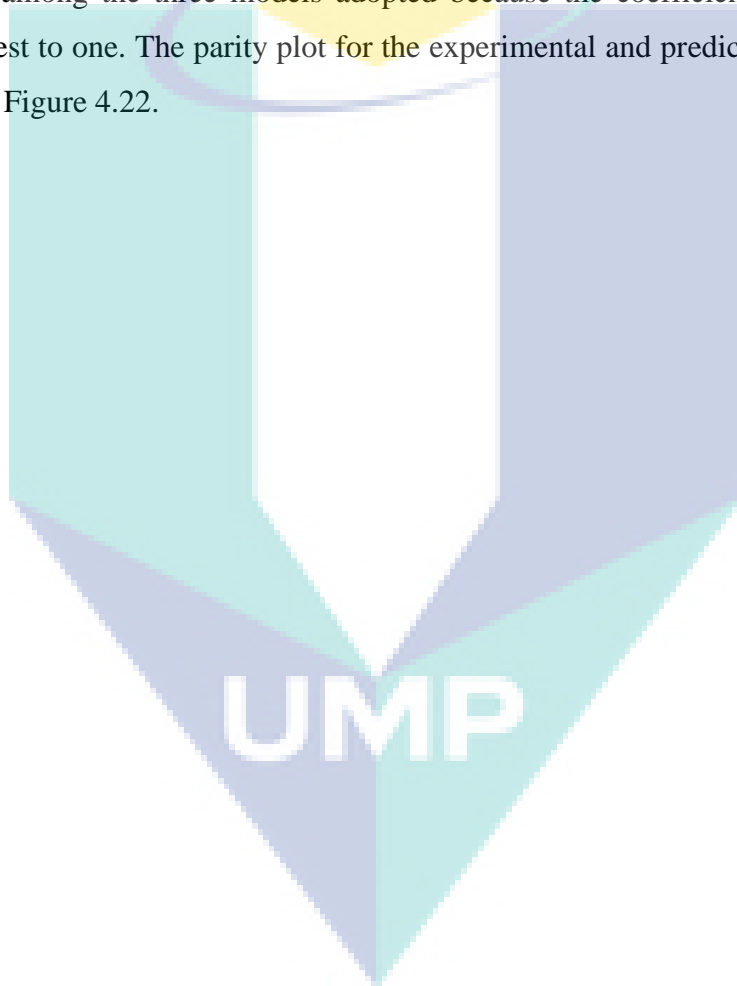
Table 4.13: Kinetic variables for the model used to fit the experimental data.

Model	Kinetic Variable		Adsorption Parameter				R^2
	k_{f0} (σk_{f0}) (mol/L.min)	Ef (σ Ef) (J/mol)	K_{AA}(σK_{AA})	K_{2EH} (σK_{2EH})	K_{2EHA}(σK_{2EHA})	K_W(σK_W)	
PH	2.04×10^8 (1.42×10^8)	72662 (264.37)	-	-	-	-	0.94
ER	1.55×10^9 (2.68×10^7)	71324 (6.55)	102.00 (2.14)	-	-	11.24 (0.94)	0.98
LHHW	4.91×10^9 (1.06×10^7)	77772 (0.82)	11.14 (0.026)	0.03 (0.003)	2.01 (0.036)	0.59 (0.015)	0.97

a)

b)

c)
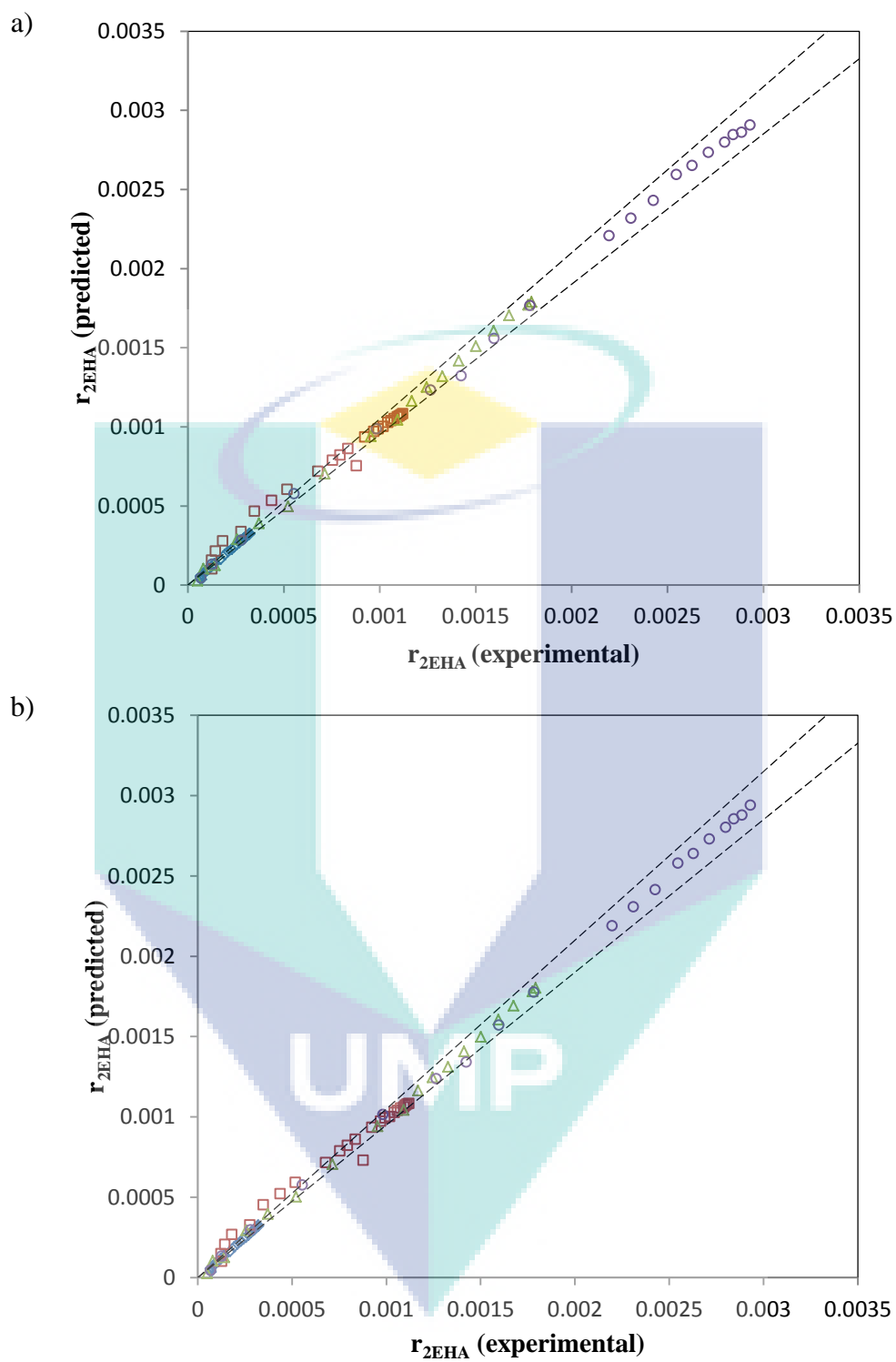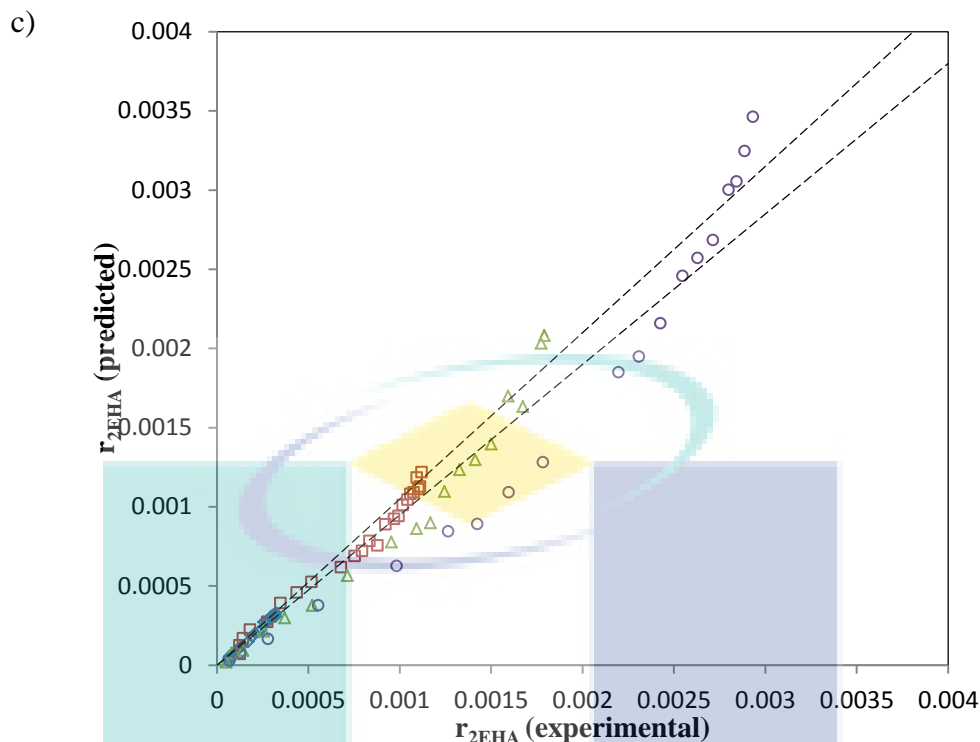
Figure 4.22: Parity plot for the experimental and predicted rate of reaction of a) LHHW; b) ER and c) PH (◊358 K □368 K Δ 378 K ○ 388 K; dotted line stand for ±5% error)

The apparent activation energy for the esterification reaction is about 71.3 kJ/mol. The activation energy of the esterification of AA with 2EH catalysed by Amberlyst 15 is in good agreement with the activation energy reported by Altiokka and Odes (2009) for the esterification of AA with propylene glycol catalysed by Amberlyst 15. However, it is higher than the activation energy reported by Komoń *et al.* (2012) and Sert *et al.* (2013) for the AA esterification catalysed by Amberlyst 70 and Amberlyst 131 respectively. Komoń *et al.* (2013) that employed Amberlyst 70 in the reaction obtain slightly lower apparent activation energy that is 50.1 kJ/mol. Fomin *et al.* (1991) which employed macroporous acidic KU-23 ion exchange resins in the reaction however come out with almost similar activation energy that is 72.8 kJ/mol.

It is proposed that the AA molecule adsorbs on the catalyst site and forms an oxonium ion intermediate, which is simultaneously attacked by the 2EH in the bulk liquid. During this exchange reaction, and the water molecule is formed in adsorbed state while 2EHA molecule is formed and desorbed immediately to the bulk liquid. All

the adsorbed molecules then desorb and give rise to a vacant catalyst site in all cases. The good agreement between the experimental data with ER model has shown that the reaction is controlled by surface reaction. This is in line with the findings in the study of the effect of temperature on the esterification reaction in section 4.4.1. Figure 4.23 summarizes the energy profile for this reaction pathway.
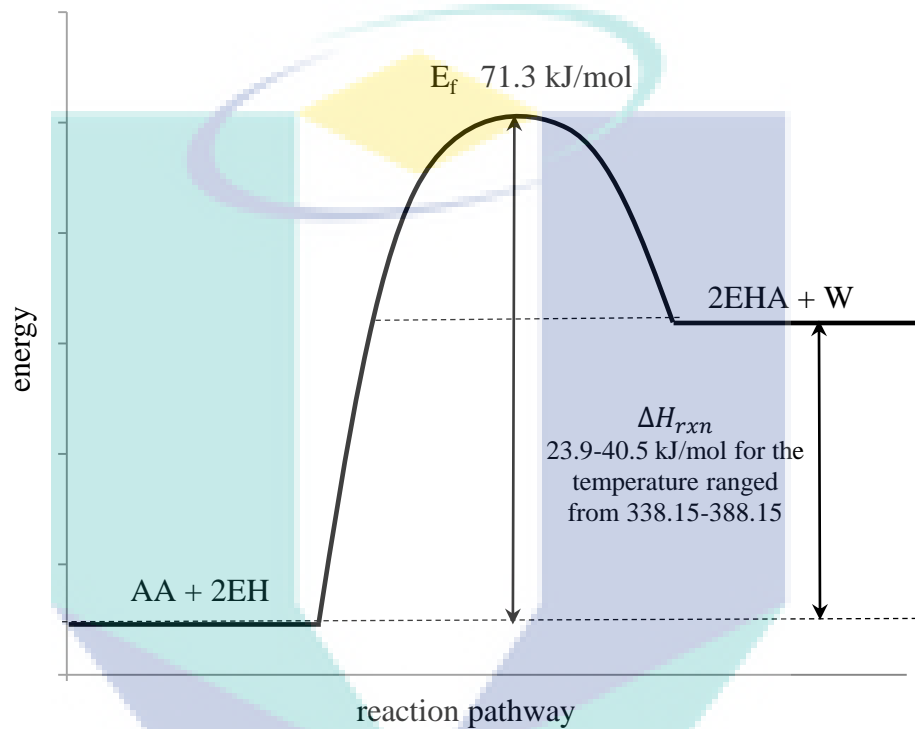
Figure 4.23 : Energy profile for reaction pathway of AA with 2EH

4.6.2   Side Reaction (Dimerization)

The best fit ER kinetic model was included into the batch reactor model to predict the concentration of the other components. In the case of this heterogeneously catalyzed reaction, the following reactor model equation was used (Cunill *et al.,* 2000):

$$r_i = \frac{dC_i}{dt} \tag{4.22}$$

Where C_i is the concentration of component i and t is the reaction time.

Figure 4.24 (a) shows that the deviation of the predicted AA concentration from the experimental data is significant when the simulation is carried out without considering the side reaction. Taking into account the general esterification reaction as well as polymerization of AA and 2EHA, the overall reaction mechanism is proposed to be:

$$2AA \xrightarrow{k_2} dimer$$
$$2(2EHA) \xrightarrow{k_3} dimer$$

(4.23)

Some of the dimer molecules formed may transform into polymer. Assuming that each reaction step is elementary, the corresponding rate expression can be written as follows:

$$r_{2,AA} = -k_2 (a_{AA})^2$$

(4.24)

$$r_{3,2EHA} = -k_3 (a_{2EHA})^2$$

(4.25)

Where k_2 and k_3 are the rate constants for the polymerisation of AA and 2EHA respectively. The reaction rate constants, k_2 and k_3 were determined using the non − linear regression analysis in POLYMATH 6.10 program

It was found that the AA polymerisation occurred profoundly when the reaction temperature was more than 358 K. k_2 can be related with temperature using:

$$k_2 = 5.05 \times 10^4 \exp(-39054/(RT)) \text{ mol/L.min}$$

(4.26)

The polymerisation of 2EHA only significant when the reaction temperature was 388 K and the rate constant, k_3=0.023 mol/L.min. The parity plot for the AA concentration after considering the polymerisation as shown in Figure 4.24 (b) depicts that the most of the errors between the predicted C_{AA} and experimental C_{AA} are within ±5%. This is verified by the statement of Altiokka and Odes (2009) in which the AA esterification reaction will never be held without the polymerisation side reactions.
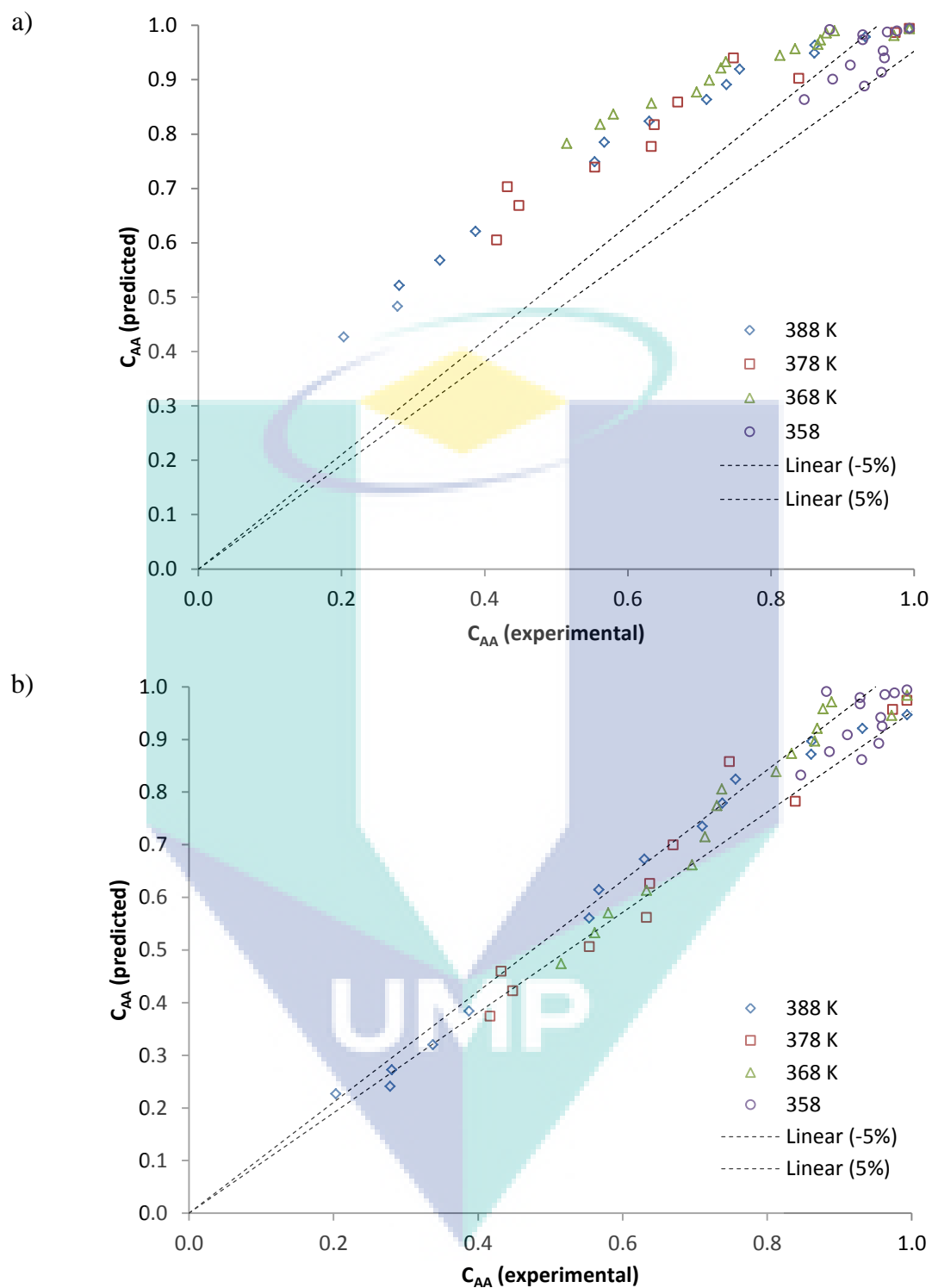
Figure 4.24 : Parity plot for the experimental and predicted rate of reaction of LHHW;
a) without considering polymerization of AA, b) considering
polymerization of AA (○358 K △368 K □378 K ◇388 K; dotted line
stand for ±5% error)

Using the numerical values of the reaction rate constants, Eq 4.17 was solved simultaneously by applying Runge–Kutta method for the chosen temperature. The concentration–time data based on the model were obtained under given reaction conditions. A reasonably good agreement between the predicted and experimental value of concentration are shown in Figure 4.25. The comparison of the predicted and experimental concentration-time data for other reaction conditions are given in Appendix G.
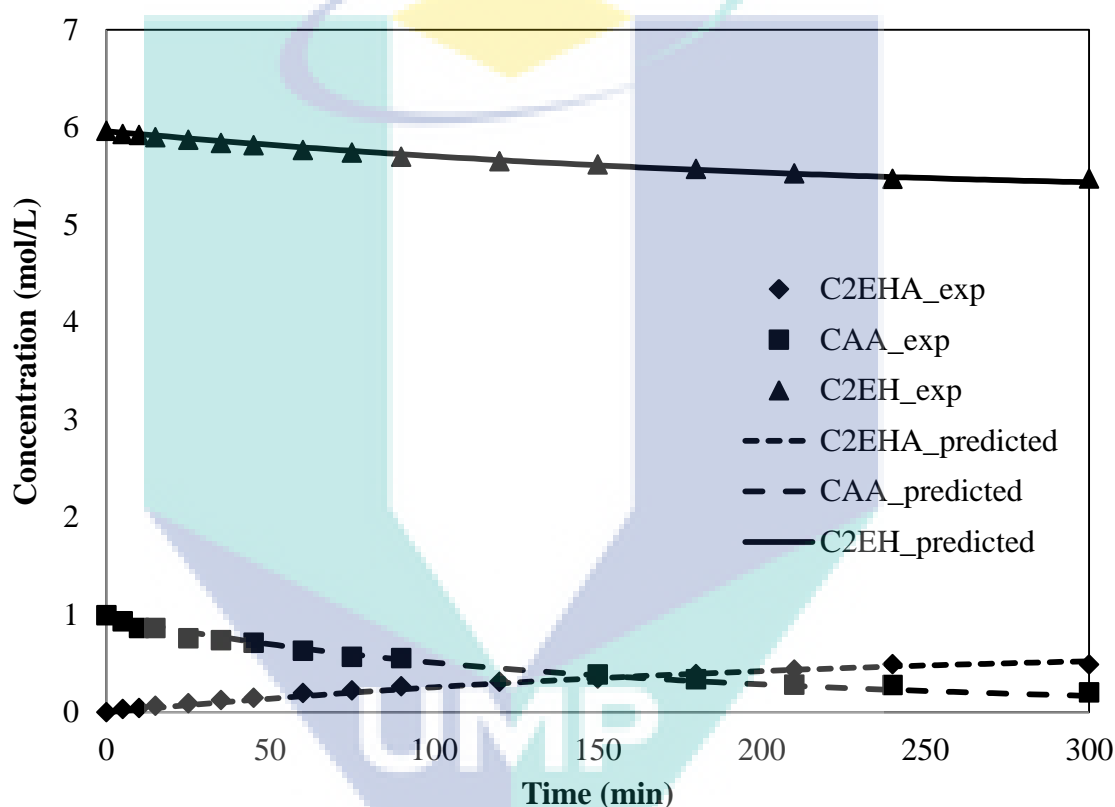
Figure 4.25 : Comparison between experimental and calculated (with ER model considering polymerization of AA) concentration profiles. Molar ratio of AA to 2EH is 1:6, temperature at 388 K, catalyst loading is 10% w/w and stirring speed at 400 rpm.

The developed kinetic models were used to fit the experimental data generated under different initial molar ratio to examine the model viability. Figure 4.25 shows that the kinetic rate constant for the main esterification reaction increases with the increase of $M_{2EH/AA}$ from 1 to 3. The excess 2EH has provided a driving force to shift the reaction to the product side. However, the kinetic rate constant decreases when the

$M_{2EH/AA}$ is further increased to 7. The excess of bulk molecule, 2EH has hindered the adsorption of AA on the catalyst surface and hence promoting the polymerisation reaction. This is indicated by the increase of the rate constant for the polymerisation reaction as shown in Figure 4.26. This phenomenon did not occur in the esterification reaction using simple alcohols such as methanol, ethanol and butanol. The rate of the these reactions increased with the rise in the amount of excess alcohol (Delgado *et al.*, 2007; Lee *et al.*, 2002; Sanz *et al.*, 2002; Singh and Sachan, 2013). The parity plots of the predicted and experimental value for C_{AA} and C_{2EHA} are shown in Figure 4.27-4.28. The experimental data is in good agreement with the predicted value.

Then, the improved kinetic model was again adopted toward different condition of initial molar ratio to check the viability of the kinetic toward different condition of system. The parity plot of the predicted and experimental value was plotted in Figure 4.28 show the dependability of the kinetic model to all condition regardless the temperature and molar ratio.
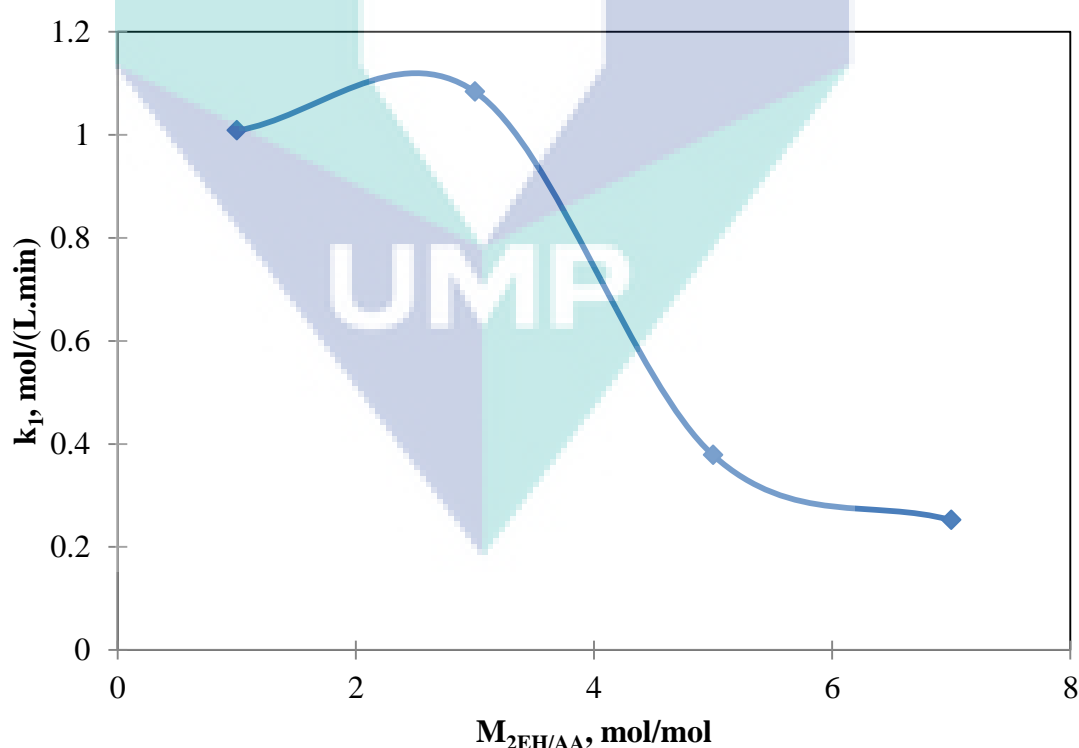
Figure 4.26: Effect of different molar ratio on the main esterification reaction rate constant. The reaction was carried out at the temperature of 388 K, catalyst loading of 10% w/w and stirring speed of 400 rpm.
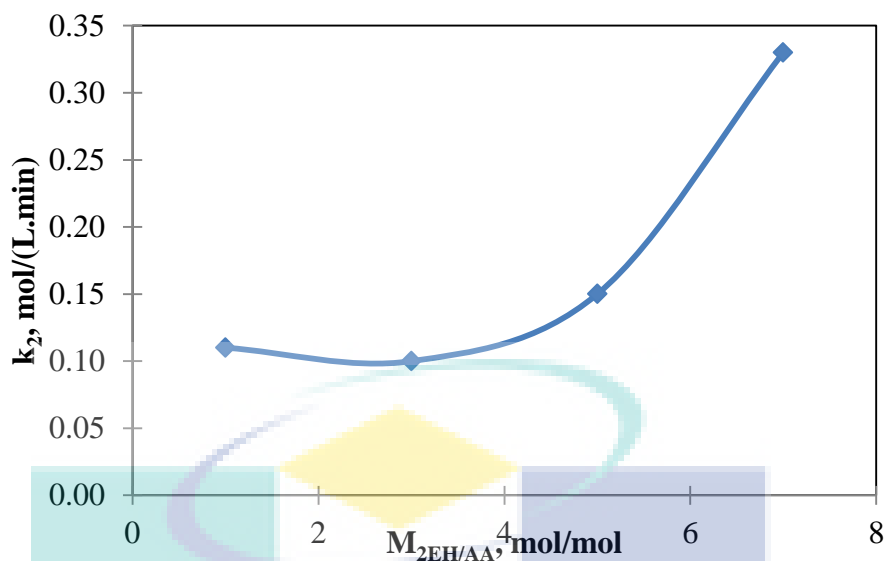
Figure 4.27: Effect of different molar ratio on the polymerisation reaction rate constant. The reaction was carried out at the temperature of 388 K, catalyst loading of 10% w/w and stirring speed of 400 rpm.
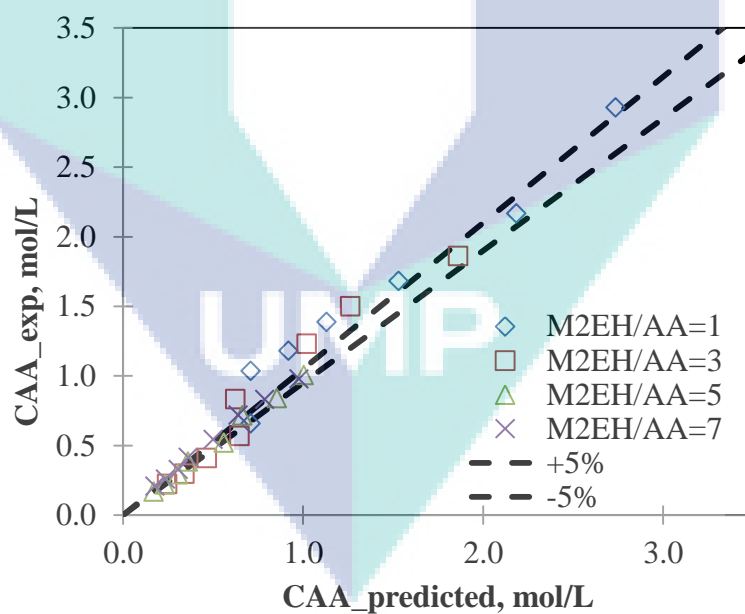
Figure 4.28 : Comparison between experimental and calculated (for ER model considering polymerization of AA) C_{AA} profiles for different molar ratio of AA to 2EH at temperature at 388 K, catalyst loading is 10% w/w and stirring speed at 400 rpm.
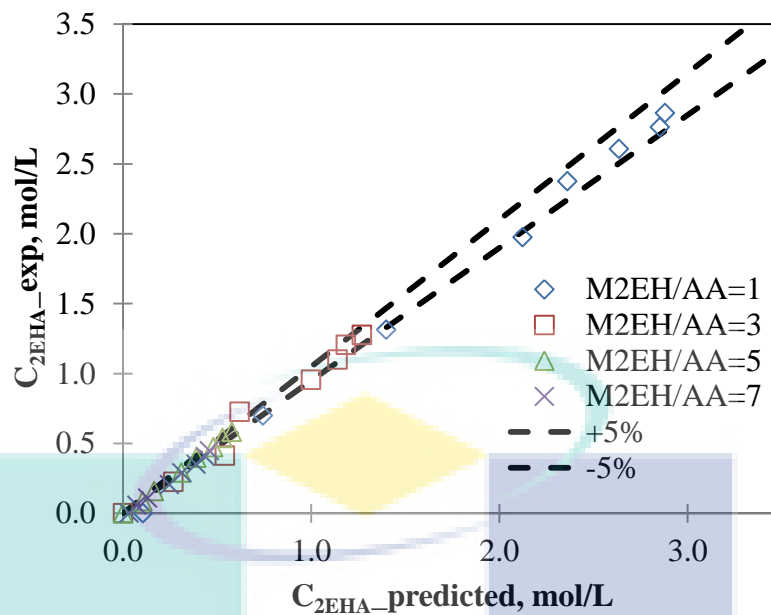
Figure 4.29 : Comparison between experimental and calculated (for ER model considering polymerization of AA) C_{2EHA} profiles for different molar ratio of AA to 2EH at temperature at 388 K, catalyst loading is 10% w/w and stirring speed at 400 rpm.

4.6.3 Water Inhibition

Due to the immiscibility of water with 2EH, most of the AA was distributed in 2EH of the reaction mixture with diluted AA. Therefore, the presence of water did not affect the equilibrium of the reaction. However, water would inhibit the activity of the Amberlyst 15 since this catalyst was well dispersed in the reaction mixture. Water has a large affinity for SO_3H of the ion exchange resin catalyst and it adsorbs preferably on acid sites, excludes the reactants and inhibits greatly the reaction rate (Bringue *et al.,* 2007). Water effect on the reaction rate was modelled by correction factors analogous to expressions derived from Langmuir isotherms as shown in Eq. 4.27. The correction factor represents the catalyst activity. Eq. 4.28 shows the kinetic models incorporated with the correction factors.

$$\frac{k_{W0}}{1 + K_W a_W} \tag{4.27}$$

$$r_{2EHA} = \left(\frac{k_f \left(a_{AA} a_{2EH} - \frac{a_{2EHA} a_W}{K_{eq}} \right)}{(1 + K_{AA} a_{AA} + K_W a_W)} \right) * \frac{k_{W0}}{1 + K_W a_W} \tag{4.28}$$

Figure 4.29 depicts the corresponding ratio of initial rate for the reaction using dilute AA to the initial rate for the reaction using pure AA. It shows that the presence of 10 wt% of water does not inhibit the activity of the catalyst. The activity of the catalyst is significantly decreased when the initial water concentration is more than 10 wt%. The activity remains constant for the water initial content of 40-80 wt%. The activity of the catalyst is almost negligible when the water concentration is 90 wt%. A more severe poisoning occurred due to the deposition of substantial amount of poly-acrylic acid when the initial water concentration is 90 wt%. The corresponding correction factor for different initial water concentration is shown in Figure 4.30. This concluding remark is supported by the SEM results as reported in section 4.5.2.

The esterification reaction of the dilute AA with 2EH was simulated using the corrected kinetic model. The comparisons of the simulation results with the experimental C_{2EHA} are shown in Figure 4.32 (a) and (b) for the dilute AA with different AA concentrations. The points scattered between ±5% errors indicates a good agreement between the predicted and experimental results. The comparison of the predicted and experimental concentration-time data for the reaction study with different AA concentration is appended is Appendix H.
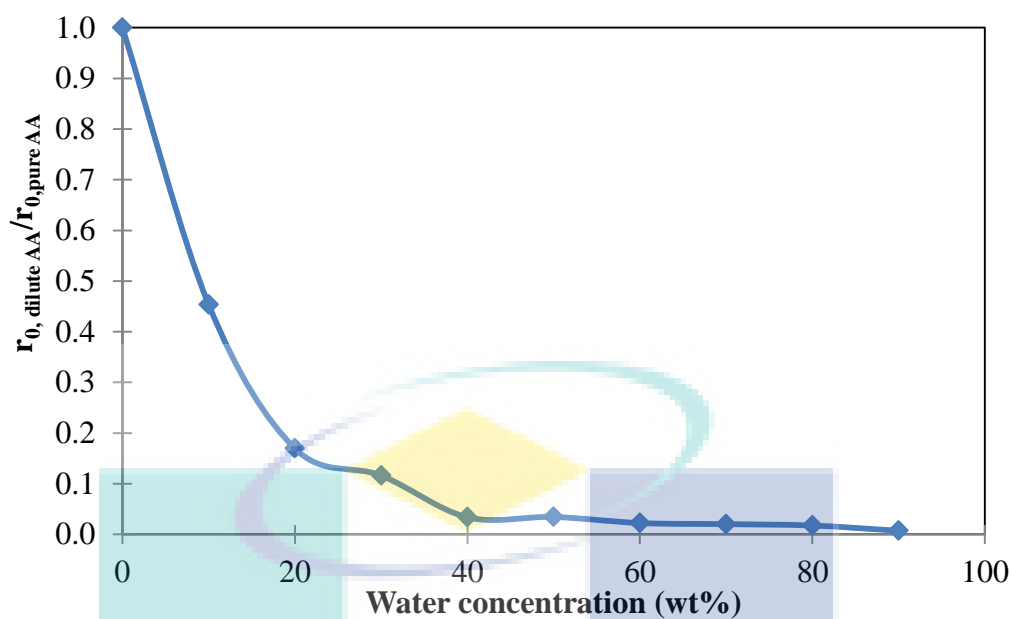
Figure 4.30 : Water inhibition correction factor at different initial water content in the reaction mixture under 373 K, molar ratio of AA:2EH, 1:3, catalyst loading of 10 % w/w, with 400 rpm stirring speed.
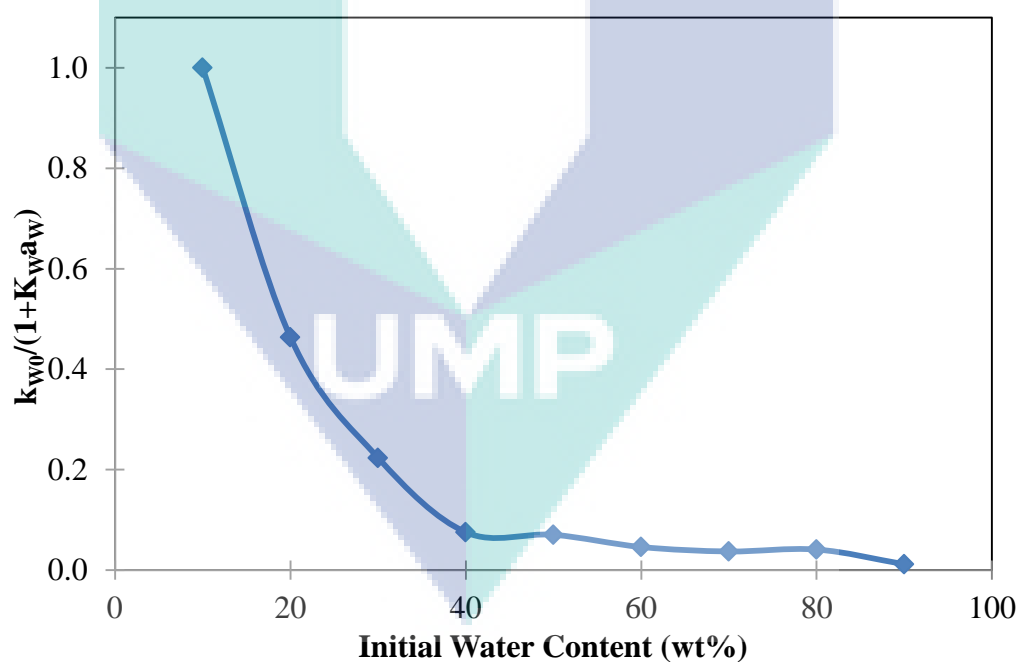
Figure 4.31 : Water inhibition correction factor at different initial water content in the reaction mixture under 373 K, molar ratio of AA:2EH, 1:3, catalyst loading of 10 % w/w, with 400 rpm stirring speed.
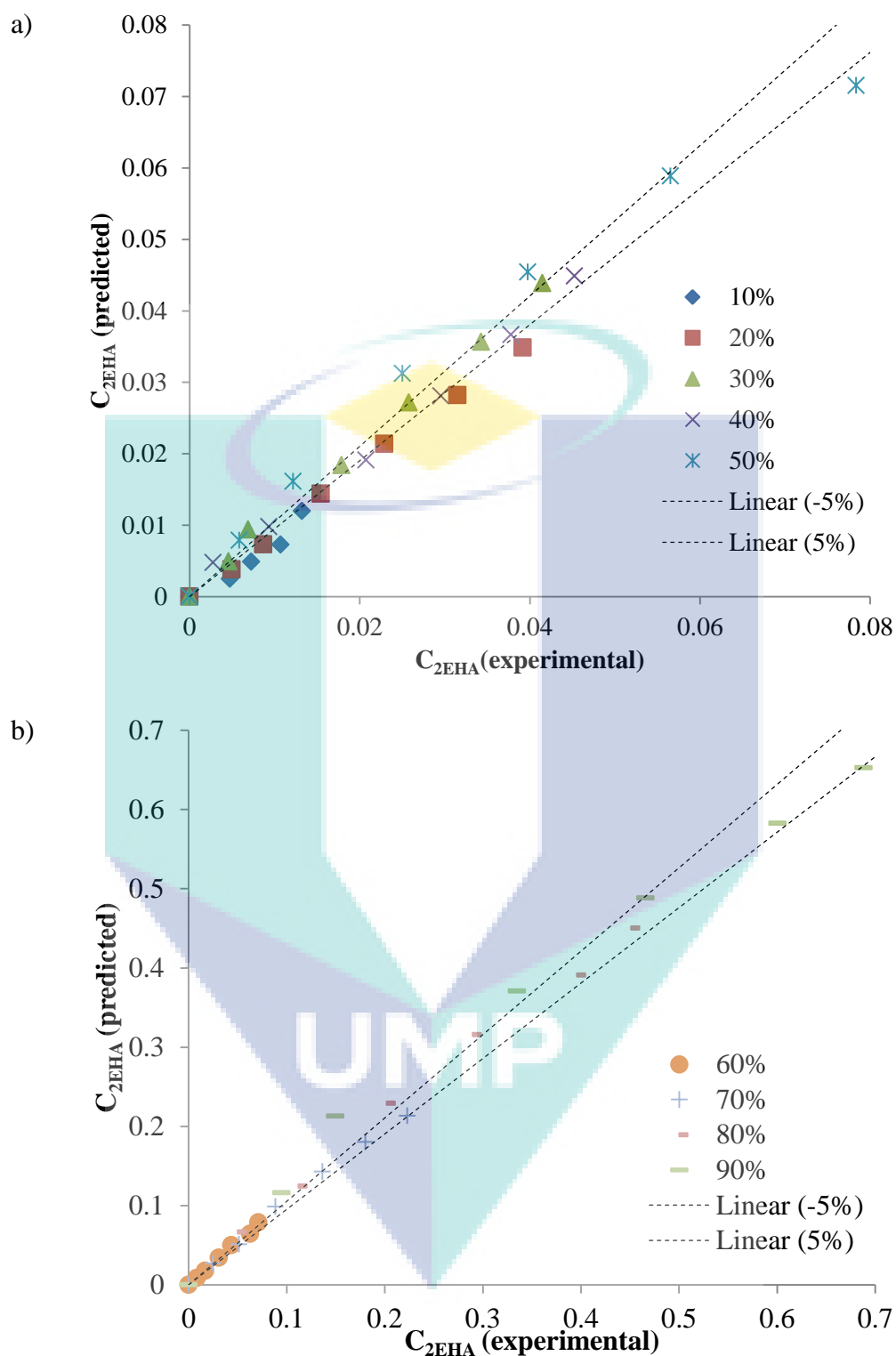
Figure 4.32 : Parity plot of predicted vs experimental 2EHA concentration, a) 10 – 50 % AA; b) 60 – 90 % AA, under 373 K, molar ratio of AA:2EH, 1:3, catalyst loading of 10% w/w, with 400 rpm stirring speed.

CHAPTER 5

CONCLUSIONS

5.1 CONCLUSIONS

The Amberlyst 15 catalysed esterification of AA with 2EH at the temperature ranged from 358 K to 388 K, initial molar ratios of AA:2EH ranged from 7:1 to 1:7 and catalyst loading ranged from 1 to 15 wt% was investigated experimentally. It was carried out in a stirred batch reactor under the reaction conditions which were not limited by mass transfer. Among the important operating variables, reaction temperature has significantly affected the conversion of AA and the yield of 2EHA. The highest yield was obtained at the temperature of 388 K, initial molar ratio of AA:2EH of 1:3 and catalyst loading of 10 wt%.

The heterogeneously catalysed esterification of 2EH with AA solutions with different concentrations was studied using two different experimental setups. The yield of reactions with the AA concentrations ranged from 30-80 wt% was increased significantly when the experimental setup with continuous water removal (CWR) was used. It did not happen in the reactions with the AA concentrations ranged from 10-20 wt% due to the catalyst poisoning. The catalyst was poisoned by the poly-acrylic acid deposits as validated by the catalyst characterisation results. AA could be potentially recovered from the waste water using the setup with CWR. The dilute AA waste water (10-20 wt%) should be concentrated or large molar ratio of 2EH to AA should be adopted to prevent the formation of poly-acrylic acid.

The increase of the equilibrium constant and equilibrium conversion with temperature indicated that the esterification of AA with 2EH an endothermic reaction.

The non-ideal PH, ER and LHHW kinetic models were applied to correlate with the experimental kinetic data for batchwise esterification reaction of AA with 2EH in the presence of Amberlyst-15. ER model was found to be the best fit model. Taking into account the esterification reaction and polymerisation of acrylic acid, as well as the correction factor which takes into account the water inhibition effect, the overall rate law well described the kinetic data of both the esterification of pure and diluted AA with 2EH.

This kinetic data is useful for the simulation and design of a reactive distillation column for recovering AA from the waste water stream.

5.2   RECOMMENDATION FOR FUTURE WORK

Based on the present study, AA is potentially to be recovered using RDC. Nevertheless, the important studies to examine the practicability of this method should be further carried out in the future. The recommended studies are included in the following section.

The present study has shown that the conversion of the esterification of AA with 2EH is high but the selectivity is relatively low. This is attributed to the polymerisation of AA. Optimisation study for the amount of the polimerization inhibitor used especially in the diluted AA system should be taken into account in the future.

The substantial amount of poly-acrylic acid formed on the Amberlyst 15 during the esterification reaction study using diluted AA with 10 wt% AA has demonstrated the complex phase equilibrium in the diluted AA system. Further investigation on the phase equilibrium is required to minimise the polymerisation reaction.

The simulation study of the esterification of the diluted AA with 2EH catalysed by Amberlyst 15 could be carried out based on the kinetic model developed in the present study. This reaction also should be tested in a lab scale reactive distillation setup. Finally, all the recommended studies must be done using the real industrial waste water.

REFERENCES

Abdul Rahman, M.B., Jumbri, K., Mohd Ali Hanafiah, N.A., Abdulmalek, E., Tejo, B.A., Basri, M., and Salleh, A.B. 2012. Enzymatic esterification of fatty acid esters by tetraethylammonium amino acid ionic liquids-coated Candida rugosa lipase. *Journal of Molecular Catalysis B: Enzymatic*. **79**: 61−65.

Adam, F., Hello, K.M., and Chai, S.J. 2012. The heterogenization of l-phenylalanine−Ru(III) complex and its application as catalyst in esterification of ethyl alcohol with acetic acid. *Chemical Engineering Research and Design*. **90**(5): 633-642.

Agilent Technologies, 2011, The Essential Chromatography & Spectroscopy Catalog 2011/2012 Edition.

Agreda, V.H. and Lilly, R.D. 1990. *Preparation of ultra high purity methyl acetate*. US4939294.

Agreda V.H., Partin L.R., and Heise W.H. 1990 High-Purity Methyl Acetate via Reactive Distillation, *Chemical Engineering Progress*. **86**: 40-46.

Akbay, E.Ö. and Altıokka, M.R. 2011. Kinetics of esterification of acetic acid with n-amyl alcohol in the presence of Amberlyst-36. *Applied Catalysis A: General*. **396**(1-2): 14−19.

Allen, S.J., Koumanova, B., Kircheva, Z., and Nenkova, S. 2005. Adsorption of 2-nitrophenol by technical hydrolysis lignin: kinetics, mass transfer, and equilibrium studies. *Industrial & Engineering Chemistry. Res.*. **44:** 2281−2287.

Allison, M., Singh, K., Webb, J., and Grant, S. 2011. Treatment of Acrylic Acid Production Wastewater Using a Submerged Anaerobic Membrane Bioreactor. *Proceedings of the Water Environment Federation, WEFTEC 2011: Session 101 through Session*. **110**: pp. 6554-6564(11).

Altıokka, M.R. and Ödeş, E. 2009. Reaction kinetics of the catalytic esterification of acrylic acid with propylene glycol. *Applied Catalysis A: General*. **362**(1-2): 115−120.

Ayranci, E. and Duman, O. 2006. Adsorption of aromatic organic acids onto high area activated carbon cloth in relation to wastewater purification. *Journal Hazard Material*. **136**(3): 542-52.

BASF, AG 1988. *Analytisches Labor; unveröffentlichte Untersuchung* (J.Nr. 129304/01 vom 02.09.88).

BASF, AG 1994. *Sicherheitsdatenblatt Acrylsäure rein* (22.08.1994). BASF

Bauer Jr., W., Kroschwitz, J.I., Howe-Grant, M., and Kirk-Othmer, 1991. *Encyclopedia of Chemical Technology*. **vol. 1**. fourth ed., Wiley-Interscience, New York: 287–314.

Berg, L. 1992. *Dehydration of acetic acid by extractive distillation*, US 5167774.

Bhattacharyya, D., Allison, M.J., Webb, J.R., Zanatta, G.M., Singh, K.S., and Grant, S.R. 2013. Treatment of an Industrial Wastewater Containing Acrylic Acid and Formaldehyde in an Anaerobic Membrane Bioreactor. *Journal of Hazardous Toxic and Radioactive Waste*. **17** (2): 74-79.

Bianchi, C.L., Ragaini, V., Pirola, C., and Carvoli, G.A. 2003. New Method to Clean Industrial Water from Acetic Acid Via Esterification, *Journal Applied Catalysis B: Environmental*. **40**: 93–99.

Bock, H., Wozny, G., and Gutsche, B. 1997. Design and control of a reaction distillation column including the recovery system. *Journal Chemical Engineering Process*. **36:** 101–109

Bringué, R., Tejero, J., Iborra, M., Izquierdo, J. F., Fité, C., and Cunill, F. 2007. Water effect on the kinetics of 1-pentanol dehydration to di-n-pentyl ether (DNPE) on amberlyst 70. *Topics in Catalysis*. **45**(1-4): 181–186.

Calvar, N., Gonzalez, B., and Dominquez, A. 2007. Esterification of Acetic Acid with Ethanol: Reaction Kinetics and Operation in a Packed Bed Distillation Column, *Chemical Engineering Process*. **46:** 1317.

Chandrasekhar, S., Narsihmulu, C., and Sultana S.S. 2002. Poly(ethylene glycol) (PEG) as a reusable solvent medium for organic synthesis. *Application in the Heck reaction. Organic Letters*. **4**(25): 4399-4401.

CHEMSAFE. *National database for safety data of the Physikalisch-technische Bundesanstalt Braunschweig*, established by expert judgement.

Chen, X., Xu, Z., and Okuhara, T. 1999. Liquid phase esterification of acrylic acid with 1-butanol catalyzed by solid acid catalysts. *Applied Catalysis A: General*. **180:** 261-269

Chiang, W. and Huang, C. 1993, Separation of liquid mixtures by using polymer membranes. IV. water-alcohol separation by pervaporation through modified acrylonit- rile grafted polyvinyl alcohol copolymer (PVA-G-AN) membranes. *Journal of Applied Polymer Science* **48**: 199-203.

Chiang, W.Y. and Hu, C.M. 1991. Separation of liquid mixtures by using polymer membranes. I. Water/alcohol separation by pervaporation through PVA-G-MMA:MA membrane. *Journal of Applied Polymer Science*. **43**: 2005-2012.

Choi, J., and Hong, W.H. 1999. Recovery of lactic acid by batch distillation with chemical reactions using ion exchange resin. *Journal of Chemical Engineering of Japan*. **32**: 184-189.

Chubarov, G.A., Danov, S.M., Logutov, V.I., and Obmelyukhina, T.N. 1984. Esterification of acrylic acid with methanol. *Journal of Applied Chemistry of the USSR*. **57**: 192–193.

Cordeiro, C.S., Arizaga, G.G.C., Ramos, L.P., and Wypych, F. 2008. A new zinc hydroxide nitrate heterogeneous catalyst for the esterification of free fatty acids and the transesterification of vegetable oils. *Catalysis Communications*. **9**: 2140–2143

Cunill, F., Ibbora, M., Fite, C., Tejero, J., and Izquierdo, J.F. 2000. Conversion, selectivity and kinetics of the addition of isopropanol to isobutene catalyzed by a macroporous ion-exchange resin. *Industial & Engineering Chemistry. Res.*. **39**: 1235-1241.

David, M.O., Nguyen, Q.T., and Neel, J. 1992. Pervaporation membranes endowed with catalytic properties based on polymer blends, *Journal of Membrane Science.* **73:** 129-141.

Delgado, P., Sanz, M. T., and Beltrán, S. 2007. Kinetic study for esterification of lactic acid with ethanol and hydrolysis of ethyl lactate using an ion-exchange resin catalyst. *Journal Chemical Engineering Journal.* **126**(2-3): 111–118.

Demirbas, A. 2008. Biofuels sources, biofuel policy, biofuel economy and global biofuel projections. *Journal Energy Conversion and Management*. **49**: 2106–2116.

Devulapelli, V. G. and Weng, H.-S. 2009. Esterification of 4-methoxyphenylacetic acid with dimethyl carbonate over mesoporous sulfated zirconia. *Catalysis Communications*. **10**(13): 1711–1717.

Dirk-Faitakis, C.B., An, W., Lin, T.B., and Chuang, K.T. 2009. Catalytic distillation for simultaneous hydrolysis of methyl acetate and etherification of methanol. *Journal Chem. Eng. Process.* **48**: 1080–1087.

Disteldorf, W., Peters, J., Morsbach, B., Kummer, M., and Rühl, T. 2002. *Method for the production of phthalic anhydride to a specification.* BASF, WO/2002/064539

Dupont, P. Vcdrine, J. C. Paumard, E. Hecquet, and G. 1995. Heteropolyacids supported on activated carbon as catalysts for the esterification of acrylic acid by butanol, *Journal Applied Catalysis A: General*. **129**(2): 17-227

ECETOC, 1995. *European Centre for Ecotoxicology and Toxicology of Chemicals. Acrylic Acid.* CAS No. 79-10-7. Joint Assessment of Commodity Chemicals No. 34. ECETOC, Brussels.

Essayem, N., Martin, V., Riondel, A., and Védrine, J.C. 2007. Esterification of acrylic acid with but-1-ene over sulfated Fe- and Mn-promoted zirconia. *J. Applied Catalysis A: General.* **326**(1): 74–81.

Faber, K. 1997. *Biotransformations. In Organic Chemistry*: A Textbook, 3rd Ed.; Springer-Verlag: Berlin, Germany,

Falbe, J., Rebitz, M., and Römpp, H. 1995. *Römpp Chemie Lexikon*. Thieme, Stuttgart

Farnetti, E., Monte, R.D., and Kaspar, J. 2004. Homogeneous and Heterogeneous Catalyst. *J. Inorganic and Bio-inorganic Chemistry*, **2**(2)

Fernandes, S.A., Cardoso, A.L., and José da Silva, M. 2012. A novel kinetic study of $H_3PW_{12}O_{40}$-catalyzed oleic acid esterification with methanol via ^1H NMR spectroscopy. *J. Fuel Processing Technology.* **96**: 98–103

Fogler, H.S. 2008. *Elements of Chemical Reaction Engineering* Fourth Edition, United State of America, Pearson Education.

Fomin, V.A., Etlis, I.V., and Kulemin, V.I. 1991. Some aspects of esterification of acrylic acid with 2-ethylhexyl alcohol on sulfonic cation-exchangers. *Journal Applied Chemistry. USSR*. **64**: 1811–1815.

Fox, M., Gibson, T., Mulach, R., and Sasano, T. 1990. *CEH Marketing research report*. SRI International.

Gangadwala, J., Mankar, S., Mahajani, S., Kienle, A., and Stein, E. 2003. Esterification of Acetic Acid with Butanol in the Presence of Ion-Exchange Resins as Catalysts, *J. Ind. Eng. Chem. Res.* **42**: 2146–2155.

Garcia, T., Coteron, A., Martinez, M., and Aracil, J. 2000. Kinetic model for the esterification of oleic acid and cetyl alcohol using an immobilized lipase as catalyst. *J. Chemical Engineering Science*. **55**: 1411-1423.

Gerpen, J.V. 2005. Biodiesel processing and production. *Journal Fuel Processing Technology*. **86**: 1097–1107.

Gómez-Castro, F.I., Rico-Ramírez, V., Segovia-Hernández, J.G., and Hernández-Castro, S. 2011. Esterification of fatty acids in a thermally coupled reactive distillation column by the two-step supercritical methanol method. *Journal Chemical Engineering Research and Design*. **89**(4): 480–490.

Gonçalves, C.E., Laier, L.O., Cardoso, A.L., and Silva, M.J. 2012. Bioadditive synthesis from $H_3PW_{12}O_{40}$-catalyzed glycerol esterification with HOAc under mild reaction conditions. *Journal Fuel Processing Technology*. **102**: 46–52.

Gorak, A., Hoffmann, A., and Kreis, P. 2007. Prozessintensivierung: Reaktive und Membran- unterstützte Rektifikation. *Journal Chemical Engineering & Technology*. **79**: 1581-1600.

Gref, R., Nguyen, Q.T., Schaetzel, P., and Neel, J. 1993. Transport properties of poly (vinyl alcohol) membranes of different degrees of crystallinity. I. Pervaporation results. *Journal Appl. Polym. Sci*. **49**: 209-218.

Haas, M.J. 2005. Improving the economics of biodiesel production through the use of low value lipids as feedstock: vegetable oil, soapstock. *Fuel Processing Technology*. **86**: 1087–1096.

Hanika, J., Smejkal, Q., and Kolena, J. 2001. 2-Methylpropylacetate synthesis via catalytic distillation. *Catalysis Today*. **66**(2-4): 219–223.

Harmer, M.A. and Sun, Q. 2001. Solid acid catalysis using ion-exchange resins. *Journal Applied Catalysis A: General*. **221**: 45–62.

Hayashi, S., Hirai, T., Hayashi, F., and Hojo, N. 1983. Permeation characteristics of poly(vinyl alcohol) poly(vinyl acetate) composite porous membranes. *Journal Applied Polymer Science*. **28**: 3041-3048.

Hino, M. and Arata, K. 1981. Synthesis of esters from acetic acid with methanol, ethanol, propanol, butanol and iso-butyl alcohol catalysed by solid superacid. *Chemistry Letter*. 1671–1672.

Hoechst Celanese Corp. 1992. *Material Safety Data Sheet: 2-Ethylhexyl Acrylate (41)*, Dallas, TX

Hsiue, G.H., Yang, Y.S., and Kuo, J.F. 1987. Permeation and separation of aqueous alcohol solutions through grafted poly(vinyl alcohol) latex membranes. *Journal Applied Polymer Science*. **34**: 2187–2196.

Hui Y.H. 1996. *Bailey's Industrial Oil and Fat Products*. Wiley-Interscience, New York.

Hüls 1995. *Determination of the surface tension.* Unpublished test report (Report No. AN-ASB 0066, 28.06.1995).

ICB Chemical Profile, 2008, Acrylic Acid Uses and Market Data. http://www.icis.com/v2/chemicals/9074870/acrylic+acid/uses.html, (13 October 2013)

Ingale, M.N. and Mahajani, V.V. 1996. Recovery of Carboxylic Acids, C2-C6, from an Stream using Tributylphosphate (TBP): Effect Aqueous Waste of Presence of Inorganic Acids and their Sodium Salts. *Journal Separation Science Technology.* **6**: 1−7.

Iranpoor, N. and Shekarriz, M. 1999. Ring Opening of Epoxides with Sodium Cyanide Catalyzed with Ce(OTf)₄. *Journal Synthetic Communications*. **29**(13): 2249-2254.

Ishihara, K., Nakayama, M., Ohara, S., and Yamamoto, H. 2001. A green method for the selective esterification of primary alcohols in the presence of secondary alcohols or aromatic alcohols, *SYNLETT*. **7**: 1117-1120

Ishihara, K., Nakayama, M., Ohara, S., and Yamamoto, H. 2002. Direct ester condensation from a 1:1 mixture of carboxylic acids and alcohols catalyzed by hafnium(IV) or zirconium(IV) salts. *Journal Tetrahedron.* **58**: 8179-8188

Ishihara, K., Ohara, S., and Yamamoto, H. 2000 Direct condensation of carboxylic acids with alcohols catalyzed by hafnium(IV) salts. *Journal Science*. **290**: 1140-1142.

Izci, A. and Bodur, F. 2007. Liquid Phase Esterification of Acetic Acid with iso-Butanol Catalyzed by Ion Exchange Resins. *Reactive and Functional Polymers* **67**(12): 1458−1464.

Jagadeeshbabu, P.E., Sandesh, K., and Saidutta, M.B. 2011. Kinetics of Esterification of Acetic Acid with Methanol in the Presence of Ion Exchange Resin Catalysts. *Journal of Industrial Engineering Chemistry. Res.* **50:** 7155−7160.

Jaques, D. and Leisten, J.A. 1964. Acid-catalysed ether fission. Part II. Diethyl ether in aqueous acids. *J. Chem. Soc.* 2683-2689

Johannessen, T., Larsen, J.H., Chorkendorff, I., Livbjerg, H., and Topsøe, H. 2000. Catalyst dynamics: consequences for classical kinetic descriptions of reactors. *Journal Chemical Engineering Journal*. **82**(1-3): 219- 230.

Kadaba, P.K. 1974. New compounds: Convenient selective esterification of aromatic carboxylic acids bearing other reactive groups using a boron trifluoride etherate—alcohol reagent. *Journal of Pharmaceutical Sciences*. **63**(8): 1333-1335

Katz, M.G. and Wydeven, T. 1982. Selective permeability of PVA membranes. II. Heat treated membranes. *Journal Applied Polymer Science*. **27**: 79-87.

Keshav, A., Chand, S., and Wasewar, K.L. 2009. Recovery of propionic acid from aqueous phase by reactive extraction using quarternary amine (Aliquat 336) in various diluents. *Chemical Engineering Journal*. **152**(1), 95–102.

Khurana, J.M., Sahoo, P.K., and Maitkap, G.C. 1990. *Synth. Commun.*. **20**, 2267.

Kimura, T. and Ito, Y. 2001. Two bacterial mixed culture systems suitable for degrading terephthalate in wastewater. *Journal Bioscience Bioengineering*. **91**: 416–418.

Kiss, A.A. 2011. Heat-integrated reactive distillation process for synthesis of fatty esters. *Fuel Processing Technology*. **92:** 1288–1296.

Klein, G., Houérou, V.L., Muller, R., Gauthier, C., and Holl, Y. 2012. Friction properties of acrylic-carboxylated latex films. 1. Effects of acrylic acid concentration and pH *Tribology International*. **53**: 142–149.

Kojima, Y., Fruhata, K.I., and Miyasaka, K. 1985. Sorption and permeation of iodine in water-swollen poly (vinyl alcohol) membranes and iodine complex formation. *Journal Applied Polymer Science*. **30**: 1617-1628.

Komoń, T., Niewiadomski, P., Oracz, P., and Jamróz, M.E. 2013. Esterification of acrylic acid with 2-ethylhexan-1-ol: Thermodynamic and kinetic study. *Journal Applied Catalysis A: General*. **451**: 127– 136.

Kraai, G.N., Winkelman, J.G.M., de Vries, J.G., and Heeres, H. J. 2008. Kinetic studies on the Rhizomucor miehei lipase catalyzed esterification reaction of oleic acid with 1-butanol in a biphasic system. *Journal Biochemical Engineering*. **41**(1): 87–94.

Kudła, S. and Kaledkowska, M. 1998. Production and Use of Acrylic-Acid and It's Esters. *Przemysl Chemiczny*. **77**(3): 86–91.

Kuila, S. B. and Ray, S. K. 2011. Dehydration of acetic acid by pervaporation using filled IPN membranes, *J. Separation and Purification Technology*. **81**: 295–306.

Kumar, A., Prasad, B., and Mishra, I.M. 2008. Optimization of process parameters for acrylonitrile removal by a low-cost adsorbent using Box–Behnken design. *Journal of Hazardous Materials*. **150**: 174–182.

Kumar, M.V.P. and Kaistha, N. 2009. Evaluation of ratio control schemes in a two-temperature control structure for a methyl acetate reactive distillation column. *J. Chemical Engineering Research and Design*. **87**(2): 216–225.

Lam, M.K., Lee, K.T., and Mohamed, A.R. 2010. Homogeneous, heterogeneous and enzymatic catalysis for transesterification of high free fatty acid oil (waste cooking oil) to biodiesel: A review. *J. Biotechnology advances*, **28**(4), 500–18.

Lee, L.S. and Kuo, M.Z. 1996. Phase and reaction equilibria of the acetic acid-isopropanol-isopropyl acetate-water system at 760 mmHg. *J. Fluid Phase Equilibrium*. **123**: 147–165.

Lee, M., Chiu, J., and Lin, H. 2002. Kinetics of Catalytic Esterification of Propionic Acid and n -Butanol over Amberlyst. *J. Ind. Eng. Chem. Res*. **35**: 2882–2887.

Lei, Z., Li, C., Li, Y., and Chen, B. 2004. Separation of acetic acid and water by complex extractive distillation. *J. Separation and Purification Technology*. **36**(2): 131–138.

Li, S., Zhuang, J., Zhi, T., Chen, H., and Zhang, L. 2008. Combination of complex extraction with reverse osmosis for the treatment of fumaric acid industrial wastewater. *Desalination*. **234**: 362–369.

Li, S.J., Chen, H.L., and Zhang, L. 2009. Recovery of fumaric acid by hollow-fiber supported liquid membrane with strip dispersion using trialkylamine carrier. *J. Separation and Purification Technology*. **66**: 25–34.

Liljaa, J., Murzina, D.Y., Salmia, T., Aumoa, J., Mäki-Arvelaa, P., and Sundell, M. 2002. Esterification of different acids over heterogeneous and homogeneous catalysts and correlation with the Taft equation. *Journal of Molecular Catalysis A: Chemical*. **182–183**, 555–563.

Lutze, P., Dada, E.A., Gani, R., and Woodley, J.M.. 2010. Heterogeneous catalytic distillation – a patent review. *Rec. Pat. Chem. Eng*. **3**: 208-229.

Mahajan, Y. S., Shah, A. K., Kamath, R. S., Salve, N. B., and Mahajani, S. M. 2008. Recovery of trifluoroacetic acid from dilute aqueous solutions by reactive distillation. *J. Separation and Purification Technology*. **59**(1), 58−66.

Malshe, V.C. and Chandalia, S.B. 1977. Kinetics of liquid-phase esterification of acrylic-acid with methanol and ethanol. *J. Chemical Engineering Science*. **32**: 1530−1531.

Manabe, K., Iimura, S., Sun, X.M., and Kobayashi, S. 2002. Dehydration reactions in water. Brønsted acid-surfactant-combined catalyst for ester, ether, thioether, and dithioacetal formation in water. *J. Am. Chem. Soc.* **124**: 11971−11978.

Merchant, S.Q., Almohammad, K.A., Al Bassam, A.A.M., and Ali, S. H. 2013. Biofuels and additives: Comparative kinetic study of Amberlite IR 120-catalyzed esterification of ethanol with acetic, propanoic and pentanoic acids to produce eco-ethyl-esters. *J. Fuel*. **111**: 140−147.

Merck Index, 1996. *The Merck Index.* 12th edition. Merck & Co., Inc., Whitehouse Station, NJ. Miller

Neier W., 1991, *Ion exchangers as catalysts*, in: K. Dorfner (Ed.), Ion Exchangers, Walter de Gruyter, p. 981.

Neumann, R. and Sasoon, Y. 1984. Recovery of dilute acetic acid by esterification in a packed chemorectification column. *J. Ind. Eng. Chem. Process Des. DeV.*. **23** (4), 654-659.

Nowak, P. 1999. Kinetics of The Liquid Phase Esterification of Acrylic Acid With n Octanol and 2-ethylhexanol catalyzed by Sulphuric Acid. *J. React. Kinetic Catalyst Lett.* **66**(2): 375-380.

Ogawa, T., Hikasa, T., Ikegami, T., Ono N., and Suzuki, H. J. (1994). Selective Activation of Primary Carboxylic Acids by Electron-rich Triarylbismuthanes. Application to Amide and Ester Synthesis under Neutral Conditions. *Chem. Soc.*, Perkin Trans. **1**, 3473-3478.

Ohya, H., Matsumoto, K., Negishi, Y., Hino, T., and Choi, H.S. 1992. The separation of water and ethanol by pervaporation with PVA-PAN composite membranes. *J. Memb. Sci.* **68**: 141-148.

Okuhara, T. 2002. New catalytic functions of heteropoly compounds as solid acids. *J. Catal. Today*. **73**: 167-176

Orjuela, A., Yanez, A. J., Santhanakrishnan, A., Lira, C. T., and Miller, D. J. 2012. Kinetics of mixed succinic acid/acetic acid esterification with Amberlyst 70 ion exchange resin as catalyst. *Chemical Engineering Journal*. **188**: 98–107.

Osorio-Viana, W., Duque-Bernal, M., Fontalvo, J., Dobrosz-Gómez, I., and Gómez-García, M.Á. 2013. Kinetic study on the catalytic esterification of acetic acid with isoamyl alcohol over Amberlite IR-120. *J. Chemical Engineering Science*. **101**: 755–763.

Otera, J.; Dan-oh, N.; and Nozaki, H. 1991. Distannoxane-catalysed transesterification of 1,n-diols. Selective transformation of either of chemically equivalent functional groups. *J. Chem. Soc., Chem. Commun.* 1742-1743.

Pappu, V.K.S., Yanez, A.J., Peereboom, L., Muller, E., Lira, C.T., and Miller, D.J. 2011. A kinetic model of the Amberlyst-15 catalyzed transesterification of methyl stearate with n-butanol. *J. Bioresource technology*. **102**(5): 4270–4272.

Pappu, V.K.S., Kanyi, V., Santhanakrishnan, A., Lira, C.T., and Miller, D.J. 2013. Butyric acid esterification kinetics over Amberlyst solid acid catalysts: The effect of alcohol carbon chain length. *J. Bioresource Technology*. **130**: 793–797

Park, D.W., Haam, S., Ahn, I.S., Lee, T.G., Kim, H.S., and Kim, W.S. 2004. Enzymatic esterification of beta-methylglucoside with acrylic/methacrylic acid in organic solvents. *Journal of biotechnology.* **107**: 151–160.

Paul, J.M. and Samuel, Y. 1995. *Method of manufacturing secondary butyl acrylate by reaction of acrylic acid and butene isomers*. M. Esch, European Patent, No.745579

Paumard, E. 1990. *Heteropolyacid catalysts in the preparation of esters of unsaturated carboxylic acids, The preparation of unsaturated carboxylic acid esters by liquid phase trans-esterification using heteropolyacids as catalysts*. French Patent FR PP.007.368.

Peters, T.A., Benes, N.E., Holmen, A., and Keurentjes, J.T.F. 2006. Comparison of commercial solid acid catalysts for the esterification of acetic acid with butanol *Appl. Catalyst. A: General*. **297**: 182–188.

Peykova, Y., Lebedeva, O.V., Diethert, A., Müller-Buschbaum, P., and Willenbacher, N. 2012. Adhesive properties of acrylate copolymers: effect of the nature of the substrate and copolymer functionality. *Int. J. Adhes. Adhes.* **34**: 107–116.

Ping, Z., Nguyen, Q.T., and Neel, J. 1994. Investigation of poly(vinyl alcohol):poly(N-vinyl-2)-pyrolidone blends. 3. Permeation properties of polymer blend membranes. *Macromol. Chem. Phys.* **195**: 2107-2116.

Qu, Y., Peng, S., Wang, S., Zhang, Z., and Wang, J. 2009. Kinetic Study of Esterification of Lactic Acid with Isobutanol and n-Butanol Catalyzed by Ion-exchange Resins. *Chinese Journal of Chemical Engineering*. **17**(5): 773–780.

Ragaini, V., Bianchi, C.L., Pirola, C., and Carvoli, G. 2006. Increasing the value of dilute acetic acid streams through esterification. *Applied Catalysis B: Environmental*. **64**(1-2): 66–71.

Rahmanian, A., and Ghaziaskar, H.S. 2008. Selective extraction of maleic acid and phthalic acid by supercritical carbon dioxide saturated with trioctylamine. *The Journal of Supercritical Fluids*. **46**(2): 118–122.

Ram R.N. and Charles, I. 1997. Selective Esterification of Aliphatic Nonconjugated Carboxylic Acids in the Presence of Aromatic or Conjugated Carboxylic Acids Catalysed by $NiCl_2.6H_2O$. *J. Tetrahedron*. **53**: 7335.

Rat, M., Zahedi-Niaki, M.H., and Kaliaguine, S.T.O.D 2008. Sulfonic acid functionalized periodic mesoporous organosilicas as acetalization catalysts. *Microporos Mesoporous Mater.* **112**: 26–31.

Rattanaphra, D., Harvey, A. P., Thanapimmetha, A., and Srinophakun, P. 2011. Kinetic of myristic acid esterification with methanol in the presence of triglycerides over sulfated zirconia. *J. Renewable Energy*. **36**(10): 2679–2686.

Rohe, D. 1995. *Märkte und Unternehmen, Acrylsäure, Chemische Industrie* **1**-2/95, pp 12-13.

Rohm, Haas, 2006. *Amberlyst 15 Dry, Product data sheet*. Philadelphia, USA.

Saha, B. and Streat, M. 1999. Transesterification of cyclohexyl acrylate with n -butanol and 2-ethylhexanol: acid-treated clay, ion exchange resins and tetrabutyl titanate as catalysts. *J. Reactive and Functional Polymers*. **40**: 13–27.

Saha, B., Chopade, S.P., and Mahajani, S.M. 2000. Recovery of dilute acetic acid through esterification in a reactive distillation column. *J. Catalysis Today*. **60**: 147–157.

Saha, B. and Sharma, M. 1996. Esterification of formic acid, acrylic acid and methacrylic acid with cyclohexene in batch and distillation column reactors: ion-

exchange resins as catalysts. *J. Reactive and Functional Polymers*. **28**(3): 263–278.

Salem, I.A. (2001). Activation of H_2O_2 by Amberlyst-15 resin supported with copper(II)-complexes towards oxidation of crystal violet. *Chemosphere*, **44**(5), 1109–19.

Santia, V.D., Cardellinia, F., Brinchib, L., and Germani, R. 2012. Novel Brønsted acidic deep eutectic solvent as reaction media for esterification of carboxylic acid with alcohols. *Tetrahedron Letters*. **53**: 5151–5155.

Sanz, M.T., Murga, R., Beltràn, S., and Cabezas, J.L. 2002. Autocatalyzed and Ion-Exchange-Resin-Catalyzed Esterification Kinetics of Lactic Acid with Methanol, *J. Ind. Eng. Chem. Res.* **41**: 512-517.

Sarkar, A., Ghosh, S. K., and Pramanik, P. 2010. Investigation of the catalytic efficiency of a new mesoporous catalyst SnO_2/WO_3 towards oleic acid esterification. *Journal of Molecular Catalysis A: Chemical*. **327**(1-2): 73–79.

Sayyed Hussain, S., Mazhar Farooqui, N., and Gaikwad Digambar, D. 2010. Kinetic and Mechanistic Study of Oxidation of Ester By $KMnO_4$. *International Journal of ChemTech Research*. **2**(1): 242-249.

Scates, M.O., Parker, S.E., Lacy, J.B., and Gibbs, R.K. 1997. *Recovery of acetic acid from dilute aqueous streams formed during carobonylation process.* US Patent 5,599,976

Scholz, N. 2003. Ecotoxicity and biodegradation of phthalate monoesters. *J. Chemosphere.* **53**(8): 921-926

Schwegler, M. A., van Bekkum, H., and de Munck, N. A. 1991. Heteropoly acids as catalysts for the production of phthalate diesters. *Appl. Catal. A*. **74**: 191-204.

Sejidov, F.T., Mansoori, Y., and Goodarzi, N. 2005. Esterification reaction using solid heterogeneous acid catalysts under solvent-less condition. *Journal of Molecular Catalysis A: Chemical*. **240**: 186–190.

Sert, E., Buluklu, A.D., Karakuş, S., and Atalay, F.S. 2013. Kinetic study of catalytic esterification of acrylic acid with butanol catalyzed by different ion exchange resins. *J. Chemical Engineering and Processing: Process Intensification.* Article in Press

Sert, E. and Atalay, F.S. 2012. Determination of Adsorption and Kinetic Parameters for Transesteri fi cation of Methyl Acetate with Hexanol Catalyzed by Ion

Exchange Resin. *J. Industrial and Engineering Chemistry Research*. **51**: 6350−6355.

Shafaei, A., Nikazar, M., and Arami, M. 2010. Photocatalytic degradation of terephthalic acid using titania and zinc oxide photocatalysts: Comparative study. *J. Desalination*. **252**(1-3): 8-16.

Shanmugam, S., Vieswanathan, B., and Varadarajan, T.K. 2004. Esterification by solid acid catalysts—a comparison. *J. Mol. Catal. A*. **223**: 143-147.

Shantora, V. and Huang, R.Y.M. 1981. Separation of liquid mixtures by using polymer membranes. III. Grafted poly(vinyl alcohol) membranes in vacuum permeation and dialysis. *Journal of Applied Polymer Science*. **26**(10): 3223-3243.

Sharma, M. M. 1995. Some novel aspects of cationic ion-exchange resins as catalysts. *Reactive and Functional Polymers*. **26**(1-3): 3−23.

Shi, W., He, B., and Li, J. (2011). Esterification of acidified oil with methanol by SPES/PES catalytic membrane. *J. Bioresource technology*. **102**(9): 5389-93.

Shin, C.H., Kim, J.Y., Kim, J.Y., Kim, H.S., Lee, H.S., Mohapatra, D., and Bae, W. 2009. A solvent extraction approach to recover acetic acid from mixed waste acids produced during semiconductor wafer process. *Journal of hazardous materials*. **162**(2-3): 1278−1284.

Sigma-Aldrich (2013, July 25). Acrylic acid [Material Safety Data Sheet]. Retrieved from http://www.sigmaaldrich.com/MSDS/MSDS/DisplayMSDSPage.do?country=MY&language=en&productNumber=147230&brand=ALDRICH&PageToGoToURL=http%3A%2F%2Fwww.sigmaaldrich.com%2Fcatalog%2Fproduct%2Faldrich%2F147230%3Flang%3Den

Siirola, J.J. 1995. *An industrial perspective on process synthesis.* In: Biegler, L.T., Doherty, M.F. (Eds.), A.I.Ch.E. Symposium Series No. 304, **91**, 222−233.

Sing, K.S.W. 1982. *Reporting physisorption data for gas/solid systems with special reference to the determination of surface area and porosity (Provisional).* **54**(11): 2201-2218

Singh, A., Tiwari, A., Mahajani, S.M., and Gudi, R.D. 2006. Recovery of Acetic Acid from Aqueous Solutions by Reactive Distillation. *J. Industrial & Engineering Chemistry Research*. **45**(6): 2017−2025.

Singh, N. and Sachan, P.K. 2013. Kinetic Study of Catalytic Esterification of Butyric Acid and Ethanol over Amberlyst 15. *ISRN Chemical Engineering.* **2013**:1–6.

Smitha, B. 2004. Separation of organic–organic mixtures by pervaporation ─ a review, *Journal of Membrane Science.* **241**: 1–21.

Song, C., Qi, Y., Deng, T., Hou, X., and Qin, Z. 2010. Kinetic model for the esterification of oleic acid catalyzed by zinc acetate in subcritical methanol. *J. Renewable Energy.* **35**(3): 625–628.

Ströhlein, G., Assunção, Y., Dube, N., Bardow, A., Mazzotti, M., and Morbidelli, M. 2006. Esterification of acrylic acid with methanol by reactive chromatography: Experiments and simulations. *Chemical Engineering Science.* **61**(16): 5296–5306.

Sundmacher, K. and Kienle, A. 2003. *Reactive Distillation*, 1 ed., Wiley-VCH, Weinbeim.

Takegami, S., Yamada, H., and Tsujii, S. 1992. Dehydration of water:ethanol mixtures by pervaporation using modified poly(vinyl alcohol). *Polym. J.* **24** (11): 1239-1250.

Taylor, R. and Krishna, R. 2000. Modelling reactive distillation. *J. Chemical Engineering Science.* **55**(22): 5183–5229.

Teo, H.T.R. and Saha, B. 2004. Heterogeneous catalysed esterification of acetic acid with isoamyl alcohol: kinetic studies. *Journal of Catalysis.* **228**: 174–182.

Thil, L., Breitscheidel, B., Disteldorf, W., Dornik K., and Morsbach, 2000. *Mixture of diesters of adipic or phthalic acid with isomers of nonanols*. B. DE 19924339 (2000).

Tsai, Y.T., Lin, H., and Lee, M.J. 2011. Kinetics behavior of esterification of acetic acid with methanol over Amberlyst 36. *J. Chemical Engineering Journal.* **171**(3): 1367–1372.

Tsukamoto, J. and Franco, T.T. 2009. Enzymatic esterification of d-fructose with acrylic acid in organic media, *J. New Biotechnology.* **25**: 108-109.

Tuyun, A.F., Uslu, H., Gökmen, S., and Yorulmaz, Y. 2011. Recovery of Picolinic Acid from Aqueous Streams Using a Tertiary Amine Extractant. *Journal of Chemical and Engineering Data.* **56**(5): 2310–2315.

Vicente, G., Martinez, M., and Aracil, J. 2004. Integrated biodiesel production: a comparison of different homogeneous catalysts systems. *Bioresource Technology*. **92**, 297–305.

Wakasugi, K., Misaki, T., Yamada, K., and Tanabe, Y. 2000. Diphenylammonium Triflate (DPAT): Efficient Catalyst for Esterification of Carboxylic Acids and for Transesterification of Carboxylic Esters with Nearly Equimolar Amounts of Alcohols. *Tetrahedron Lett.* **41**: 5249-5252.

Wang, Q., Cheng, G., and Sun, X. 2006. Recovery of lactic acid from kitchen garbage fermentation broth by four-compartment configuration electrodialyzer. *J. Process Biochemistry.* **41**: 152–158.

Wang, Y.Z., Liu, Y.P., and Liu, C.G. 2008. Removal of Naphthenic Acids of a Second Vacuum Fraction by Catalytic Esterification. *J. Petrol Sci Technol.* **26**(12): 1424–32.

Weast, R.C. 1989. *Handbook of Chemistry and Physics*. 69th edition. CRC Press Inc., Boca Raton, FL, C-673.

Wesslein, M., Heintz, A., and Lichtenthaler, R.N. 1990. Pervaporation of liquid mixtures through poly(vinyl alcohol) (PVA) membranes. II. The binary systems methanol:1-propanol and methanol:dioxane and the ternary system water:methanol:1-propanol. *J. Memb. Sci.* **51**: 181-188.

Will, B. and Lichtenthaler, R.N. 1992. Comparison of the separation of mixtures by vapor permeation and by pervaporation using PVA composite membranes. II. The binary systems ammonia-water, methylamine-water, 1-propanol-methanol and the ternary system 1-propanol-methanol-water. *J. Memb. Sci.* **68**: 127-131.

Wu, L.G., Zhu, C.L., and Liu, M. 1994. Study of a new pervaporation membrane, Part 1. Preparation and characteristics of the new membrane. *J. of Membrane Science* **90:** 199-205.

Xiang, S., Zhang, Y.L., Xin, Q., and Li, C. 2002. Enantioselective epoxidation of olefins catalysed by Mn (salen)/MCM-41 synthesized with a new anchoring method. *J. Chem. Commun.* **22**: 2696-2697.

Xu, T.W. and Yang, W.H. 2002. Citric acid production by electrodialysis with bipolar membranes. *Chem. Eng. Process.* **41**: 519–524.

Xu, X., Lin, J., and Cen, P. 2006. Advances in the Research and Development of Acrylic Acid Production from Biomass. *Chinese J. Chem. Eng.* **14**(4): 419-427.

Xu, Z.P., Afacan, A., and Chuang, K.T. 1999. Removal of Acetic Acid from Water by Catalytic Distillation. Part 1. Experimental Studies. *Can. J. Chem. Eng.* **77**: 676

Yadav, G.D., and Rahuman, M.S.M.M. 2003. Synthesis of fragrance and flavour grade esters: activities of different ion exchange resins and kinetic studies. *J. Clean Tech. Environ. Policy*. **5**: 128−135.

Yin, P., Chen, W., Liu, W., Chen, H., Qu, R., Liu, X., and Xu, Q. 2013. Efficient bifunctional catalyst lipase/organophosphonic acid-functionalized silica for biodiesel synthesis by esterification of oleic acid with ethanol. *J. Bioresource technology*. **140**: 146−151.

Yu, L., Lin, T., Guo, Q., and Hao, J. 2003. Relation between mass transfer and operation parameters in the electrodialysis recovery of acetic acid. *J. Desalination*. **154**(2): 147−152.

Yu, W., Hidajat, K., and Ray, A.K. 2004. Determination of adsorption and kinetic parameters for methyl acetate esterification and hydrolysis reaction catalyzed by Amberlyst 15. *Applied Catalysis A: General*. **260**: 191−205.

Yuzhong, Z., Keda, Z., and Jiping, X. 1993. Preferential sorption of modified PVA membrane in pervaporation. *J. Memb. Sci.* **80**: 297-308.

Zhang, X., Li, C., Wang, Y., Luo, J., and Xu, T. 2011. Recovery of acetic acid from simulated acetaldehyde wastewaters: Bipolar membrane electrodialysis processes and membrane selection. *Journal of Membrane Science.* **379**(1-2): 184−190.

Zhicai, Y., Xianbao, R.C., and Jings, G. 1998. Esterification − distillation of butanol and acetic acid, *J. Chemical Engineering Science.* **53**(11): 2081-2088.

APPENDIX A

STANDARD CALIBRATION CURVE OF ACRYLIC ACID

Figure A1-A6 shows the chromatogram of standard AA with various concentrations.
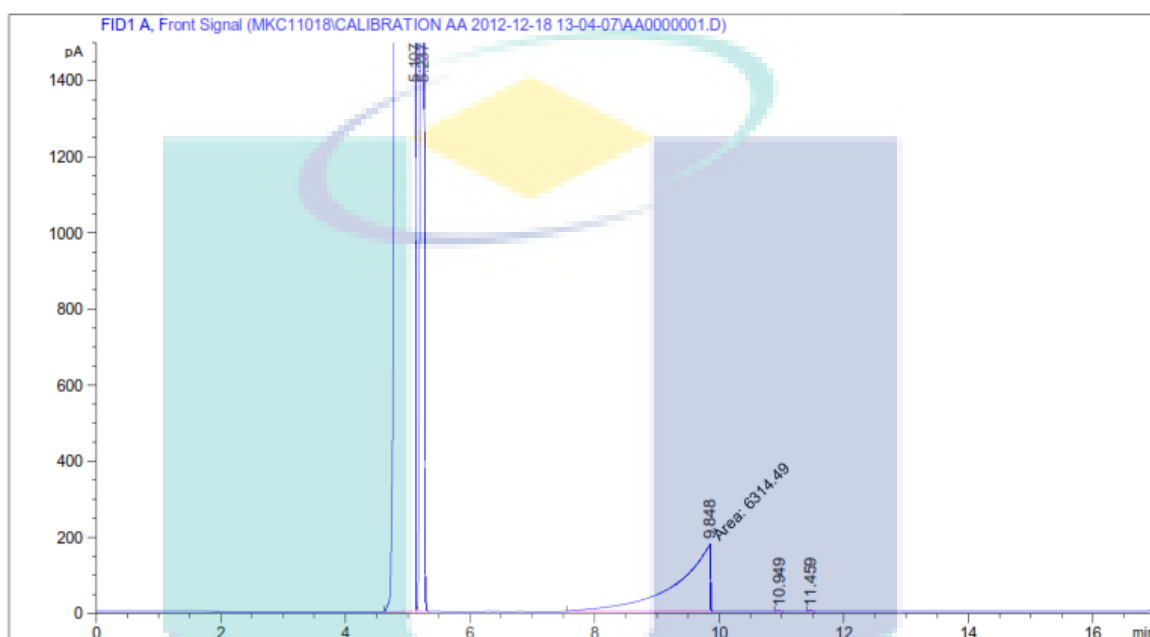
Figure A1 : GC-FID spectrometry of 6,393.27 ppm AA
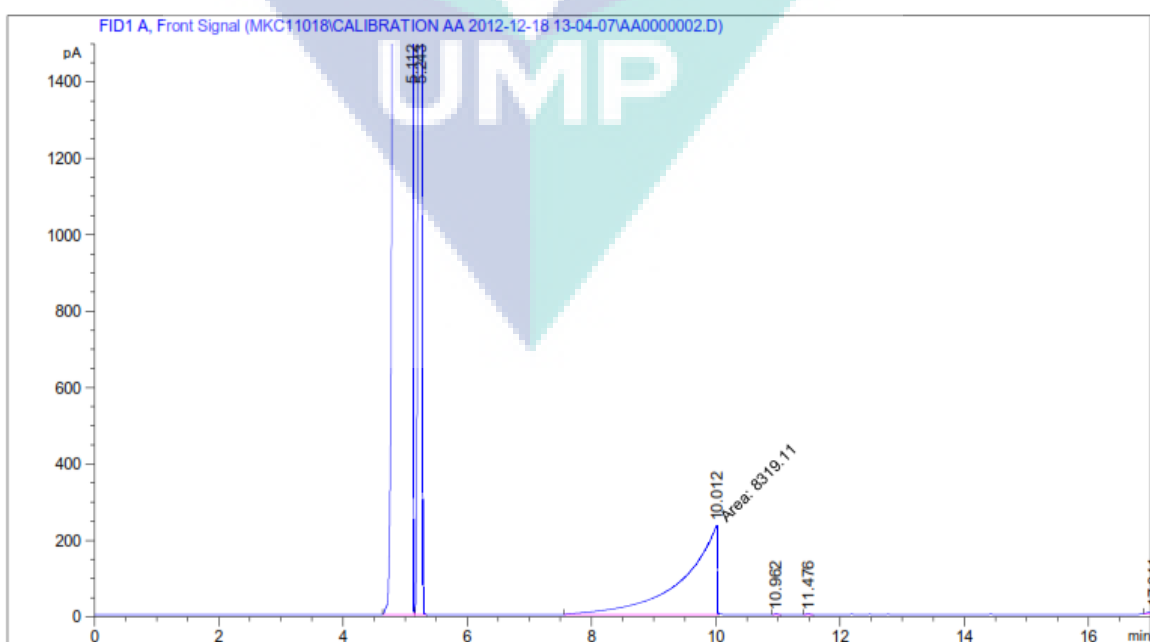
Figure A2 : GC-FID spectrometry of 12,786.55 ppm AA
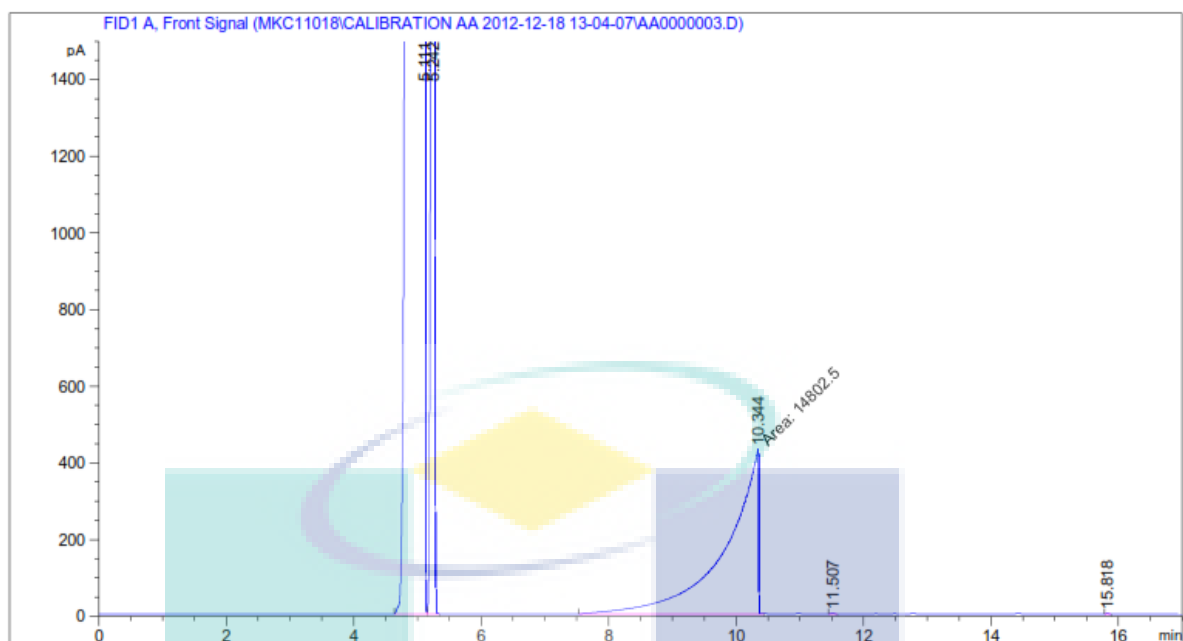
Figure A3 : GC-FID spectrometry of 25,573.10 ppm AA
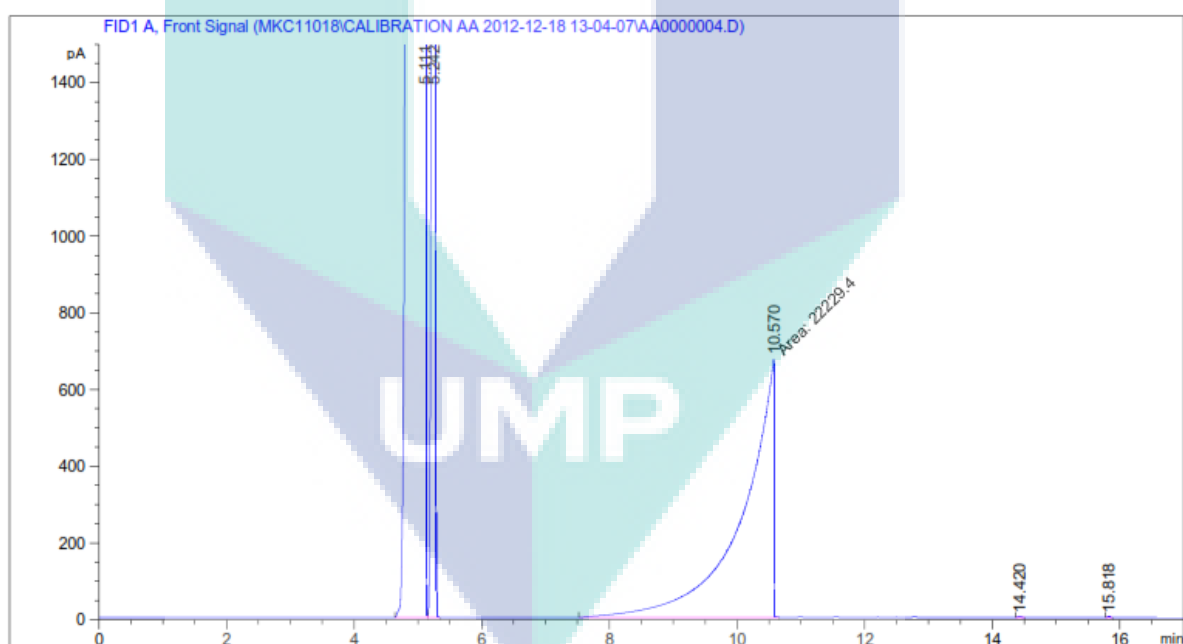
Figure A4 : GC-FID spectrometry of 38,359.64 ppm AA
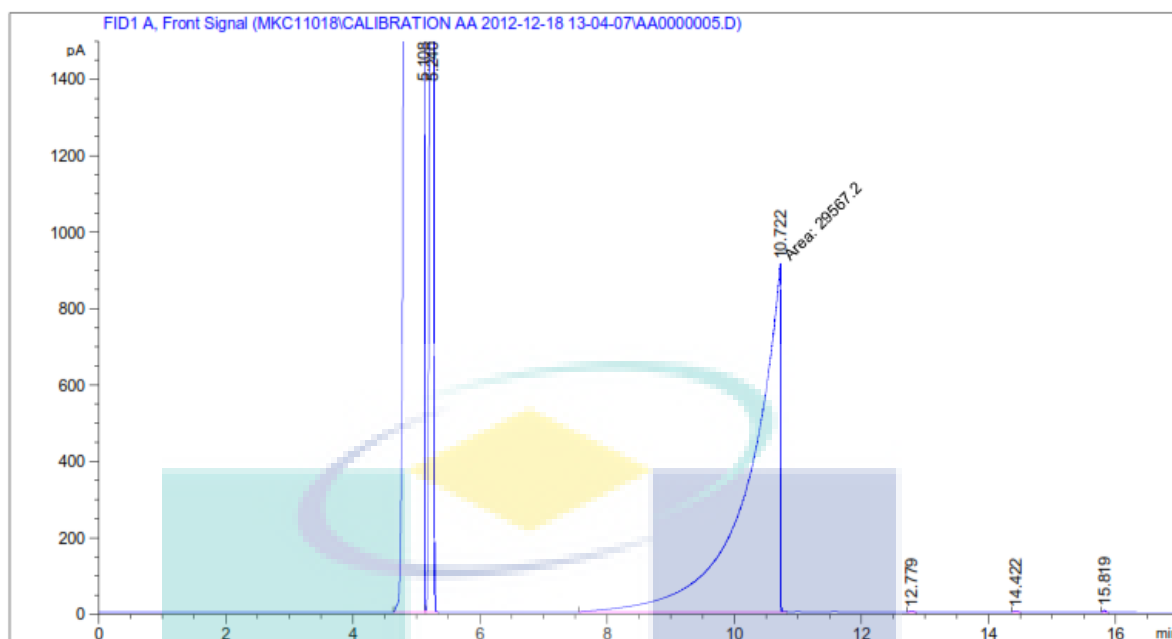
Figure A5 : GC-FID spectrometry of 51,146.19 ppm AA
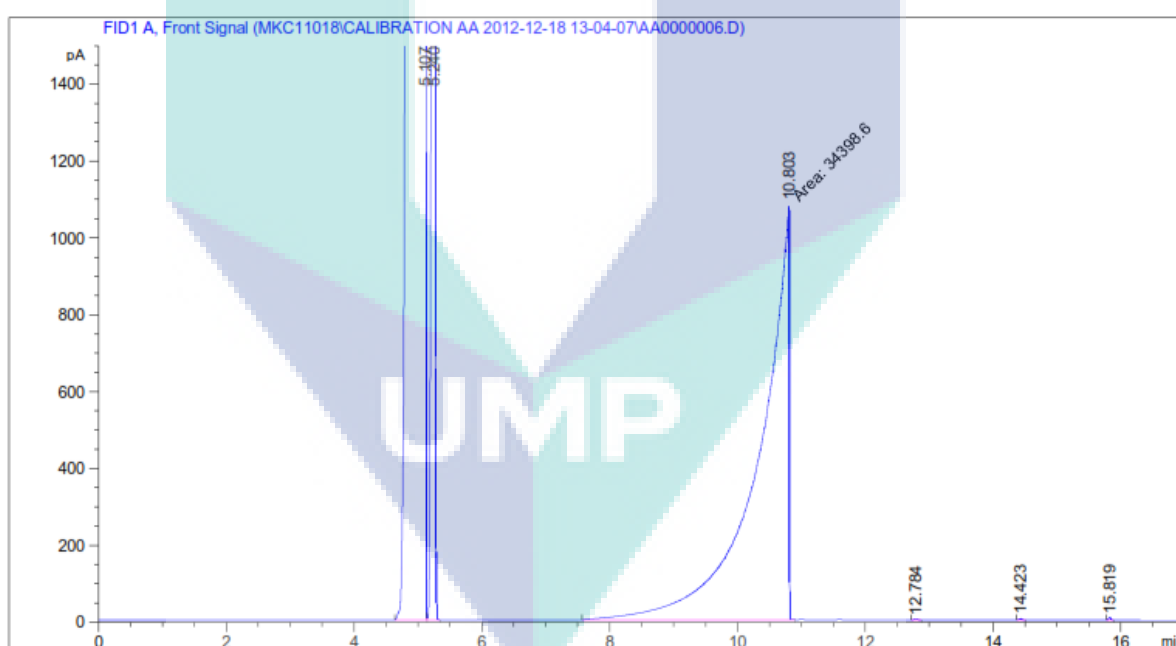
Figure A6 : GC-FID spectrometry of 63,932.74 ppm AA

The retention time for AA was detected at 10 min. The ABS-concentration data of standard calibration curve was included in table A1 and plotted in Figure A7.

Table A1: Concentration versus ABS for standard calibration curve plot of AA.

concentration (ppm)	ABS (pA*s)
0.00	0.000
6,393.27	6,314.490
12,786.55	8,319.110
25,573.10	14,802.500
38,359.64	23,229.400
51,146.19	29,567.200
63,932.74	34,398.600
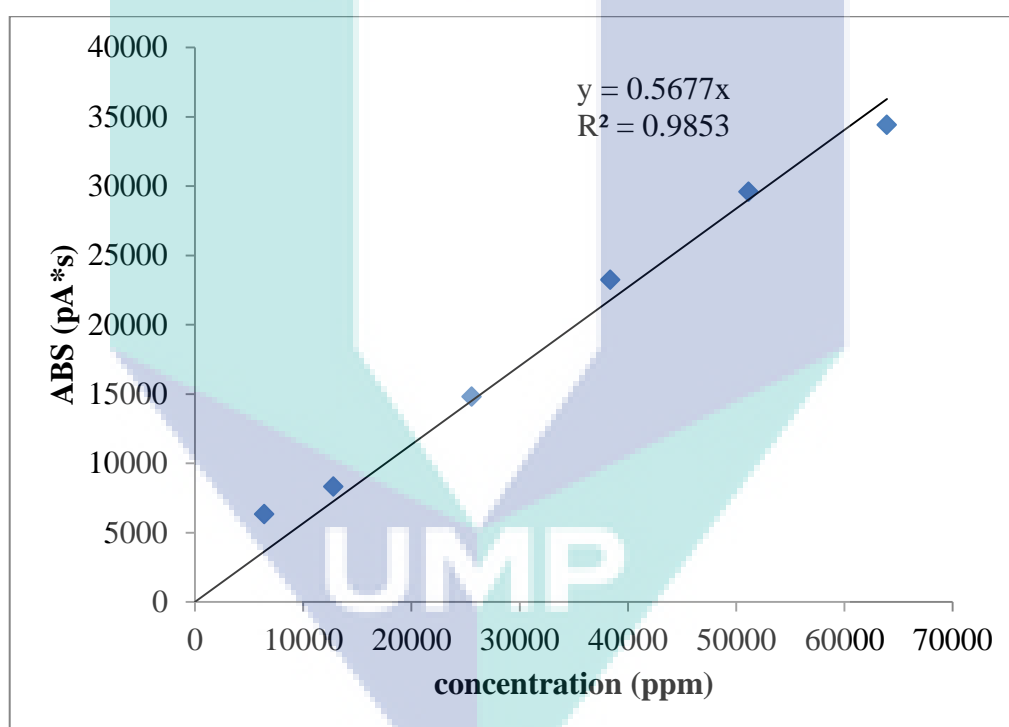
Figure A7: Calibration curve for AA using GC-FID

From the Figure A7, the following equation was developed to calculate the unknown concentration of AA for each sample using the absorbance given by GC-FID analysis:

$$ABS_{AA} = m \ x \ C_{AA} \tag{A1}$$

$$C_{AA} = \frac{ABS_{AA}}{m} \qquad (A2)$$

$$C_{AA} = \frac{ABS_{AA}}{0.5677} \qquad (A3)$$

$$C_{AA} = 1.76 \; x \; ABS_{AA} \qquad (A4)$$
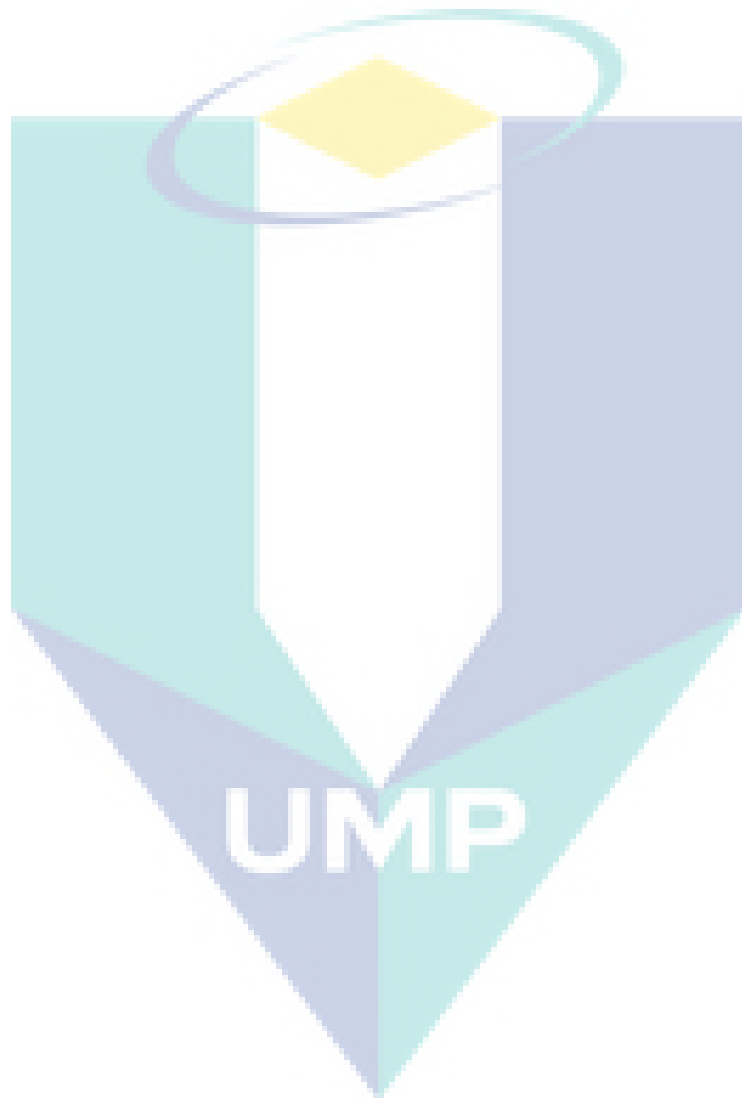
APPENDIX B

# STANDARD CALIBRATION CURVE OF 2 ETHYL HEXYL ACRYLATE

Figure B1-B8 shows the chromatogram of standard 2EHA with various concentrations.
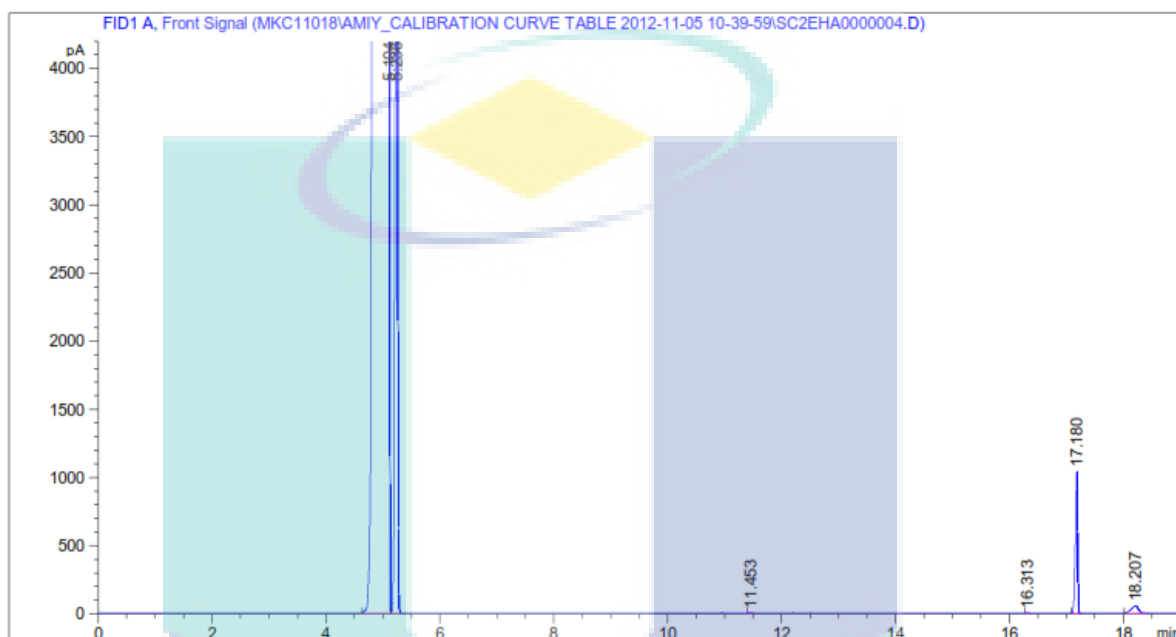
Figure B1 : GC-FID spectrometry of 2,000 ppm 2EHA
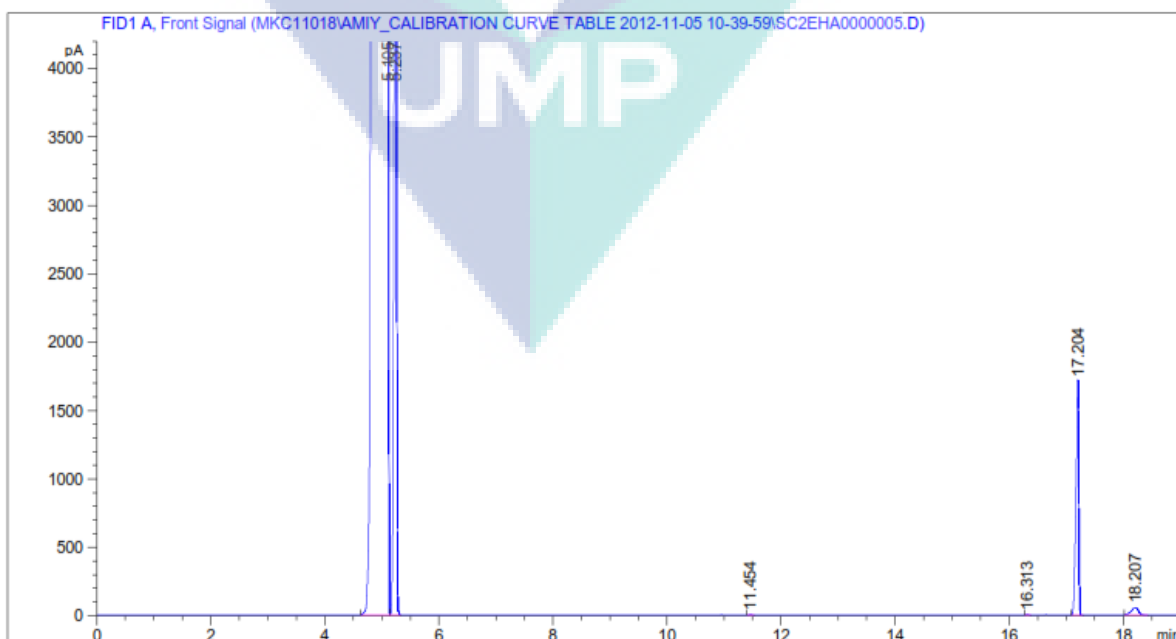
Figure B2 : GC-FID spectrometry of 4,000 ppm 2EHA
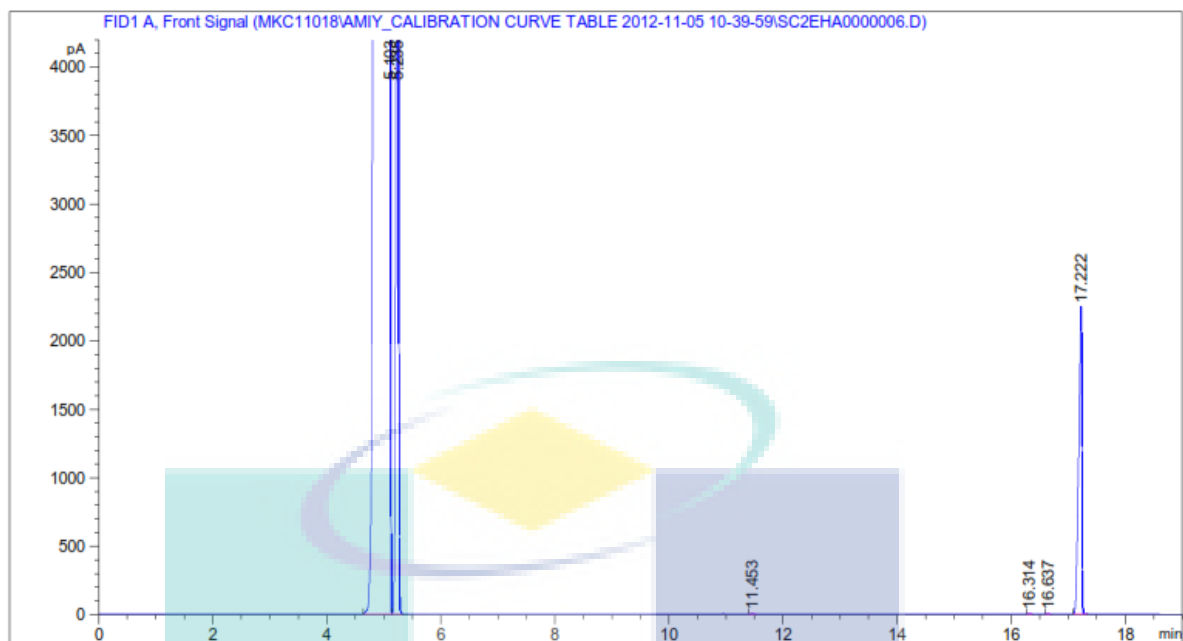
Figure B3 : GC-FID spectrometry of 6,000 ppm 2EHA
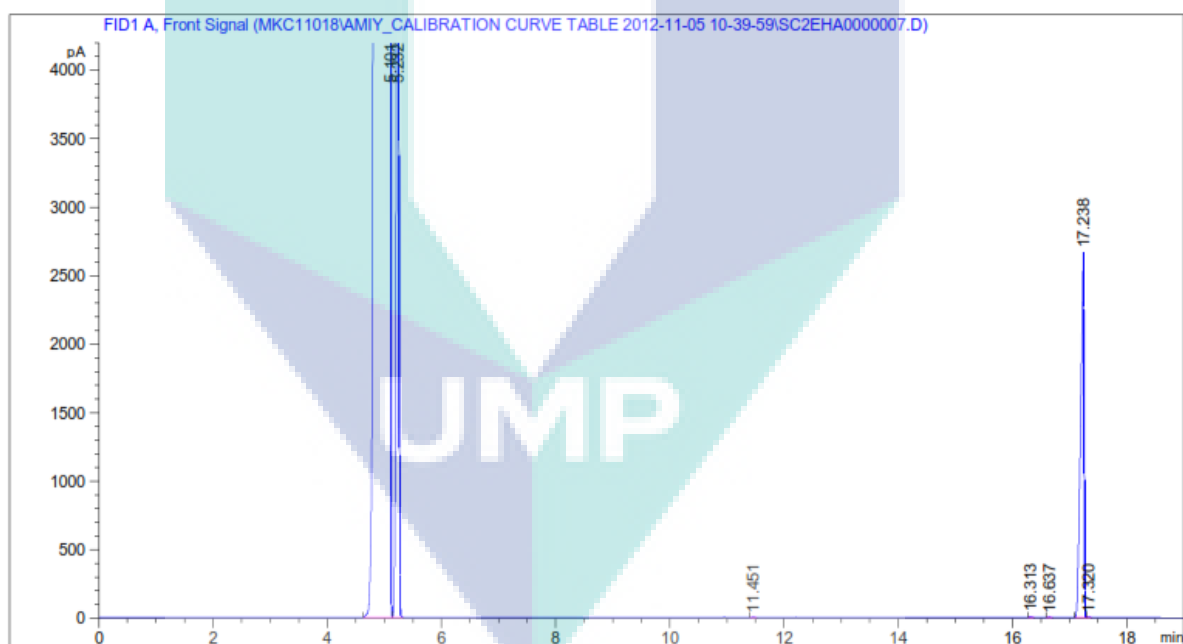
Figure B4 : GC-FID spectrometry of 8,000 ppm 2EHA
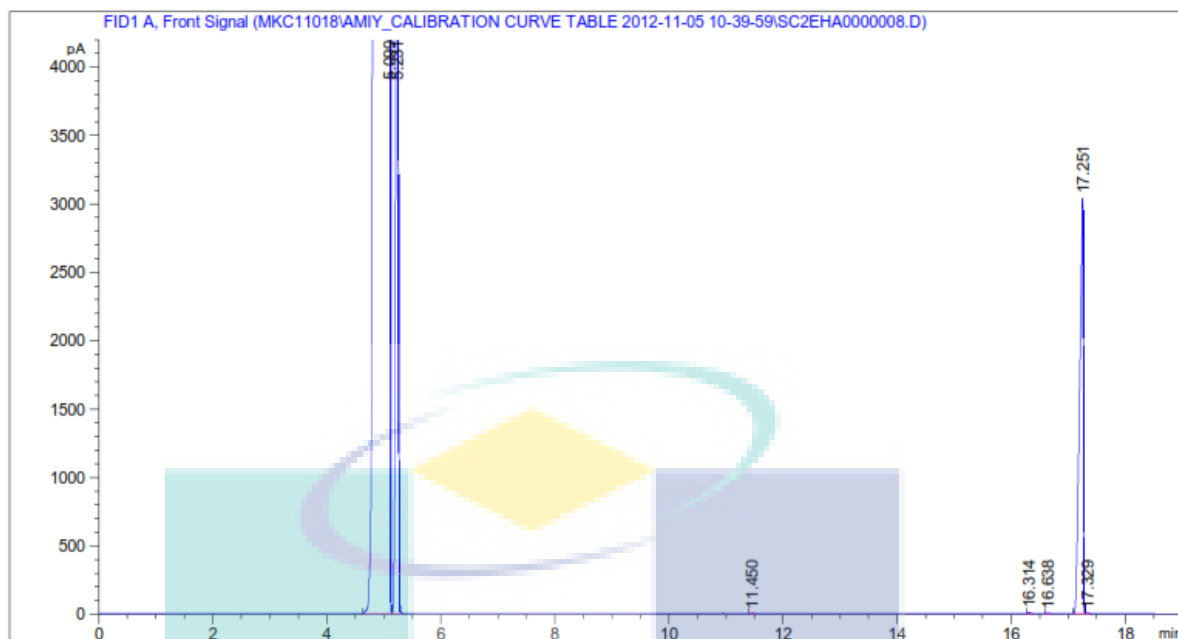
Figure B5 : GC-FID spectrometry of 10,000 ppm 2EHA
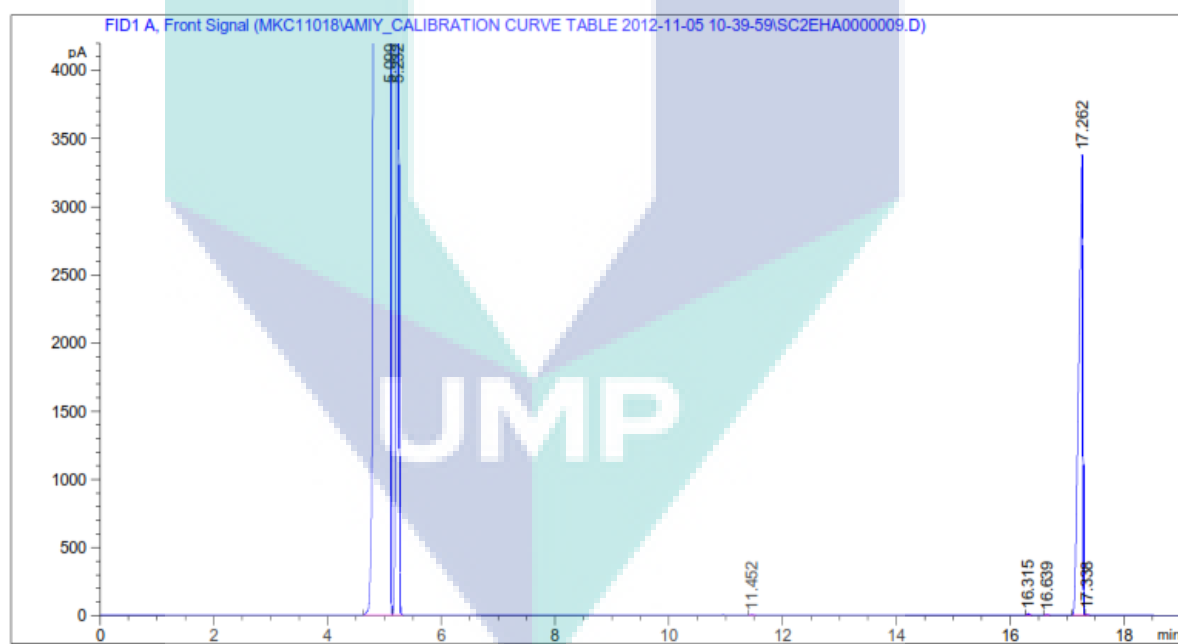
Figure B6 : GC-FID spectrometry of 12,000 ppm 2EHA
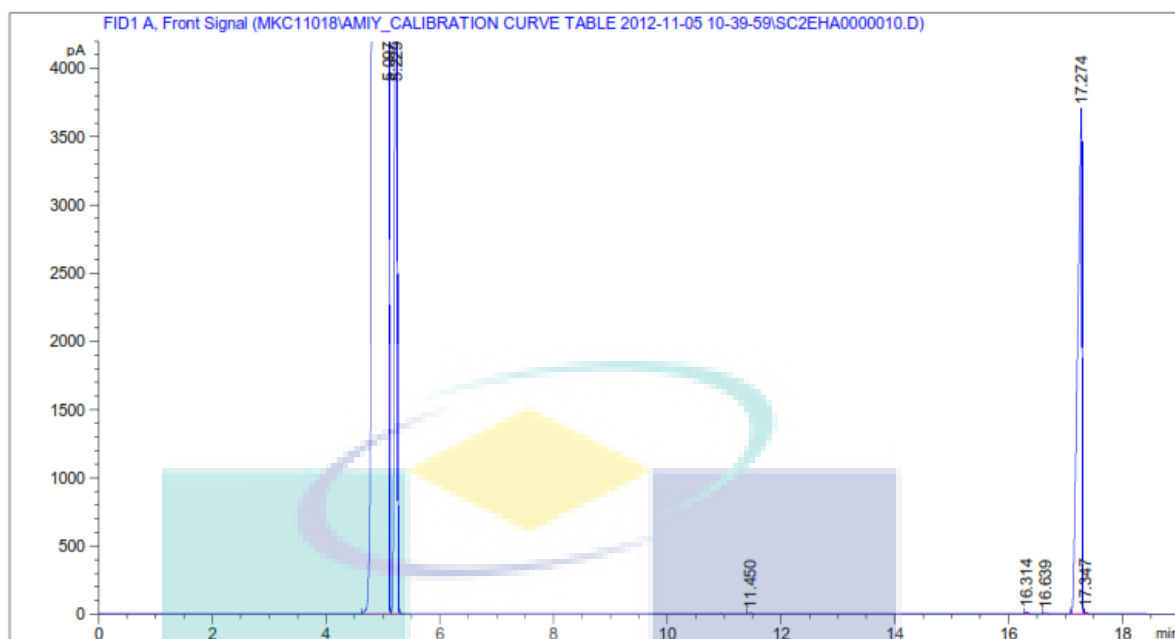
Figure B7 : GC-FID spectrometry of 14,000 ppm 2EHA
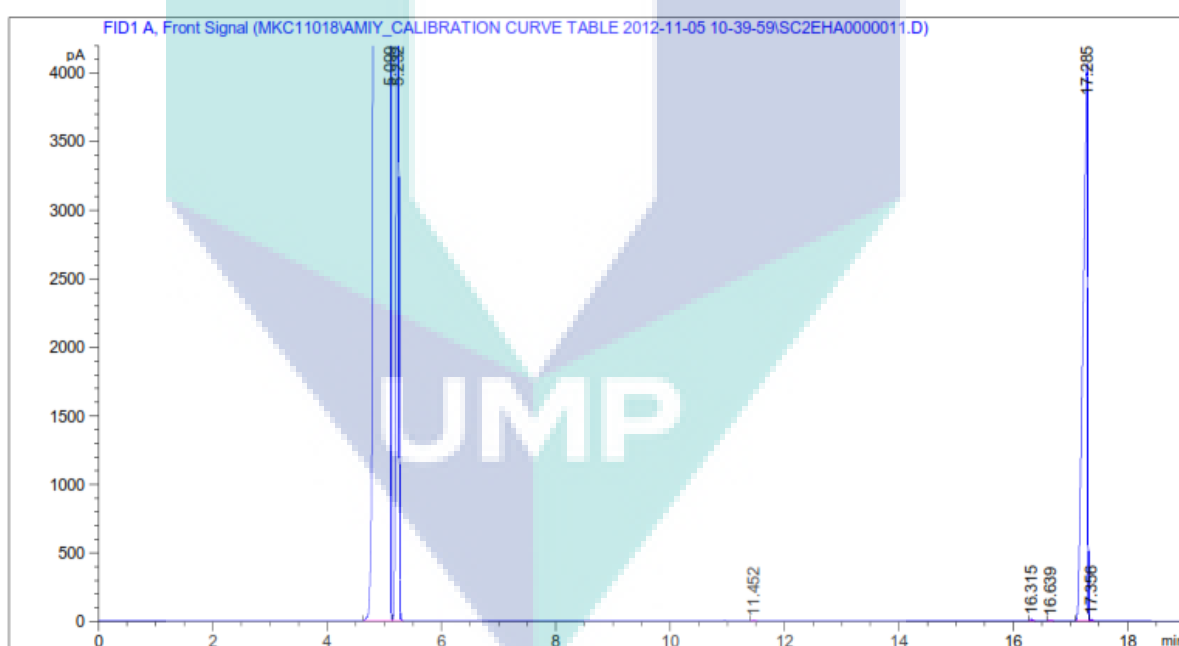

Figure B8 : GC-FID spectrometry of 16,000 ppm 2EHA

The retention time for 2EHA was detected at 17.2 min. The ABS-concentration data of standard calibration curve was included in table B1 and plotted in Figure B9.

Table B1: Concentration versus ABS for standard calibration curve plot of 2EHA

concentration (ppm)	ABS (pA*s)
0	0.000
2000	2921.603
4000	5844.755
6000	8702.682
8000	11464.200
10000	14178.100
12000	16817.200
14000	19797.600
16000	22472.300
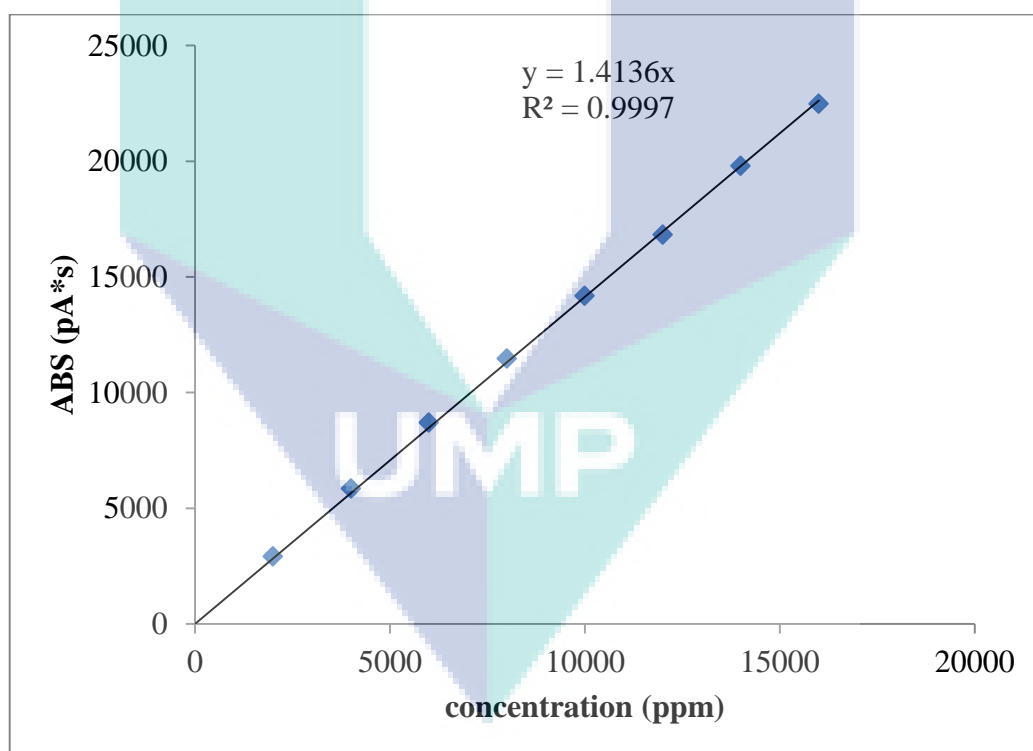
**Figure B9:** Calibration curve for 2EHA using GC-FID

From the Figure B9, the following equation was developed to calculate the unknown concentration of 2HA for each sample using the absorbance given by GC-FID analysis:

$$ABS_{2EHA} = m \ x \ C_{2EHA} \tag{B1}$$

$$C_{2EHA} = \frac{ABS_{2EHA}}{m} \tag{B2}$$

$$C_{2EHA} = \frac{ABS_{2EHA}}{1.4136} \tag{B3}$$

$$C_{2EHA} = 0.707 \ x \ ABS_{2EHA} \tag{B4}$$
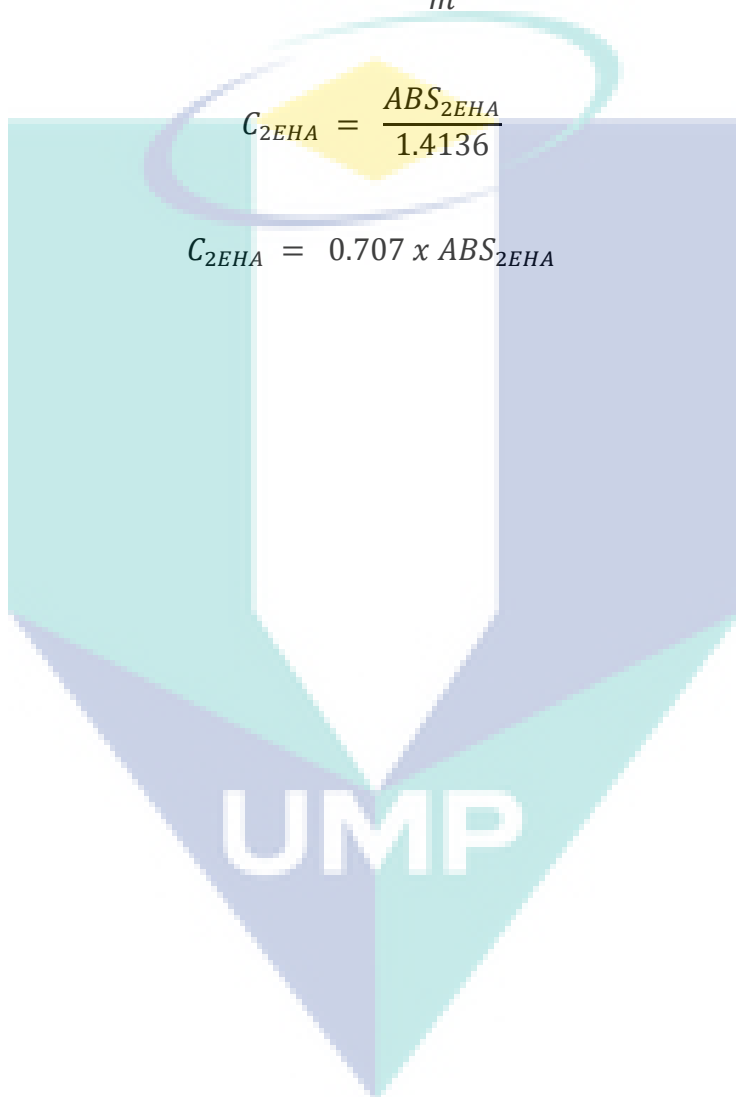
APPENDIX C

UNIFAC (VLE) FOR ESTERIFICATION SYSTEM

P=	111.0182	mmHg
T(^{o}C)=	100	^{o}C

As distributed, this cell has a formula to calculate the bubble pressure.

Table 1. Antoine Coefficients (mmHg) log10(P^{sat})=A-B/(T+C) where T[=] ^{o}C

	comp1	comp2	comp3	comp4	comp5
A	8.87829	8.07131		8.1122	6.87632
B	2010.33	1730.63		1592.864	1075.78
C	252.636	233.426		226.184	233.205
P^{sat}[mmHg]	1504.6159	760.08637		1693.832	4443.6208
y_i	1.00000	10.81294	0.00000	9.59272	0.00000

Enter Antoine constants or vapor pressures if you want bubble P and vapor phase concentrations calculated automatically.

Table 2. Component Structure Information and Activity Coefficient Calculation.

Vapor phase mole fractions calculated automatically.

		comp1	comp2	comp3	comp4	comp5
		AA	Water	2EH	2EHA	
	x_i	0.102	0.399	0.102	0.399	0.000
SubGroup	γ_i	0.727	3.963	1.213	1.578	0.951
1	CH3			2	2	1
2	CH2			5	4	1
3	CH			1	1	
5	CH2=CH	1			1	
10	AC					
11	ACCH3					
12	ACCH2					
14	OH			1		
15	CH3OH					
16	H2O		1			
17	ACOH					
18	CH3CO					
20	CHO					
21	CH3COO					
22	CH2COO				1	
36	ACNH2					
42	COOH	1				
49	CCL2					
51	CCL3					
99	CON(CH2)2					
	$\Sigma_k v_k^{(i)} x_i$	0.203	0.3985	0.9135	3.5865	2E-20
	N groups	2	1	9	9	2

Liquid phase mole fractions. Enter a very small number like 1E-20 or smaller for absent compounds - don't use zero.

*Enter the number of occurences of a chemical structure in this table for each component. Residual group interaction parameters are not available for all groups, and **are treated as zero if unavailable**. Check Table 1 on sheet "aij-UNIFAC (VLE)".*

*The sub-groups available in this table may be changed in this column by changing the SubGroup number. If you change a sub-group here, be sure to edit the component structure information in the table. Available subgroups and subgroup numbers are in Table 2 of sheet "aij-UNIFAC (VLE)".*

Note that columns H:AS are hidden. They contain intermediate calculations. Unprotect the sheet and unhide them to see the calculations.

	comp1	comp2	comp3	comp4	comp5
q	2.4000	1.4000	5.8240	6.6800	1.3880
r	2.6467	0.9200	6.6211	7.9685	1.5755
θ_i	0.0601	0.1376	0.1458	0.6565	0.0000
Φ_i	0.0599	0.0818	0.1499	0.7084	0.0000
$\ln\gamma^C$	-0.1173	0.0135	-0.0756	-0.1034	-0.3947
$\ln\gamma^{Ro}$	1.2029	0.0000	1.9433	0.9151	0.0000
$\ln\gamma^R$	1.0013	1.3636	2.2118	1.4744	0.3441

APPENDIX D

CHROMATOGRAM FOR YIELD-TIME DATA FOR ACRYLIC ACID WITH 2 ETHYL HEXANOL ESTERIFICATION

Figure D1-D4 shows the chromatogram of sample from recyclability experiment (1st run) at certain time interval.

Peak #	RetTime [min]	Type	Width [min]	Area [pA*s]	Height [pA]	Area %
1	4.997	BB S	0.1358	1.06885e6	9.60012e4	90.83128
2	9.739	MM	0.5636	6055.15137	179.05711	0.51457
3	14.123	BB	0.2149	9.53582e4	5336.70557	8.10355
4	17.067	BB	0.0494	5286.43945	1550.00916	0.44924
5	17.604	BB	0.1213	729.82324	76.23186	0.06202
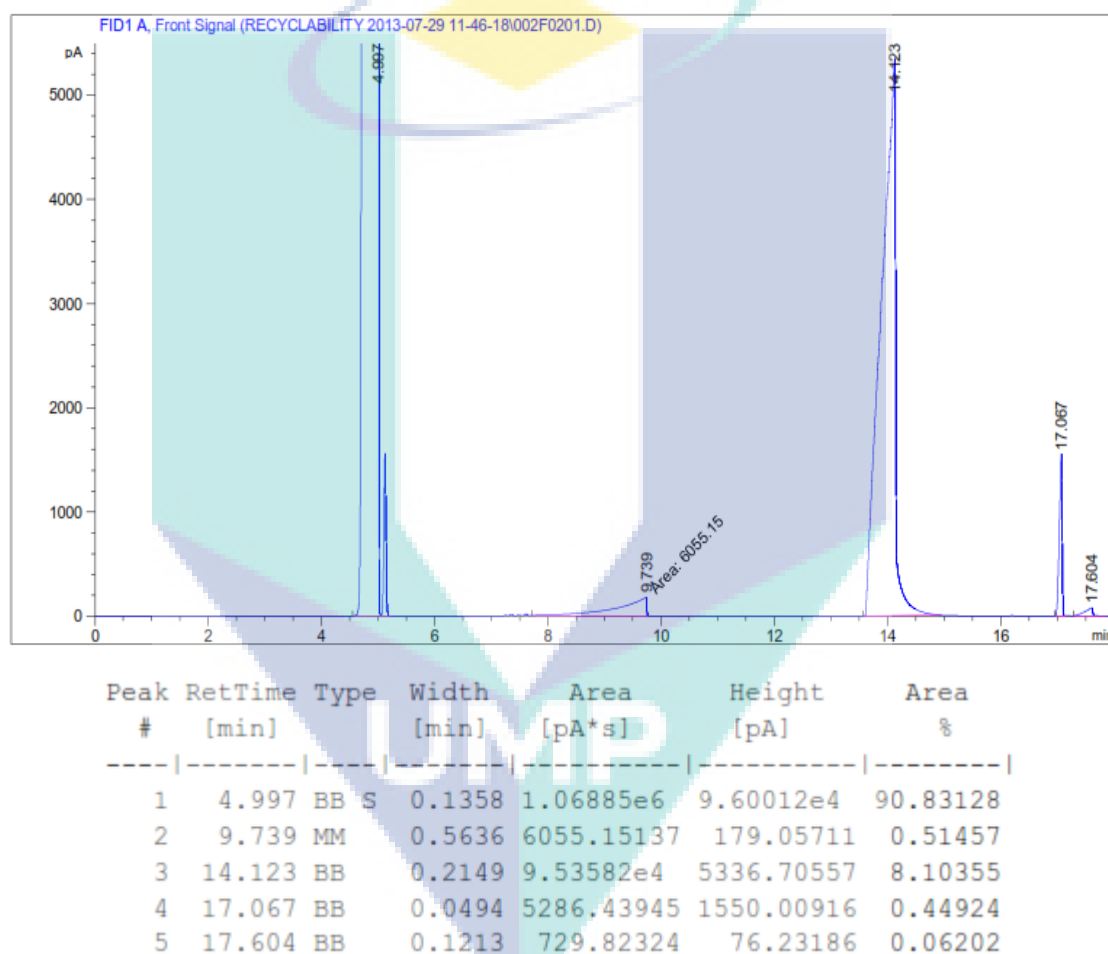
Figure D1: GC-FID chromatogram of sample from recyclability experimental (1st run) at 30 min.

FID1 A, Front Signal (RECYCLABILITY 2013-07-29 11-46-18\003F0301.D)


```
Peak RetTime Type  Width     Area       Height     Area
  #   [min]        [min]     [pA*s]      [pA]        %
----|-------|----|-------|----------|----------|--------|
  1   4.996 BB S  0.1343 1.04408e6   9.52132e4  91.06544
  2   5.119 BB T  0.0408 3953.00073 1519.18262   0.34478
  3   9.593 MM    0.5530 4664.15820  140.57298   0.40681
  4  14.085 BB    0.2042 8.27637e4  4942.17822   7.21872
  5  17.091 BB    0.0566 8863.97852 2200.90625   0.77312
  6  17.529 BB    0.1024  407.03345   52.50257   0.03550
```

Figure D2: GC-FID chromatogram of sample from recyclability experimental (1st run) at 60 min
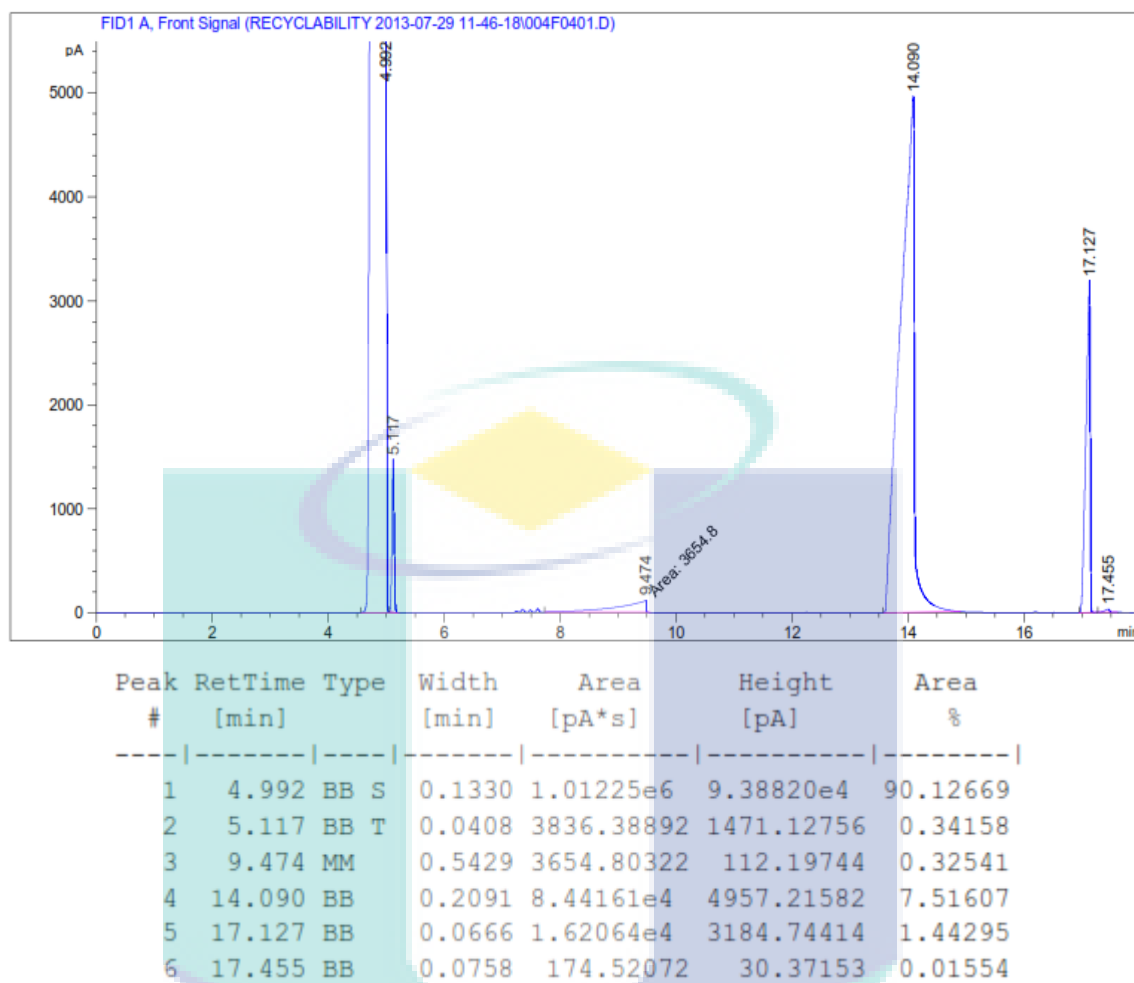
Figure D3: GC-FID chromatogram of sample from recyclability experimental (1st run) at 120 min

```
FID1 A, Front Signal (RECYCLABILITY 2013-07-29 11-46-18\005F0501.D)
```

```
Peak RetTime Type  Width     Area        Height      Area
  #    [min]        [min]    [pA*s]       [pA]         %
----|-------|----|-------|----------|-----------|--------|
  1   4.991 BB S  0.1314 1.00133e6   9.28501e4  89.97883
  2   5.116 BB T  0.0408 3797.27979 1455.49866   0.34122
  3   9.301 MM    0.5331 2758.36890   86.23648   0.24787
  4  14.076 BB    0.2007 8.00431e4  4845.96680   7.19265
  5  17.148 BV    0.0718 2.12116e4  3829.91479   1.90607
  6  17.400 VB    0.0639   75.14575   17.15597   0.00675
```

Figure D4: GC-FID chromatogram of sample from recyclability experimental (1st run) at 180 min

By applying the Eq. B4, the yield-time data was present in Table D1.

Table D1 : Yield time data for recyclability experimental (1st run)

Time (min)	ABS (pA*s)	ppm (2-EHA)	Mole 2-EHA (mol)	Yield (%)
0	228.3	1,615.03	0.00	0.47
30	5,286.4	37,396.72	0.03	10.91
60	8,864	62,705.15	0.05	18.29
120	1.62E+04	114,646.29	0.09	33.45
180	2.12E+04	150,053.76	0.12	43.78

APPENDIX E

THE CONCENTRATION-TIME DATA FOR THE REACTION STUDIES USING DIFFERENT CATALYST LOADING

Table E1 : The concentration-time data for the reaction at 1 wt% ot catalyst loading

Time (min)	ABS (pA*s)	Conversion (%)
30	403.44	1.56
60	591.02	2.28
120	1086.89	4.20
180	1619.48	6.26
240	2096.99	8.10

Table E2 : The concentration-time data for the reaction at 5 wt% ot catalyst loading

Time (min)	ABS (Pa*s)	Conversion (%)
30	692.18	2.94
120	3719.34	15.81
180	4811.43	20.45
240	6217.12	26.43

Table E3 : The concentration-time data for the reaction at 10 wt% ot catalyst loading

Time (min)	ABS (pA*s)	Conversion (%)
30	3248.54	12.55
60	5131.53	19.83
180	10166.00	39.28
240	12778.00	49.37

Table E4 : The concentration-time data for the reaction at 15 wt% ot catalyst loading

Time (min)	ABS (pA*s)	Conversion (%)
30	1974.91	8.39
60	4093.10	17.40
120	6553.84	27.86
180	7643.90	32.49
240	13257.20	56.35

APPENDIX F

THE CONCENTRATION-TIME DATA FOR THE REACTION STUDY AT DIFFERENT INITIAL REACTANT MOLAR RATIO (AA:2EH)

Table F1 : The concentration-time data for the reaction at 1:7 of initial reactant molar ratio (AA:2EH)

Time (min)	Conversion (%)	Mole product	Mole reacted AA	Mole reacted 2EH	Mole AA side product	Mole 2EH side product	Selectivity
30	16.822	0.024	0.047	0.133	0.023	0.109	15.417
60	32.400	0.043	0.090	0.330	0.047	0.287	11.278
120	47.066	0.080	0.130	0.268	0.051	0.188	24.951
180	61.802	0.101	0.171	0.394	0.070	0.293	21.840
240	67.621	0.125	0.187	0.244	0.062	0.119	40.903
300	75.201	0.141	0.208	0.387	0.067	0.246	31.098
360	81.312	0.148	0.225	0.462	0.077	0.313	27.498
						Average	33.166

Table F2 : The concentration-time data for the reaction at 1:5 of initial reactant molar ratio (AA:2EH)

Time (min)	Conversion (%)	Mole product	Mole reacted AA	Mole reacted 2EH	Mole AA side product	Mole 2EH side product	Selectivity
30	21.790	0.029	0.060	0.037	0.031	0.008	42.310
60	39.407	0.046	0.109	0.229	0.063	0.183	15.884
120	48.833	0.086	0.135	0.162	0.049	0.075	41.019
180	67.072	0.109	0.186	0.271	0.077	0.163	31.250
240	72.069	0.134	0.200	0.208	0.066	0.074	49.092
300	78.743	0.148	0.218	0.250	0.071	0.102	46.123
360	84.550	0.162	0.234	0.257	0.073	0.095	49.058
						Average	48.091

Table F3 : The concentration-time data for the reaction at 1:3 of initial reactant molar ratio (AA:2EH)

Time (min)	Conversion (%)	Mole product	Mole reacted AA	Mole reacted 2EH	Mole AA side product	Mole 2EH side product	Selectivity
30	32.161	0.040	0.088	0.127	0.048	0.087	22.985
60	45.189	0.081	0.124	0.134	0.043	0.053	45.925
120	66.491	0.093	0.184	0.289	0.091	0.196	24.537
180	65.259	0.150	0.180	0.141	0.030	-0.009	87.646
240	75.040	0.171	0.208	0.160	0.037	-0.011	86.991
300	81.705	0.178	0.226	0.204	0.048	0.026	70.358
360	86.846	0.190	0.240	0.221	0.050	0.031	70.310
						Average	75.886

Table F4 : The concentration-time data for the reaction at 1:1 of initial reactant molar ratio (AA:2EH)

Time (min)	Conversion (%)	Mole product	Mole reacted AA	Mole reacted 2EH	Mole AA side product	Mole 2EH side product	Selectivity
30	44.179	0.046	0.122	0.127	0.076	0.081	22.872
60	44.061	0.087	0.122	0.122	0.035	0.035	55.669
120	55.346	0.132	0.153	0.147	0.021	0.015	78.843
180	68.716	0.147	0.190	0.180	0.043	0.033	65.941
240	76.903	0.164	0.213	0.201	0.049	0.036	65.852
300	81.234	0.178	0.225	0.210	0.047	0.032	69.033
360	85.498	0.180	0.237	0.223	0.057	0.043	64.052
						Average	66.312

Table F5 : The concentration-time data for the reaction at 3:1 of initial reactant molar ratio (AA:2EH)

Time (min)	Conversion (%)	Mole product	Mole reacted AA	Mole reacted 2EH	Mole AA side product	Mole 2EH side product	Selectivity
30	32.008	0.044	0.089	0.073	0.045	0.030	36.862
60	40.614	0.051	0.113	0.084	0.061	0.033	35.313
120	42.055	0.066	0.117	0.091	0.051	0.025	46.417
180	50.362	0.065	0.140	0.092	0.075	0.028	38.830
240	52.833	0.069	0.146	0.092	0.077	0.023	40.929
300	59.147	0.065	0.164	0.092	0.099	0.027	34.156
360	58.742	0.070	0.163	0.092	0.093	0.023	37.569
						Average	37.551

Table F6 : The concentration-time data for the reaction at 5:1 of initial reactant molar ratio (AA:2EH)

Time (min)	Conversion (%)	Mole product	Mole reacted AA	Mole reacted 2EH	Mole AA side product	Mole 2EH side product	Selectivity
30	31.061	0.037	0.086	0.051	0.050	0.015	36.264
60	37.668	0.043	0.104	0.055	0.062	0.013	36.503
120	47.042	0.045	0.130	0.055	0.085	0.010	32.367
180	48.706	0.050	0.135	0.055	0.085	0.006	35.506
240	57.317	0.048	0.159	0.055	0.111	0.008	28.576
300	59.324	0.049	0.164	0.055	0.115	0.006	28.850
360	64.385	0.048	0.178	0.055	0.130	0.007	26.117
						Average	27.848

Table F7 : The concentration-time data for the reaction at 7:1 of initial reactant molar ratio (AA:2EH)

Time (min)	Conversion (%)	Mole product	Mole reacted AA	Mole reacted 2EH	Mole AA side product	Mole 2EH side product	Selectivity
30	13.787	0.025	0.038	0.040	0.014	0.015	46.684
60	14.974	0.030	0.042	0.040	0.012	0.010	57.337
120	26.816	0.030	0.074	0.040	0.045	0.010	35.029
180	32.405	0.032	0.090	0.040	0.058	0.008	32.430
240	36.200	0.033	0.100	0.040	0.068	0.007	30.257
300	46.951	0.032	0.130	0.040	0.098	0.007	23.526
360	53.532	0.031	0.148	0.040	0.117	0.008	19.937
						Average	24.573

APPENDIX G

THE COMPARISON OF THE PREDICTED AND EXPERIMENTAL CONCENTRATION-TIME DATA

Table G1: Experimental concentration-time data for reaction temperature at 388.15 K, $M_{aa/2eh}$ is 1:6, catalyst loading is 10% w/w and stirring speed at 400 rpm.

t (min)	C2EHA$_{exp}$ (mol/L)	CAA$_{exp}$ (mol/L)	C2EH$_{exp}$ (mol/L)
0	0.000	0.994	5.960
5	0.031	0.932	4.561
10	0.043	0.862	4.340
15	0.065	0.861	4.491
25	0.091	0.756	4.171
35	0.125	0.738	4.339
45	0.146	0.710	4.214
60	0.197	0.630	4.229
75	0.221	0.567	4.088
90	0.265	0.554	4.252
150	0.343	0.387	3.727
180	0.390	0.337	3.734
210	0.436	0.281	3.706
240	0.491	0.278	3.915
300	0.487	0.203	3.550

Table G2: Predicted concentration-time data for reaction temperature at 388.15 K, $M_{aa/2eh}$ is 1:6, catalyst loading is 10% w/w and stirring speed at 400 rpm

t (min)	C2EHA$_{predicted}$ (mol/L)	CAA$_{predicted}$ (mol/L)	C2EH$_{predicted}$ (mol/L)
0.000	0.000	0.994	5.960
6.525	0.020	0.946	5.903
11.325	0.034	0.913	5.887
13.725	0.041	0.897	5.871
16.125	0.048	0.881	5.855
18.525	0.055	0.866	5.823
23.325	0.068	0.837	5.807
25.725	0.075	0.823	5.792
28.125	0.082	0.810	5.776
30.525	0.088	0.796	5.746
35.325	0.102	0.770	5.732
37.725	0.108	0.758	5.717
40.125	0.114	0.746	5.703
42.525	0.121	0.734	5.674
47.325	0.133	0.711	5.661
49.725	0.140	0.699	5.647
52.125	0.146	0.688	5.634
54.525	0.152	0.678	5.607
59.325	0.164	0.657	5.594
61.725	0.170	0.647	5.582
64.125	0.176	0.637	5.569
66.525	0.181	0.627	5.545
71.325	0.193	0.608	5.533
73.725	0.199	0.599	5.521
76.125	0.204	0.590	5.510
78.525	0.210	0.581	5.487
83.325	0.221	0.564	5.476
85.725	0.226	0.556	5.466

88.125	0.231	0.548	5.455
90.525	0.236	0.540	5.434
95.325	0.247	0.524	5.424
97.725	0.252	0.517	5.414
100.125	0.257	0.509	5.405
102.525	0.262	0.502	5.386
107.325	0.272	0.487	5.376
109.725	0.277	0.481	5.367
112.125	0.281	0.474	5.358
114.525	0.286	0.467	5.341
119.325	0.295	0.454	5.332
121.725	0.300	0.447	5.324
124.125	0.304	0.441	5.316
126.525	0.309	0.435	5.300
131.325	0.318	0.423	5.292
133.725	0.322	0.417	5.284
136.125	0.326	0.411	5.276
138.525	0.331	0.405	5.262
143.325	0.339	0.394	5.254
145.725	0.343	0.389	5.247
148.125	0.347	0.384	5.240
150.525	0.351	0.378	5.227
155.325	0.359	0.368	5.220
157.725	0.363	0.363	5.213
160.125	0.366	0.358	5.207
162.525	0.370	0.353	5.194
167.325	0.378	0.344	5.188
169.725	0.381	0.339	5.182
172.125	0.385	0.335	5.176
174.525	0.388	0.330	5.164
179.325	0.395	0.321	5.159
181.725	0.399	0.317	5.153

184.125	0.402	0.313	5.147
186.525	0.405	0.309	5.136
191.325	0.412	0.301	5.131
193.725	0.415	0.297	5.126
196.125	0.418	0.293	5.120
198.525	0.421	0.289	5.110
203.325	0.428	0.281	5.105
205.725	0.431	0.278	5.100
208.125	0.434	0.274	5.095
210.525	0.437	0.270	5.085
215.325	0.442	0.263	5.081
217.725	0.445	0.260	5.076
220.125	0.448	0.257	5.071
222.525	0.451	0.253	5.062
227.325	0.456	0.247	5.058
229.725	0.459	0.244	5.053
232.125	0.462	0.241	5.049
234.525	0.464	0.237	5.040
239.325	0.469	0.231	5.036
241.725	0.472	0.229	5.032
244.125	0.474	0.226	5.027
246.525	0.477	0.223	5.019
251.325	0.482	0.217	5.015
253.725	0.484	0.214	5.011
256.125	0.486	0.212	5.007
258.525	0.489	0.209	4.999
263.325	0.493	0.204	4.995
265.725	0.495	0.201	4.991
268.125	0.498	0.199	4.987
270.525	0.500	0.196	4.980
275.325	0.504	0.191	4.976
277.725	0.506	0.189	4.972

280.125	0.508	0.187	4.969
282.525	0.510	0.184	4.961
287.325	0.514	0.180	4.958
289.725	0.516	0.178	4.954
292.125	0.518	0.175	4.950
294.525	0.520	0.173	4.943
299.325	0.524	0.169	4.940
300.000	0.524	0.168	4.938

Table G3: Experimental concentration-time data for reaction temperature at 378.15 K, $M_{aa/2eh}$ is 1:6, catalyst loading is 10% w/w and stirring speed at 400 rpm.

| t (min)	C2EHA$_{exp}$ (mol/L)	CAA$_{exp}$ (mol/L)	
0	0.000	0.994	
5	0.014	0.974	
10	0.012		
35	0.066	0.748	
45	0.068		
60	0.121	0.839	
75	0.113		
90	0.162	0.670	
120	0.207	0.637	
150	0.267	0.633	
180	0.279	0.554	
210	0.265	0.432	
240	0.356	0.448	
300	0.408	0.417	

Table G4: Predicted concentration-time data for reaction temperature at 378.15 K, $M_{aa/2eh}$ is 1:6, catalyst loading is 10% w/w and stirring speed at 400 rpm

t (min)	C2EHA$_{predicted}$ (mol/L)	CAA$_{predicted}$ (mol/L)
0.000	0.000	0.994
7.220	0.011	0.963
9.620	0.015	0.953
12.020	0.019	0.943
16.820	0.026	0.923
19.220	0.030	0.914
21.620	0.034	0.905
24.020	0.037	0.896
28.820	0.045	0.878
31.220	0.048	0.869
33.620	0.052	0.860
36.020	0.056	0.852
40.820	0.063	0.835
43.220	0.066	0.827
45.620	0.070	0.819
48.020	0.073	0.811
52.820	0.081	0.796
55.220	0.084	0.788
57.620	0.088	0.781
60.020	0.091	0.774
64.820	0.098	0.759
67.220	0.101	0.752
69.620	0.105	0.745
72.020	0.108	0.738
76.820	0.115	0.725
79.220	0.118	0.718
81.620	0.122	0.712
84.020	0.125	0.705

88.820	0.132	0.693
91.220	0.135	0.686
93.620	0.138	0.680
96.020	0.141	0.674
100.820	0.148	0.662
103.220	0.151	0.656
105.620	0.154	0.651
108.020	0.157	0.645
112.820	0.164	0.634
115.220	0.167	0.628
117.620	0.170	0.623
120.020	0.173	0.617
124.820	0.179	0.607
127.220	0.182	0.602
129.620	0.185	0.596
132.020	0.188	0.591
136.820	0.194	0.581
139.220	0.197	0.576
141.620	0.200	0.572
144.020	0.203	0.567
148.820	0.208	0.557
151.220	0.211	0.553
153.620	0.214	0.548
156.020	0.217	0.543
160.820	0.222	0.535
163.220	0.225	0.530
165.620	0.228	0.526
168.020	0.231	0.521
172.820	0.236	0.513
175.220	0.239	0.509
177.620	0.241	0.505
180.020	0.244	0.501

184.820	0.249	0.492
187.220	0.252	0.488
189.620	0.255	0.485
192.020	0.257	0.481
196.820	0.262	0.473
199.220	0.265	0.469
201.620	0.267	0.465
204.020	0.270	0.462
208.820	0.275	0.455
211.220	0.277	0.451
213.620	0.279	0.447
216.020	0.282	0.444
220.820	0.287	0.437
223.220	0.289	0.434
225.620	0.291	0.430
228.020	0.294	0.427
232.820	0.298	0.420
235.220	0.301	0.417
237.620	0.303	0.414
240.020	0.305	0.411
244.820	0.310	0.404
247.220	0.312	0.401
249.620	0.314	0.398
252.020	0.316	0.395
256.820	0.320	0.389
259.220	0.323	0.386
261.620	0.325	0.383
264.020	0.327	0.380
268.820	0.331	0.375
271.220	0.333	0.372
273.620	0.335	0.369
276.020	0.337	0.366

280.820	0.341	0.361
283.220	0.343	0.358
285.620	0.345	0.355
288.020	0.347	0.353
292.820	0.351	0.347
295.220	0.353	0.345
297.620	0.355	0.342
300.000	0.357	0.340
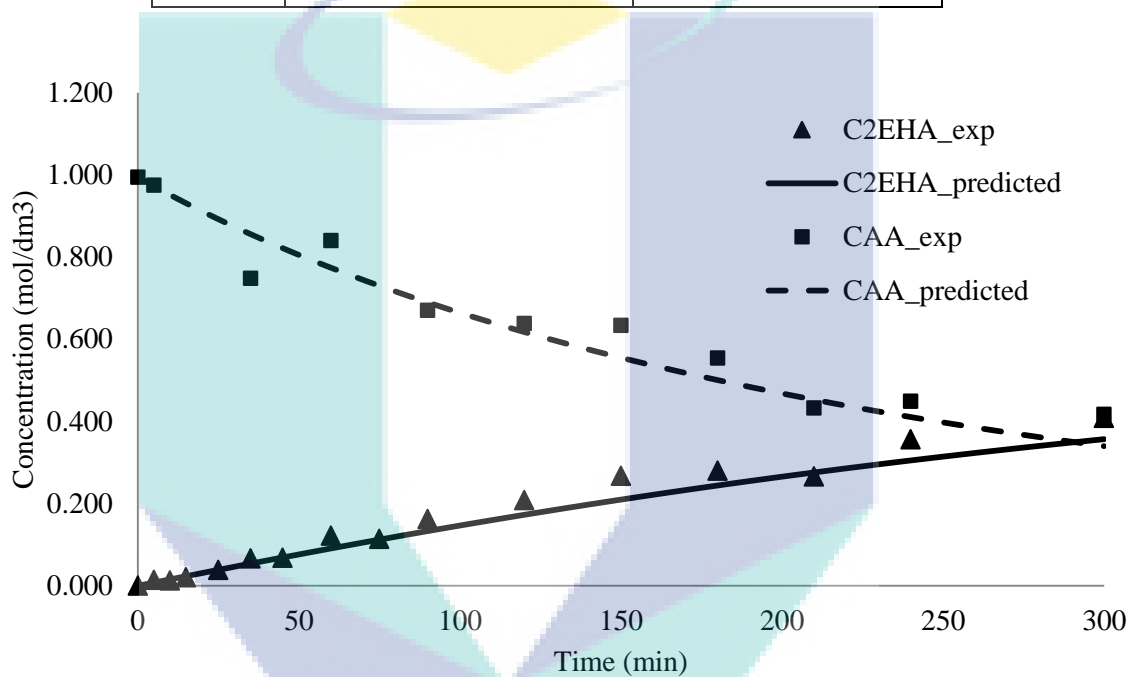
Figure G1 : Comparison between experimental and calculated (with ER model considering polymerization of AA) concentration profiles. Molar ratio of AA to 2EH is 1:6, temperature at 378.15 K, catalyst loading is 10% w/w and stirring speed at 400 rpm.

Table G5: Experimental concentration-time data for reaction temperature at 368.15 K, $M_{aa/2eh}$ is 1:6, catalyst loading is 10% w/w and stirring speed at 400 rpm

| t (min)	C2EHA$_{exp}$ (mol/L)	CAA$_{exp}$ (mol/L)
0	0.000	0.994
5	0.008	0.889
10	0.014	0.877
15	0.020	0.972
25	0.029	0.869
35	0.040	0.866
45	0.049	0.834
60	0.069	0.812
75	0.072	0.737
90	0.086	0.730
120	0.114	0.714
150	0.200	0.696
180	0.158	0.633
210	0.176	0.580
240	0.198	0.561
300	0.244	0.515

Table G6: Predicted concentration-time data for reaction temperature at 368.15 K, $M_{aa/2eh}$ is 1:6, catalyst loading is 10% w/w and stirring speed at 400 rpm

t (min)	C2EHA$_{predicted}$ (mol/L)	CAA$_{predicted}$ (mol/L)
0.000	0.000	0.994
6.448	0.006	0.972
11.248	0.007	0.965
13.648	0.009	0.959
16.048	0.013	0.945
18.448	0.015	0.938
23.248	0.017	0.932

25.648	0.018	0.925
28.048	0.022	0.913
30.448	0.024	0.907
35.248	0.026	0.900
37.648	0.028	0.894
40.048	0.031	0.882
42.448	0.033	0.877
47.248	0.035	0.871
49.648	0.037	0.865
52.048	0.040	0.854
54.448	0.042	0.848
59.248	0.044	0.843
61.648	0.045	0.837
64.048	0.049	0.827
66.448	0.051	0.821
71.248	0.052	0.816
73.648	0.054	0.811
76.048	0.058	0.801
78.448	0.059	0.796
83.248	0.061	0.791
85.648	0.063	0.786
88.048	0.066	0.776
90.448	0.068	0.772
95.248	0.070	0.767
97.648	0.071	0.762
100.049	0.075	0.753
102.449	0.076	0.749
107.249	0.078	0.744
109.649	0.080	0.740
112.049	0.083	0.731
114.449	0.085	0.727
119.249	0.086	0.723

121.649	0.088	0.718
124.049	0.091	0.710
126.449	0.093	0.706
131.249	0.095	0.702
133.649	0.096	0.698
136.049	0.099	0.690
138.449	0.101	0.686
143.249	0.103	0.682
145.649	0.104	0.678
148.049	0.107	0.671
150.449	0.109	0.667
155.249	0.110	0.663
157.649	0.112	0.660
160.049	0.115	0.652
162.449	0.117	0.649
167.249	0.118	0.645
169.649	0.120	0.642
172.049	0.123	0.635
174.449	0.124	0.631
179.249	0.126	0.628
181.649	0.127	0.625
184.049	0.130	0.618
186.449	0.132	0.615
191.249	0.133	0.611
193.649	0.135	0.608
196.049	0.138	0.602
198.449	0.139	0.598
203.249	0.141	0.595
205.649	0.142	0.592
208.049	0.145	0.586
210.449	0.147	0.583
215.249	0.148	0.580

217.649	0.149	0.577
220.049	0.152	0.571
222.449	0.154	0.568
227.249	0.155	0.565
229.649	0.157	0.562
232.049	0.159	0.557
234.449	0.161	0.554
239.249	0.162	0.551
241.649	0.164	0.548
244.049	0.166	0.543
246.449	0.168	0.540
251.249	0.169	0.537
253.649	0.170	0.535
256.049	0.173	0.529
258.449	0.174	0.527
263.249	0.176	0.524
265.649	0.177	0.522
268.049	0.180	0.516
270.449	0.181	0.514
275.249	0.182	0.511
277.649	0.184	0.509
280.049	0.186	0.504
282.449	0.188	0.502
287.249	0.189	0.499
289.649	0.190	0.497
292.049	0.193	0.492
294.449	0.194	0.490
299.249	0.195	0.487
300.000	0.196	0.485
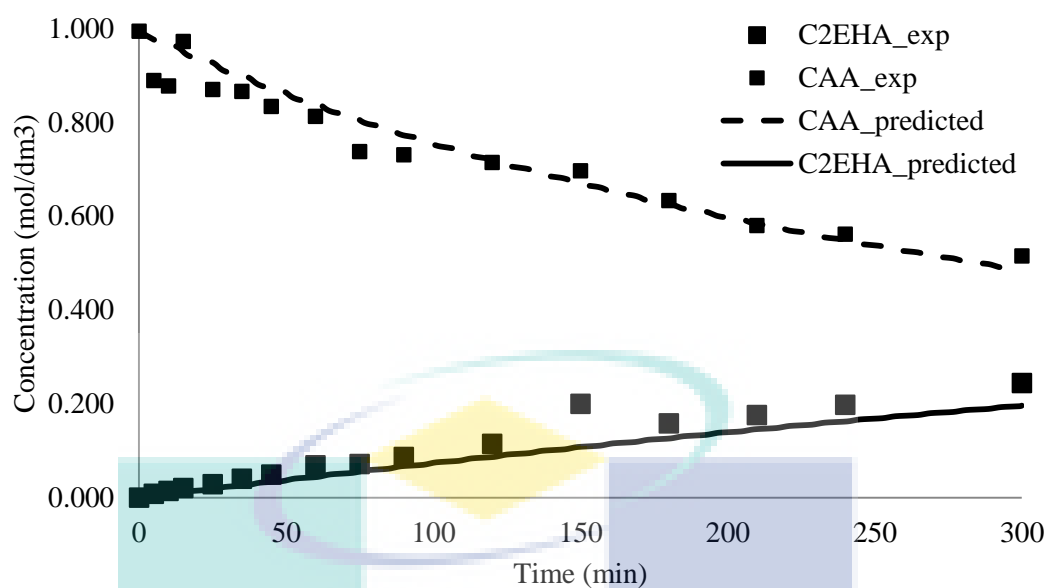
Figure G2 : Comparison between experimental and calculated (with ER model considering polymerization of AA) concentration profiles. Molar ratio of AA to 2EH is 1:6, temperature at 368.15 K, catalyst loading is 10% w/w and stirring speed at 400 rpm.

Table G7: Experimental concentration-time data for reaction temperature at 358.15 K, $M_{aa/2eh}$ is 1:6, catalyst loading is 10% w/w and stirring speed at 400 rpm

t (min)	C2EHA$_{exp}$ (mol/L)	CAA$_{exp}$ (mol/L)
0	0.000	0.994
5	0.002	0.882
10	0.005	0.977
15	0.006	0.963
25	0.009	0.929
35	0.002	
45	0.015	0.929
90	0.031	0.957
120	0.042	0.959
150	0.050	0.911
180	0.066	0.955
210	0.068	0.886
240	0.082	0.931
300	0.095	0.847

Table G8: Predicted concentration-time data for reaction temperature at 358.15 K, $M_{aa/2eh}$ is 1:6, catalyst loading is 10% w/w and stirring speed at 400 rpm

t (min)	C2EHA$_{predicted}$ (mol/L)	CAA$_{predicted}$ (mol/L)
0.000	0.000	0.994
7.239	0.003	0.990
9.639	0.003	0.988
12.039	0.004	0.987
16.839	0.006	0.984
19.239	0.007	0.983
21.639	0.008	0.981
24.039	0.009	0.980
28.839	0.010	0.977

31.239	0.011	0.976
33.639	0.012	0.974
36.039	0.013	0.973
40.839	0.015	0.970
43.239	0.016	0.969
45.639	0.016	0.968
48.039	0.017	0.966
52.839	0.019	0.964
55.239	0.020	0.962
57.639	0.021	0.961
60.039	0.021	0.959
64.839	0.023	0.957
67.239	0.024	0.955
69.639	0.025	0.954
72.039	0.026	0.953
76.839	0.027	0.950
79.239	0.028	0.949
81.639	0.029	0.947
84.039	0.030	0.946
88.839	0.032	0.943
91.239	0.032	0.942
93.639	0.033	0.941
96.039	0.034	0.940
100.839	0.036	0.937
103.239	0.037	0.936
105.639	0.037	0.934
108.039	0.038	0.933
112.839	0.040	0.930
115.239	0.041	0.929
117.639	0.042	0.928
120.039	0.042	0.927
124.839	0.044	0.924

127.239	0.045	0.923
129.639	0.046	0.921
132.039	0.046	0.920
136.839	0.048	0.918
139.239	0.049	0.916
141.639	0.050	0.915
144.039	0.051	0.914
148.839	0.052	0.911
151.239	0.053	0.910
153.639	0.054	0.909
156.039	0.055	0.908
160.839	0.056	0.905
163.239	0.057	0.904
165.639	0.058	0.903
168.039	0.059	0.901
172.839	0.060	0.899
175.239	0.061	0.898
177.639	0.062	0.896
180.039	0.063	0.895
184.839	0.064	0.893
187.239	0.065	0.892
189.639	0.066	0.890
192.039	0.067	0.889
196.839	0.068	0.887
199.239	0.069	0.886
201.639	0.070	0.884
204.039	0.071	0.883
208.839	0.072	0.881
211.239	0.073	0.880
213.639	0.074	0.878
216.039	0.075	0.877
220.839	0.076	0.875

223.239	0.077	0.874
225.639	0.078	0.872
228.039	0.078	0.871
232.839	0.080	0.869
235.239	0.081	0.868
237.639	0.082	0.867
240.039	0.082	0.865
244.839	0.084	0.863
247.239	0.085	0.862
249.639	0.085	0.861
252.039	0.086	0.860
256.839	0.088	0.857
259.239	0.089	0.856
261.639	0.089	0.855
264.039	0.090	0.854
268.839	0.092	0.851
271.239	0.092	0.850
273.639	0.093	0.849
276.039	0.094	0.848
280.839	0.095	0.846
283.239	0.096	0.845
285.639	0.097	0.844
288.039	0.098	0.842
292.839	0.099	0.840
295.239	0.100	0.839
297.639	0.101	0.838
300.000	0.101	0.837
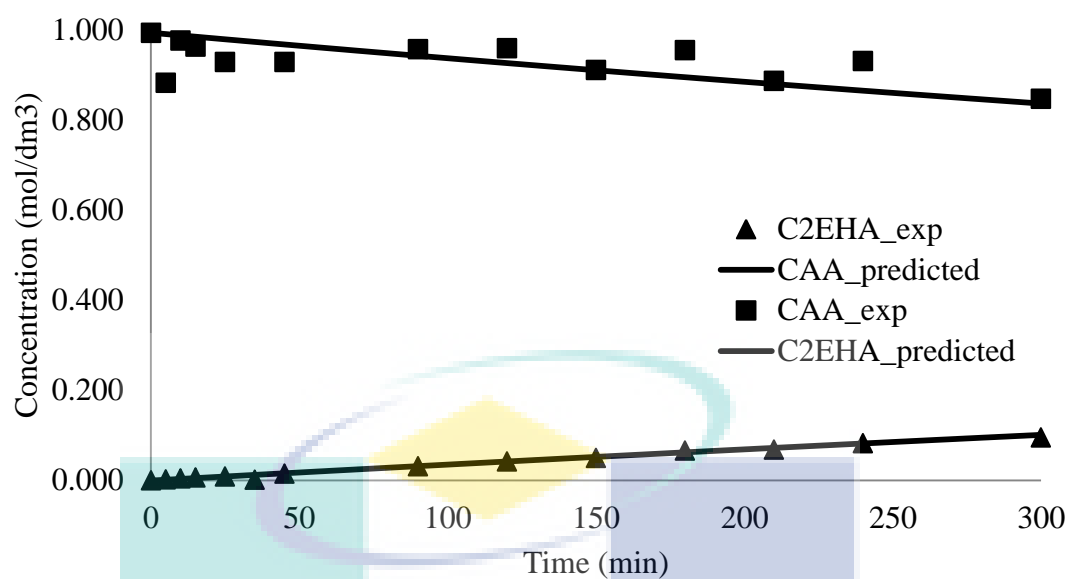
Figure G3 : Comparison between experimental and calculated (with ER model considering polymerization of AA) concentration profiles. Molar ratio of AA to 2EH is 1:6, temperature at 358.15 K, catalyst loading is 10% w/w and stirring speed at 400 rpm.

APPENDIX H

THE PREDICTED AND EXPERIMENTAL CONCENTRATION-TIME DATA
FOR THE REACTION STUDY WITH DIFFERENT AA CONCENTRATION

Table H1: The predicted and experimental concentration-time data for the reaction study with 10% w/w AA concentration

time (min)	C2EHA exp	C2EHA predicted
60	0.0048	0.0025
120	0.0073	0.0049
180	0.0107	0.0073
300	0.0132	0.0120

Table H2: The predicted and experimental concentration-time data for the reaction study with 20% w/w AA concentration

time (min)	C2EHA exp	C2EHA predicted
30	0.0050	0.0038
60	0.0087	0.0073
120	0.0154	0.0144
180	0.0229	0.0214
240	0.0315	0.0282
300	0.0392	0.0348

Table H3: The predicted and experimental concentration-time data for the reaction study with 30% w/w AA concentration

time (min)	C2EHA exp	C2EHA predicted
30	0.0046	0.0049
60	0.0069	0.0094
120	0.0179	0.0184
180	0.0258	0.0272
240	0.0343	0.0356
300	0.0415	0.0439

Table H4: The predicted and experimental concentration-time data for the reaction study with 40% w/w AA concentration

time (min)	C2EHA exp	C2EHA predicted
30	0.0028	0.0048
60	0.0093	0.0098
120	0.0207	0.0191
180	0.0296	0.0281
240	0.0378	0.0366
300	0.0452	0.0449

Table H5: The predicted and experimental concentration-time data for the reaction study with 50% w/w AA concentration

time (min)	C2EHA exp	C2EHA predicted
30	0.0059	0.0079
60	0.0122	0.0161
120	0.0250	0.0312
180	0.0398	0.0454
240	0.0565	0.0589
300	0.0784	0.0716

Table H6: The predicted and experimental concentration-time data for the reaction study with 60% w/w AA concentration

time (min)	C2EHA exp	C2EHA predicted
30	0.0085	0.0088
60	0.0168	0.0178
120	0.0308	0.0343
180	0.0435	0.0500
240	0.0627	0.0647
300	0.0712	0.0791

Table H7: The predicted and experimental concentration-time data for the reaction study with 70% w/w AA concentration

time (min)	C2EHA exp	C2EHA predicted
30	0.0250	0.0267
60	0.0513	0.0512
120	0.0887	0.0986
180	0.1366	0.1428
240	0.1804	0.1805
300	0.2231	0.2133

Table H8: The predicted and experimental concentration-time data for the reaction study with 80% w/w AA concentration

time (min)	C2EHA exp	C2EHA predicted
30	0.0503	0.0667
60	0.1121	0.1245
120	0.2021	0.2290
180	0.2899	0.3157
240	0.3962	0.3909
300	0.4513	0.4505

Table H9: The predicted and experimental concentration-time data for the reaction study with 90% w/w AA concentration

time (min)	C2EHA exp	C2EHA predicted
30	0.095	0.1162
60	0.1496	0.2132
120	0.3348	0.3708
180	0.4659	0.4886
240	0.6006	0.5826
300	0.6881	0.6528